WHAT KILLS TREES?

DRIVERS, MECHANISMS, AND TIMING OF

CLIMATE-INDUCED TREE MORTALITY.

By

WILLIAM MICHAEL HAMMOND

Bachelor Arts in Biology
University of Central Oklahoma
Edmond, Oklahoma
2016

Submitted to the Faculty of the
Graduate College of the
Oklahoma State University
in partial fulfillment of
the requirements for
the Degree of
DOCTOR OF PHILOSOPHY
May, 2021

WHAT KILLS TREES?

DRIVERS, MECHANISMS, AND TIMING OF

CLIMATE-INDUCED TREE MORTALITY.

Dissertation Approved:

Dr. Henry Adams

Dissertation Adviser

Dr. Andrew Doust

Committee Chair

Dr. Daniel Johnson

Committee Member

Dr. Monica Papeş

Committee Member

Dr. Gerald Schönknecht

Committee Member

Dr. Rodney Will

Outside Committee Member

for Sharayah

In 2011, you asked what I would do with my life, if I could do anything. The answer, a decade later, lies in these pages.

Acknowledgements reflect the views of the author and are not endorsed by committee members or Oklahoma State University.

ACKNOWLEDGEMENTS

First, I wish to acknowledge my advisor, Henry Adams. You took a chance on me, against advice of experienced peers, supporting admission of a non-traditional student directly to the PhD program. More than that, you supported my wildest ideas, reminded me of successes when I failed, and always shared ample time (and whiteboard space) with me. To my advisory committee—Dan Johnson, Gerald Schönknecht, Mona Papeș, and Rod Will—I am eternally grateful. You collectively taught me what great mentorship and careful science look like. To my committee and department chair, Andrew Doust, I am grateful for your wisdom, humor, and frequent reminders that it will all work out. My eternal gratitude extends to my lab mates, especially the first, for all our shared ideas, dreams, fears, and cups of coffee.

Of all my many teachers, none left a greater impact upon me than the undergraduates I've had the honor to mentor—you revealed to me that more than answering any particular question (even, 'what kills trees'), I most enjoy the collaborative nature of science, especially the discoveries we shared. Of course, when I was an undergraduate, I knew the feeling already—as my mentor Paul Stone provided the space to discover my passion for trees in the Peloncillos, even if we were supposed to be looking for turtles. Paul, from the bottom of my heart, thank you for your lasting mentorship.

I am grateful for so many mentors from afar—particularly Chris Still, José Torres-Ruiz and Tamir Klein for hosting my research trips to Oregon, France, and Israel respectively, and welcoming me into their labs. Our collaborations opened my mind to new ways of thinking. Especially, I wish to thank Craig Allen—for all the time he poured into me, for encouraging me

to ‘think bigger’, and for helping me find my own voice as a writer, even if I do tend to gild the lily. To my many collaborators and coauthors of these last five years—thank you for your partnership in the pursuit of knowledge.

I also must thank the financial supporters of my dissertation work—the National Science Foundation, Campus France, the US-Israel Binational Science Foundation, and the McPherson Fund—your support took me around the world, kept a roof over my family, and provided the time and freedom to both learn from and contribute to my field.

Finally, and most importantly—I must thank my family for so very much. My grandfather (and namesake, Bill), for igniting my passion for the natural world, and especially for sharing his fondness of trees with me as a boy. My grandmother Francile, and my mother Terri, for both being proud of me ‘no matter what’. My father Michael, for engraining the value of working hard for something deserving of your time—I wish you were still here and could see the lesson stuck. To my siblings, for my competitive spirit. To my daughter Hannah—for the shining example of kindness and care for others that you are. To my son Michael, for reminding me there’s always more questions. To my son Harrison, for always being ready to play, and forget my studies for a while. Above all others, I thank my partner, Sharayah—you were the only one who believed that we should take the leap and begin this journey, together. I’d never have begun, let alone finished, without your enduring love and support.

Name: WILLIAM MICHAEL HAMMOND

Date of Degree: MAY, 2021

Title of Study: WHAT KILLS TREES? DRIVERS, MECHANISMS, AND TIMING OF CLIMATE-INDUCED TREE MORTALITY.

Major Field: PLANT BIOLOGY

Abstract:

In recent decades, drought-induced tree mortality has been observed on every forested continent of the planet. This is of great concern, as trees support some of the most biodiverse communities on Earth, are keystones in the planetary carbon and water cycles, and provide both economic and structural support for human civilizations. Determining the drivers, mechanisms, and timing of climate-induced tree mortality is an important step toward understanding the central question of this dissertation: what kills trees? I began searching for an answer locally, in the Cross Timbers of Oklahoma—developing a past-to-present species distribution modeling method to predict present-day range contractions since the 1950s, field-testing these predictions through vegetation surveys and tree-ring studies. While I found higher mortality of juvenile trees in areas predicted unsuitable in the present day, the model overpredicted mature tree mortality. This simple model, and more generally the field of research, lacked critical information: (1) what climate conditions trigger tree mortality during hotter droughts? (2) what is a lethal dose of drought stress for a tree?, and (3) what determines the time-to-mortality under hotter drought stress? The balance of this dissertation seeks to provide initial answers to these pressing questions. Here, I demonstrate that global forests share a common and detectable 'hotter-drought fingerprint', a climate signal for Earth's observed forest mortality sites. This global climate fingerprint reveals that the frequency of potentially lethal climate conditions will accelerate with further warming. Next, I quantify a lethal dose of drought stress for a physiological state (xylem) ubiquitously associated with drought-induced tree mortality. Through drought-rewatering experiments, this work identifies when trees stop living, and start dying. Surprisingly, trees survived much higher levels of xylem dysfunction than expected—revealing that surviving trees retain legacies of dysfunction with long-term consequences. These legacies of dysfunction may reduce resilience and predispose eventual tipping points—initially in community compositions—and eventually in ecosystem states, so their consideration should refine future efforts to model forest mortality. Having bounded environmental drivers and physiological thresholds of tree mortality, I propose a framework of coordinated suites of physiological traits that will improve prediction for time-to-mortality of trees.

TABLE OF CONTENTS

Chapter Page

LIST OF TABLES

Table Page

LIST OF FIGURES

Figure Page

Figure Page

CHAPTER I

INTRODUCTION: WHAT KILLS TREES? DRIVERS, MECHANISMS, AND TIMING OF CLIMATE-INDUCED TREE MORTALITY.

William Michael Hammond

Trees are the tallest, eldest, and most massive living things on Earth. The scales of time and space occupied by trees dwarfs that of humans. Yet, for all their enormity, we know relatively little about what kills trees. Recent decades have underscored this lack of knowledge—as all vegetated continents have experienced forest collapse under hotter-drought in recent decades (Allen *et al.*, 2010), understanding not just what kills trees—but where, and when will they may die next—has emerged as a pressing challenge of the fields of forest ecology, physiology, and Earth system modeling (Brodribb *et al*., 2020). In the chapters that follow, I relay my attempts to understand what kills trees during hotter droughts. In the end, I have raised more questions than answers about what kills trees—but this dissertation is only the beginning.

Local tree mortality: The Cross Timbers

The first chapter to follow this introduction began the summer before I started my Ph.D. I had been handed a binder full of forest inventory data from a state-wide survey conducted by Elroy Rice and William Penfound (Rice & Penfound, 1959), by then retiring professor Stephen Hallgren. I was eager to get started. I digitized and used this data to train a species distribution model in the 1950s, to predict how the warming over six decades may have caused a shift in the range of co-dominant oak species. The model predicted significant reductions in suitable range—

reducing the contemporary suitable area in Oklahoma by a quarter, relative to the 1950s. I then conducted vegetation surveys, and sampled post oaks to build tree-ring chronologies, at sites distributed broadly across the East/West precipitation and North/South temperature gradients of the Cross Timbers. Half of my sites had been predicted suitable by the model, and the other half had not. Analysis of the vegetation surveys and tree-ring data showed that recruitment was significantly impaired at sites predicted unsuitable in the present day, while mature trees (in both vegetation surveys, and in ring-width from the tree-ring chronologies) were indistinguishable based on site suitability predictions. The method developed (past-to-present distribution modeling, with contemporary field validation) provides a framework to test the predictive power of widely deployed species distribution models.

Author's note: This chapter is in preparation for submission to *Global Change Biology*.

Global tree mortality: a hotter-drought fingerprint

Similar pursuits as my investigation in the Cross Timbers are not possible at the global scale—yet. One reason for this is that while precise records of occurrence are plentiful for global forests, the same cannot be said for observations of tree mortality (Hartmann *et al*., 2018). Foresters, primarily tasked with production and management of forests, have often paid dead and dying trees less attention than the growing, productive ones. For this reason, my third chapter is focused on assembling, precisely georeferencing, and performing a climatological analysis on the first global database of hotter-drought triggered tree mortality. Surveying 230 peer-reviewed studies which documented tree mortality at stand to regional scales, requiring more than a hundred data requests to authors, I (along with mentor Dr. Craig Allen) assembled a global database of precise locations where trees died due to hotter drought, and the year mortality began. Covering all forested continents and biomes, this database includes observations at sites ranging in mean

annual temperature from < 3 °C to < 30 °C, and in mean annual precipitation from < 50 mm to > 3,900 mm. Using a climatological approach, in this chapter I quantify the 'hotter-drought fingerprint'—a multivariate hotter-drought climate signal—for global forest mortality since 1970.

Across two warming scenarios (+2°C, +4°C), I also found that the frequency of these historically lethal climate conditions (the hotter-drought fingerprint) will likely accelerate under further warming—which should be received as an alarm bell for the threats further warming poses to Earth's forests. I propose that especially Earth's historical forests (established ca. 1880 or earlier) are at risk. Much like the oak trees in my second chapter, their recruitment occurred under bygone climate conditions—and their replacement if lost to an extreme hotter-drought event—may not be possible. There is more than just despair in this chapter, as limiting warming to +2°C or less over pre-industrial levels (we are presently +~0.7°C) will significantly reduce the acceleration of hotter-drought triggered tree mortality. Finally, this database is served at tree-mortality.net, a website of the international tree mortality monitoring network, where I serve as the data management and access group leader. There, I encourage the continued growth and expansion of this database—itself an initial footing—to further our understanding of local to global drivers of tree mortality.

Author's note: This chapter is presently in review at *Nature Climate Change since November, 2020*.

Dead, or dying? Quantifying a physiological mechanism of tree mortality.

With drivers of tree mortality described, my fourth chapter (Hammond *et al*., 2019) focuses on the mechanisms of mortality within an individual tree. As a recent global synthesis had just revealed the ubiquitous association between failure of the xylem to conduct water (drought induces air emboli, causing dysfunction in water transport) and tree mortality (Adams *et al*.,

2017), I set out to quantify the lethal dose of this so-called hydraulic failure for trees. Through a greenhouse study, I imposed drought on sapling trees of *Pinus taeda*, loblolly pine, and by relieving drought at various levels (from mild, to surely lethal stress), monitoring to see which trees would survive, and which would die. With this data I quantified that the lethal dose of hydraulic failure (a level when mortality became more likely than survival) was ~80% loss of hydraulic conductivity in the xylem. As our initial estimates (based on leading expertise in the field, e.g., Adams *et al.*, 2017; Breshears *et al.*, 2018; Choat *et al.,* 2018) were that 50-60% might be a lethal dose for a gymnosperm species, this was somewhat surprising. Staining of xylem revealed that in trees surviving the most extreme levels of stress (> 90% loss of conductivity), the remaining functional xylem was uniformly adjacent to the vascular cambium. I proposed that this evidence highlights the need to understand the dehydration tolerance of the vascular cambium, as its eventual dehydration may prove the 'final straw' in survival or mortality of an individual tree. Also, and importantly, this paper demonstrated through simple documentation of foliar color that the most commonly used indicator of when a tree is dying (visual signs of mortality, via foliar color change—in conifers, browning) lags for months behind the actual physiological stress, or hydraulic failure, from which the tree is irrecoverable. This finding has since been replicated by others, further supporting the large lag between visual indicators and eventual tree mortality (Blackman *et al*., 2019). Thus, the chapter is titled dead or dying—as it sheds light on the moment that trees become committed to death—that is, when they stop living, and start dying. Since dying can be such a long process in trees, being able to reliably detect this moment provides the opportunity for investigations into other critical mechanisms in tree survival and mortality, in the days to weeks that matter most (at maximum levels of survivable stress).

Author's note: This chapter was published in *New Phytologist* in 2019, doi: 10.1111/nph.15922.

Trees not dead yet; legacies of dysfunction in trees surviving hotter droughts

While chapter four set out to describe what happens to trees that die, and the mechanisms that underpin death—chapter five (Hammond *et al.*, 2020) turns to the survivors. It was remarkable that trees survived such high levels of stress, and given the common convention that visual signs of mortality (complete canopy browning) are so often used to determine mortality, it occurred to me that survivors of extreme stress may be hiding a significant legacy of dysfunction beneath their green canopies. To demonstrate this, and in response to a comprehensive examination question from Henry, I wrote chapter five as a perspective on alternative stable states in trees, from xylem to ecosystems. If trees are surviving significant levels of xylem dysfunction, it begs the question of what happens after drought is relieved.

In follow-up studies to chapter four, I waited to see how trees might recover their prior dysfunction. Through active xylem staining, I was able to determine that radial growth (and not xylem refilling) was required in the studied conifers to restore plants to the pre-droughted condition. This created a large hysteresis—trees could not simply return to pre-drought physiological function once drought was relieved, but instead would require months to years of radial growth (depending on the age of tree, and intensity of drought) to fully recover lost water transport and storage capacity. Thus, a common indicator used in both field observations (and to drive many models of plant response to environment stress), water potential, can become disconnected from the functional hydraulic state of a particular tree. I suggest a framework for applying alternative stable states theory (Scheffer *et al.,* 2001) to this problem, and encourage this approach to incorporate legacies of hydraulic dysfunction into models—because even if trees survive, they may be significantly different as individuals (and as forests, collectively dysfunctional) until these legacies are erased.

Author's note: This chapter was published in *Frontiers in Forests and Global Change* in 2020, doi: 10.3389/ffgc.2020.560409.

Time-to-mortality for trees

Finally, in chapter six (Hammond & Adams, 2019), I comment on recent work that has identified drivers of time-to-mortality for trees (Blackman *et al*., 2019). Here, I present a framework under which suites of physiological traits regulate the time-to-mortality, and propose that some trees will be 'quick' to race from incipient mortality risk to the point-of-no-return, while others may persist for quite a time longer. As there is much interest in understanding which trees will be able to best persist under future climates, testing of this framework may be an essential step to identifying trees well-suited to the warming, drying world we have imposed upon them.

Author's note: This chapter was an invited commentary in *Tree Physiology*, published in 2019, doi: 10.1093/treephys/tpz050.

References

Adams HD, Zeppel MJB, Anderegg WRL, Hartmann H, Landhäusser SM, Tissue DT, Huxman TE, Hudson PJ, Franz TE, Allen CD, et al. 2017. A multi-species synthesis of physiological mechanisms in drought-induced tree mortality. *Nature Ecology & Evolution* 1: 1285–1291. DOI:10.1038/s41559-017-0248-x.

Allen CD, Macalady AK, Chenchouni H, Bachelet D, McDowell N, Vennetier M, Kitzberger T, Rigling A, Breshears DD, Hogg ET. 2010. A global overview of drought and heat-induced tree mortality reveals emerging climate change risks for forests. *Forest ecology and management* 259: 660–684.

Blackman CJ, Creek D, Maier C, Aspinwall MJ, Drake JE, Pfautsch S, O'Grady A, Delzon S, Medlyn BE, Tissue DT, et al. 2019. Drought response strategies and hydraulic traits contribute to mechanistic understanding of plant dry-down to hydraulic failure. *Tree Physiology* 39: 910–924. DOI:10.1093/treephys/tpz016.

Brodribb TJ, Powers J, Cochard H, Choat B. 2020. Hanging by a thread? Forests and drought. *Science* 368: 261–266. DOI:10.1126/science.aat7631.

Choat B, Brodribb TJ, Brodersen CR, Duursma RA, López R, Medlyn BE. 2018. Triggers of tree mortality under drought. *Nature* 558: 531–539. DOI:10.1038/s41586-018-0240-x.

Hammond WM. 2020. A Matter of Life and Death: Alternative Stable States in Trees, From Xylem to Ecosystems. *Frontiers in Forests and Global Change* 3. DOI:10.3389/ffgc.2020.560409.

Hammond WM, Adams HD. 2019. Dying on time: traits influencing the dynamics of tree mortality risk from drought. *Tree Physiology* 39: 906–909. DOI:10.1093/treephys/tpz050.

Hammond WM, Yu K, Wilson LA, Will RE, Anderegg WRL, Adams HD. 2019. Dead or dying? Quantifying the point of no return from hydraulic failure in drought-induced tree mortality. *New Phytologist*. DOI:10.1111/nph.15922.

Hartmann H, Moura CF, Anderegg WR, Ruehr NK, Salmon Y, Allen CD, Arndt SK, Breshears DD, Davi H, Galbraith D. 2018. Research frontiers for improving our understanding of drought-induced tree and forest mortality. *New Phytologist* 218: 15–28.

Rice EL, Penfound WT. 1959. The upland forests of Oklahoma. *Ecology* 40: 593–608.

Scheffer M, Carpenter S, Foley JA, Folke C, Walker B. 2001. Catastrophic shifts in ecosystems. *Nature* 413: 591–596. DOI:10.1038/35098000.

CHAPTER II

THE FUTURE IS NOW: TESTING PREDICTIONS OF SPECIES DISTRIBUTION MODELS

William M. Hammond[1], Justin R. Dee[2], Alissa J. Freeman[1], Kaitlyn H. McNiel[1], Monica Papeş[3], Stephen W. Hallgren[4], and Henry D. Adams[1].

[1]Department of Plant Biology, Ecology, and Evolution, Oklahoma State University, Stillwater, OK
[2]School of Natural Resources, University of Missouri, Columbia, MO
[3]Department of Ecology and Evolutionary Biology, University of Tennessee, Knoxville, TN
[4]Department of Natural Resource Ecology and Management, Oklahoma State University, Stillwater, OK

Author's note: This chapter is in preparation for submission to *Global Change Biology*.

Abstract

Species distribution models (SDMs) predict drastic shifts for many species under future climate scenarios. Combining records of species occurrence, environment (e.g., temperature, precipitation derived variables), and other factors (e.g., geology, disturbance regime) these models provide a means to predict the fundamental niche of species. Advances in machine learning and user-friendly software have led to the rapid, widespread adoption of SDMs across many disciplines of science, with exponential increases in publishing of SDM papers. Despite their wide application to most forms of life on Earth, direct testing of predictions from these models against observed species distribution changes in the field over time is lacking. Here we show the first direct test of an SDM, which we built to predict changes in the range of co-dominant oak trees in the Cross Timbers—an ecoregion representing the westernmost dry edge of temperate hardwood forests of eastern North America. We trained an SDM in the recent past, predicted the current-day distribution, and field-tested model predictions through field surveys.

Our findings showed some support for model predictions (especially within early developmental stages), but also serve to caution against broad interpretations/applications of untested SDMs, as mature trees did not respond as the model predicted. We discuss the extension of this work by proposing a conceptual framework to test the predictive power of SDMs through past-to-present model construction paired with contemporary occurrence records or surveys.

Introduction

Worldwide, anthropogenic climate change is altering every ecosystem on the planet (IPCC 2014). Predicting species-specific responses to changing environmental conditions is an urgent task for many scientists (Thomas et al. 2004). Since the inception of ecology, the relationship between environmental conditions and species distributions has been a central focus. In the early 1980s, Elgene Box created the first climate-envelope models of species distributions (Box 1981). In recent years, species distribution models (hereafter SDMs) have been widely employed to meet this need—utilizing advanced machine learning to make future predictions of species distributions (Phillips et al. 2006). Since 2001, when machine learning methods for species distribution modeling first appeared, an exponential increase in both publications per year and citations per year has been underway, with over 1,000 new publications in 2019 containing either "ecological niche modeling" or "species distribution modeling" in their topics (Fig. 1A). Similarly, this body of work is widely cited, with over 40,000 citations of these papers in the year 2019 alone. These articles have appeared in journals across many fields, including over 40% (102 of 254) of Web of Science journal categories. Despite rapid adoption by scientists spanning extant taxa and many disciplines (Fig. 1C), the future predictions of these models remain largely untested in the field. An obvious reason for this is that field-testing future predictions would require abundant patience, or a time machine. Lacking both, here we present a testable species distribution model—a model trained with data from the past, projected to the present day and then field-tested with on-the-ground measurements and observations to assess model predictions.

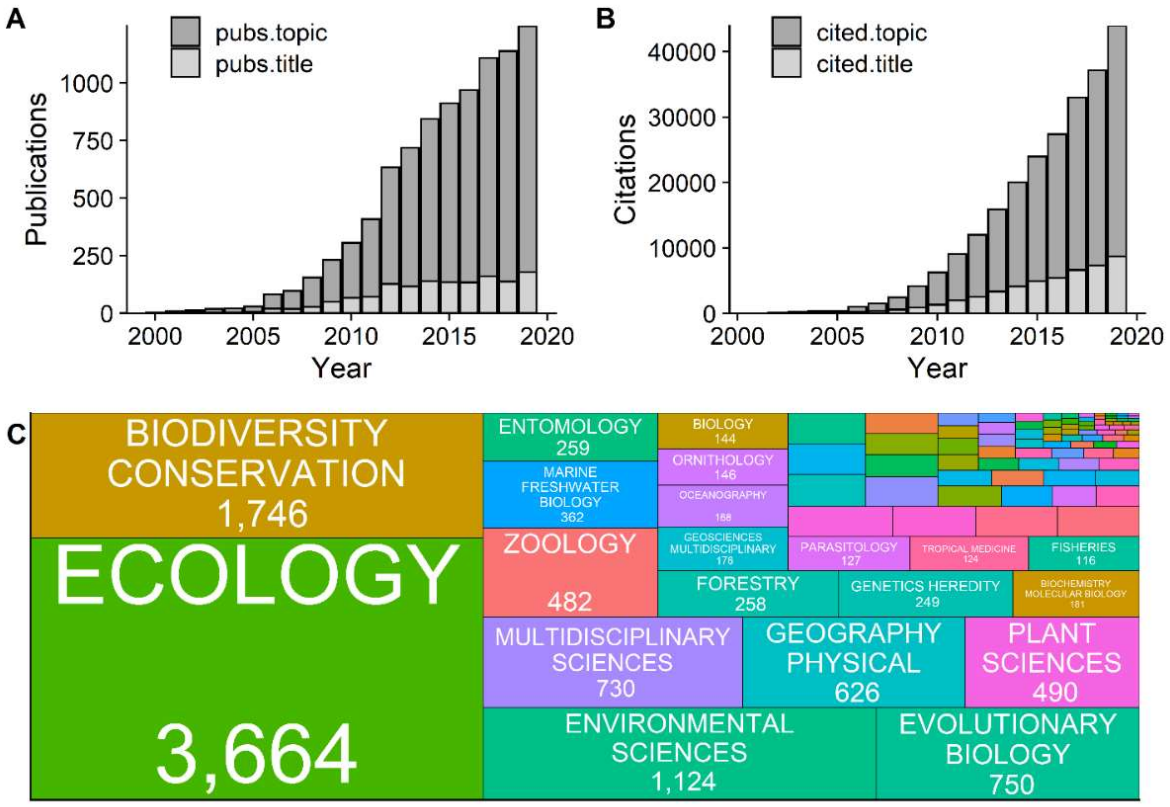

Figure 1: Panel A: Publications per year with "ecological niche modeling" OR "species distribution modeling" in their title. Panel B: Citations per year of publications with "ecological niche modeling" OR "species distribution modeling" in title. Data were collected via search on Web of Science. Panel C: By field, a break-down of the 27,855 papers citing the publications with "ecological niche model" or "species distribution model" in their titles through 2017. While many citations lie within the field of Ecology, SDM concepts are often used across many disciplines (data source: Web of Science, 2019).

Existing Species Distribution Models

SDMs, also referred to as ecological niche models, bioclimatic envelope models or habitat suitability models, use a climate-envelope approach to approximate climate utilized by existing presence observations, and projecting to future climate scenarios (Elith and Leathwick 2009, Araújo and Peterson 2012). This approach has several ecological assumptions that must be acknowledged as limitations (Dormann et al. 2013), and indeed virtual testing of various methods has shown that no single method is best at predicting known species distributions (Qiao et al. 2015). Moreover, SDMs are most often constructed using presence data that are incomplete.

Addressing the concern of these assumptions, and their impact on the projections of SDMs, has often occurred through cross-validation using subsets of presence data (most commonly, area under the curve, AUC), and other techniques for validating predictive power of SDMs (Elith et al. 2011). SDMs have been used to predict distribution changes in oak-dominated forests in recent years (Bertrand et al. 2012, Vessella and Schirone 2013). Maximum Entropy Modelling (MaxEnt) has been demonstrated an effective algorithm for modelling species distributions from presence-only data (Elith et al. 2006). However, species rarely occupy the entirety of their fundamental niche at any point in time, causing presence-only models to come under criticism for using only the presently realized niche to inform the model for suitability (Araújo and Peterson 2012, Law et al. 2019). While presence-only MaxEnt modelling utilizes observed realized niche to train the model, this has been shown predictive for oak over long time scales (15,000+years) when projecting the species range under novel climate scenarios (Veloz et al. 2012).

While predicting known presences within the current climate-envelope is an important step, it begs the question—will the predictive specificity and sensitivity of these models hold under novel climate space? To test this question, we set out to build an SDM in the recent past, project to the present-day, and use field observations of species presence, absence, demographics, and mortality to validate model projections in the Cross Timbers, an oak dominated forest ecosystem of Oklahoma, USA.

Study System

Anthropogenic climate change forecasts increasing temperatures, drought intensity, and drought duration in the Cross Timbers, an ecoregion covering 7 million hectares in the south-central US (IPCC 2014). Globally, elevated tree mortality and forest die-off events have been associated with all three of these forecasted climatic changes (Allen et al. 2010, Allen et al. 2015, Adams et al. 2017). Elevated tree mortality events can be defined as significant departures from

background mortality rates, which range between 0.5 to 2.0% globally. Recently, widespread elevated tree mortality events have been observed in the western United States (Van Mantgem et al. 2009), and elevated tree mortality events have been documented in oaks of eastern deciduous hardwood forests during intense, prolonged drought (Stringer et al. 1989), but recent drivers of mortality in these systems also include pollution and stand density (Dietze and Moorcroft 2011). Present mortality rates in the Cross Timbers are not well understood, although sizeable numbers of dead trees have been observed following past droughts (Rice and Penfound 1959). Forest die-off events can be described as mass (e.g., 50-100%) mortality events that occur during extreme environmental conditions (Allen et al. 2010, Fettig et al. 2019). Shifting species distributions may be gradual (evidenced by increasing background rates of mortality) or sudden (e.g., more immediate shifts due to wide-spread die-off at the edge of a species' range, as in Allen and Breshears, 1998).

Cross Timbers forests are a patchwork ecotone between two ecosystems—the Central Great Plains Prairie, and Eastern Deciduous Hardwood Forests (Hoagland et al., 1999). Ecotones contain species at the limits of their ranges from adjoining communities, are important in supporting regional biodiversity (Risser 1995), and are particularly sensitive to rapid shifts in climate (Allen and Breshears 1998, Rehm et al. 2015). Two climatic gradients predominate in the Cross Timbers—an East-West precipitation gradient, and a North-South temperature gradient. Paleobotanical study of pollen records in the Cross Timbers suggests that during the late Paleozoic, *Picea*, *Abies*, and *Pinus* were dominant. *Carya* became dominant, and *Quercus* first appeared ~ 12,000 years ago, while *Quercus* did not become dominant until ~ 1,000 years ago (Hall 1982). Each of these shifts coincides with a period of rapid change in climate: the end of the Paleozoic saw the warming of the modern interglacial period, while 800-1200 years ago, the medieval climate anomaly was regionally responsible for rapid warming, and increased drought (Trouet et al. 2009). From the earliest botanical records in the late 19th century, until the present

day, two species of oaks are co-dominant in the Cross Timbers: a white oak, *Quercus stellata*—post oak, and a red oak, *Quercus marilandica*—blackjack oak (Hill 1887, Desantis et al. 2010).

Between 1953 and 1957, a comprehensive statewide survey of 208 forest stands (across all forested counties) was conducted in Oklahoma, USA, to quantify stand composition (Rice and Penfound 1959). Combined basal area of *Q. stellata* and *Q. marilandica* accounted for 74% of total basal area of all trees in Oklahoma. Of the 208 sites surveyed, 113 were classified Cross Timbers, with *Q. stellata* and *Q. marilandica* codominant.

As the dry, westernmost edge of the eastern deciduous hardwood forests, the Cross Timbers ecosystem is likely to be among the first regions of the North American eastern deciduous hardwood forest to experience widespread climate-driven vegetation change. Here, we develop a predictive SDM, trained using data from the comprehensive 1950s survey (Rice and Penfound 1959), to predict suitability for *Q. stellata* and *Q. marilandica* codominance in the present day. Using this past-to-present method, we then conducted field surveys to test SDM predictions. With predictions of present-day occurrence, and observations from field surveys—we set out to test SDM predictions for this important ecotone, susceptible to impacts from global change, over a 70 year period.

Methods

Model construction

We trained our SDM with presence and environmental data from the 1950s. Presences were the co-occurrence of *Q. stellata* and *Q. marilandica* determined from the 1953-1957 field data of Rice and Penfound (1959). Although that survey assessed 208 forest stands across the state, only sites from areas classified as Cross Timbers in a 1943 survey of wildlife habitat types of

Oklahoma (Duck & Fletcher 1943) were utilized as presences to train the model (n = 134, Fig. 2), as *Q. stellata* and *Q. marilandica* co-occur in many vegetation types where they are not co-dominant. While spatial filtering to reduce sampling bias can improve model predictions (Boria et al. 2014), we did not perform it in this study due to the nature of the occurrence collection—Rice and Penfound (1959) set out to obtain representative sample data and determined their study plots before conducting the survey. We obtained centroids for all sites from the Oklahoma Biological Survey to georeference occurrence data (Hoagland & Hough 2008).

Bioclimatic variables are widely used in SDMs, and most often consist of 19 "bioclimatic" (precipitation and temperature derived) variables available from the WorldClim database (Hijmans et al. 2005). In order to generate these bioclimatic variables from 1950s and current climate data, we used 1950-1959 and 2006-2015 monthly data from PRISM Climate Group at 4 km^2 spatial resolution for precipitation, maximum temperature, and minimum temperature (PRISM Climate Group 1991). Average climate rasters were created for each month across the ten-year training and projection timeframes. Bioclimatic variables were generated from these average climate rasters using the R package "dismo." Additionally, we also downloaded monthly maximum vapor pressure deficit (VPD_{max}) data to include in the SDM (PRISM Climate Group 1991). VPD_{max} is a quantification of the highest daily atmospheric demand for water, averaged over a month. These values are informative of the maximum atmospheric drought stress on plant water relations at a site, and are biologically meaningful as water transport is driven via transpiration dependent on atmospheric vapor pressure deficit (Dixon and Joly 1895, Breshears et al. 2013, Buckley 2019).

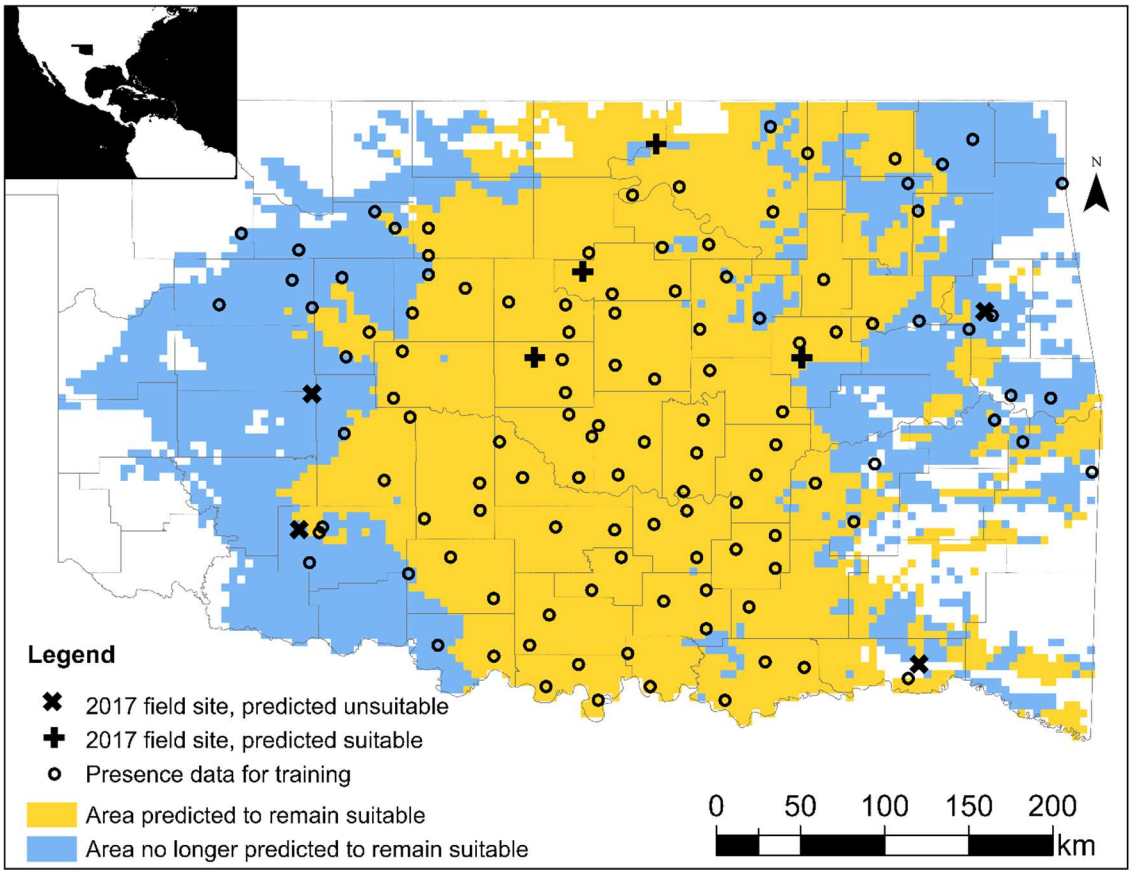

Figure 2: Map of model extent, representing most of the state of Oklahoma. Top-left inset shows location of Oklahoma (shaded black) within North America. On the main panel, black circles represent sites of *Q. stellata*/*Q. marilandica* co-dominance during the 1950s, and were considered occurrence locations for model training. Field sites are indicated by either a black "x" (predicted unsuitable) or black "+" (predicted suitable), where validation was conducted during the summer of 2017 through both increment coring of mature trees, and tree mortality surveys using belt transects. Blue shading indicates area potentially suitable in the 1950s which are predicted to no longer be suitable by our model. Gold shading represents area predicted to remain suitable in the present day, which was suitable in the 1950s.

We also added two soil information layers available from the United States Geologic Survey (USGS) to the model, as inclusion of edaphic variables in modelling *Quercus* niches has been found to reduce overestimation of future suitability predictions (Bertrand et al. 2012). The first layer informed the model on the lithographic parent material from which soils in the area were derived). Strong affinities to specific parent material have been demonstrated previously in forests (Schwartz 1994). Additionally, a soil texture (surficial materials) layer was included to characterize composition of the uppermost (10 cm) soil layer. Both soil datasets were obtained as

polygon shapefiles, and converted in ArcMap using the ArcToolbox conversion tool "Polygon to Raster" (ESRI 2011).

Training extent of the model included all counties in the state of Oklahoma, except for the panhandle region. In order to provide sufficient background for presences at the border of the training area, ArcMap was used to create an 8km (two pixel) buffer beyond any perimeter presences. Finally, to enhance the selection of background, Cross Timbers area was removed from background in all training datasets, with an $8km^2$ buffer around all presences remaining, such that environmental variables for presences would be included in the training dataset. This insured that background selections would not be drawn from the area identified as Cross Timbers during the 1943 survey (Duck and Fletcher 1943). We masked all environmental variables to this training extent.

One factor important to consider when constructing an SDM that is trained in one time period and projected to another, is collinearity between predictor variables (Dormann et al. 2013). Collinearity was identified between layers utilizing SDMToolbox, running a Pearson's correlation test (Brown 2014), and variables with ≥ 0.7 R^2 were removed from the model.

Model development

We used the maximum entropy (MaxEnt) model to construct our SDM from presence data, environmental variables, and projection layers (Phillips et al. 2006). We ran MaxEnt with 5,000 background points and 10 replicate cross validations using a random seed. Model performance was evaluated using mean area under the curve (AUC) and the ten-percentile test omission from an average of the cross-validation replicates. Average outputs for the 1950s and 2000s projections were converted to binary outputs, utilizing the minimum training presence logistic threshold. Changes in projected suitability were calculated using ArcMap's raster calculator, with the

equation (2*1950s)-(2000s), providing an output raster with four classes for 1950s/2000s: present/present, present/absent, absent/present, absent/absent (ESRI 2011).

Field Validation sites

Based on model predictions for present-day suitability (Fig. 3), we identified four field validation sites which were predicted to remain suitable in the present day, and four that were predicted to no longer remain suitable. We selected sites representative of the geographic extent of Cross Timbers for both sites predicted to remain suitable, and those predicted to no longer be suitable for oak co-dominance. As much of the Cross Timbers is privately held, site selection was limited to locations at which we could gain permission for access and sampling. Selected validation sites predicted to remain suitable were the Tall Grass Prairie preserve, E.C. Hafer Park, Lexington Wildlife Management Area, and Kaw Lake State Park. Selected sites predicted to no longer remain suitable in the present day were the Wichita Mountains National Wildlife Refuge, Canton Lake State Park, Sequoyah State Park, and Okmulgee Wildlife Management Area (Fig. 2).

Field validation: transects

At each site in 2017, we established four transects from the forest edge toward the interior. Transects were 100m in total length and 10m in width, with quadrats every 3 meters. Within each quadrat, we identified all trees, and measured their diameter at breast height (dbh). We classified each individual as either a seedling (height < breast height), sapling (dbh < 5cm), or mature tree (dbh > 5cm). To aid in identification of woody stems that were dead, we used a field guide specific to identification of woody stems in the winter (leafless) condition for Oklahoma (Buck 1983). When identification was not possible due to decay, we recorded the species as unknown, and it was not considered in the final analysis.

Field validation: dendrochronology

Within each field site, we used increment borers to core ten or more *Q. stellata* with a dbh > 30 cm. We did not core *Q. marilandica* trees, as they are shorter-lived (generally, < 100 years) and prone to heartwood decay, unlike the long-lived *Q. stellata*. We transported cores to the laboratory to dry and glue them to wooden mounts. Once the glue dried, we progressively sanded the surface of cores with a series of increasing grit (120, 240, 320, 400) using a belt sander. Micro-sanding of the cores was conducted by hand in the laboratory (45, 30, 15, 9 um, 3M, USA) to improve the identification of annual growth rings, and the boundary between early and latewood portions of annual growth within rings. Visual cross-dating of tree-rings was conducted using a compound microscope, after which individual rings were measured in the program WinDendro (Regent Instruments, Quebec City, QC, Canada). Raw ring-width measurements and cross-dating were validated using COFECHA (Speer 2010). Using program R package dplR (the dendrochronology program library) we de-trended ring widths using a negative exponential function to remove age-related growth effects and construct ring-width index (RWI) chronologies for each site (Bunn 2008).

Statistical analyses

We conducted statistical analysis comparing sites predicted unsuitable to those predicted suitable for field observations of mortality, density, and tree-ring data. For all tests, we pooled observations across sites such that each observation occurred at a site predicted "suitable" or "unsuitable" in the present day by our SDM. To test for differences in density between model predictions, we further grouped data by ontogeny (within model prediction). After checking for homogeneity of variances (leveneTest function, *car* package in R), we conducted a two-sample t-test for each size class (Tree, Seedling, Sapling, see above). Proportion of observed living and dead trees was compared between suitability type using a chi-squared test. For tree-ring data, we

compared RWI (pooled from all sites, by model prediction) for years of model training (1950s, n = 10 per site) to prediction (2006-2015, n=10 per site) using an ANOVA test in R (function aov() in R package '*stats*'). All statistical tests were performed in Program R, version 3.5 (R Core Team 2013).

Results

Model Results

Model mean AUC was 0.799, ±0.034, with a 10-percentile test omission of 0.1667. Model contribution was highest from four variables: mean annual temperature 36.5%, VPDmax 25.3%, precipitation of the wettest week 21.1%, and soil texture (surficial material) 10.2%. Our model predicted *Q. stellata* and *Q. marilandica* Cross Timbers co-dominance no longer suitable at 27% of the 134 sites Rice and Penfound visited in the 1950s, and saw no change at 73% of sites. Decreased suitability was observed in general at the eastern and western extremities of the Cross Timbers. No large change was observed in the central Cross Timbers (Fig. 2). By area, present-day suitability occupied just (73%) of the historically suitable area during the 1950s, a reduction of (27%).

Field Validation Results

In our field validation, we surveyed 5,978 individuals across the eight sites, of which 2,169 were *Q. marilandica* or *Q. stellata*. Our model predictions of suitability changes for Cross Timbers oaks were supported by field observations of mortality for seedlings and saplings, but not for mature trees. Seedling mortality was not observed at sites predicted suitable, while sites predicted to be unsuitable in the present day saw seedling mortality of 18.8%. Sapling results were similar, with 17.8% mortality at suitable sites, and 31.3% at unsuitable sites. There was not a significant difference between observed mature tree mortality, with 22.0% of stems dead at sites predicted suitable, and 25.4% at unsuitable sites (Fig. 3). Here, it is important to acknowledge

that percent dead is inclusive of multiple years of mortality—with dense wood and relatively slow decay, we are uncertain how many years of mortality are represented by our observation of dead, mature trees. Chi-square tests revealed that significantly more saplings ($c^2 = 4.913$, df=1, $p = 0.027$) and seedlings ($c^2 = 236.960$, $p < 0.001$) were dead at sites predicted unsuitable than sites predicted suitable, while there was no difference for mature trees ($c^2 = .288$, df=1, $p = 0.592$, Fig. 3B).

Density results also varied across ontogeny. Seedling density of *Q. marilandica* and *Q. stellata* was highest at sites predicted to remain suitable, with a mean of 6,150 stems/ha, and was significantly lower at sites predicted unsuitable 2,130 stems/ha. Sapling density was not significantly different based on model predictions (645 stems/ha suitable; 495 stems/ha unsuitable). Additionally, mature tree density was not different based on model predictions (840 stems/ha suitable, 630 stems/ha +- SE unsuitable). Seedlings density was significantly higher at suitable sites than at unsuitable sites (t-test, $p = 0.010$), while there was no significant difference for mature trees ($p=0.212$) or saplings ($p=0.564$, Fig. 3A).

Our analysis of tree-rings revealed that canopy trees at the eight study sites ranged in age from > 250 years (inner ring = 1768 C.E.) to 50 years (inner ring = 1968 C.E.). Mean sensitivity of the chronologies to climate was 0.27 for total-ring width, 0.22 for earlywood, and 0.44 for latewood chronologies respectively. When comparing the decade of model training (1950-1959) to decade of model prediction (2006-2015), there was not a significant difference in RWI for total-ring, early, or latewood chronologies (Fig. 3C).

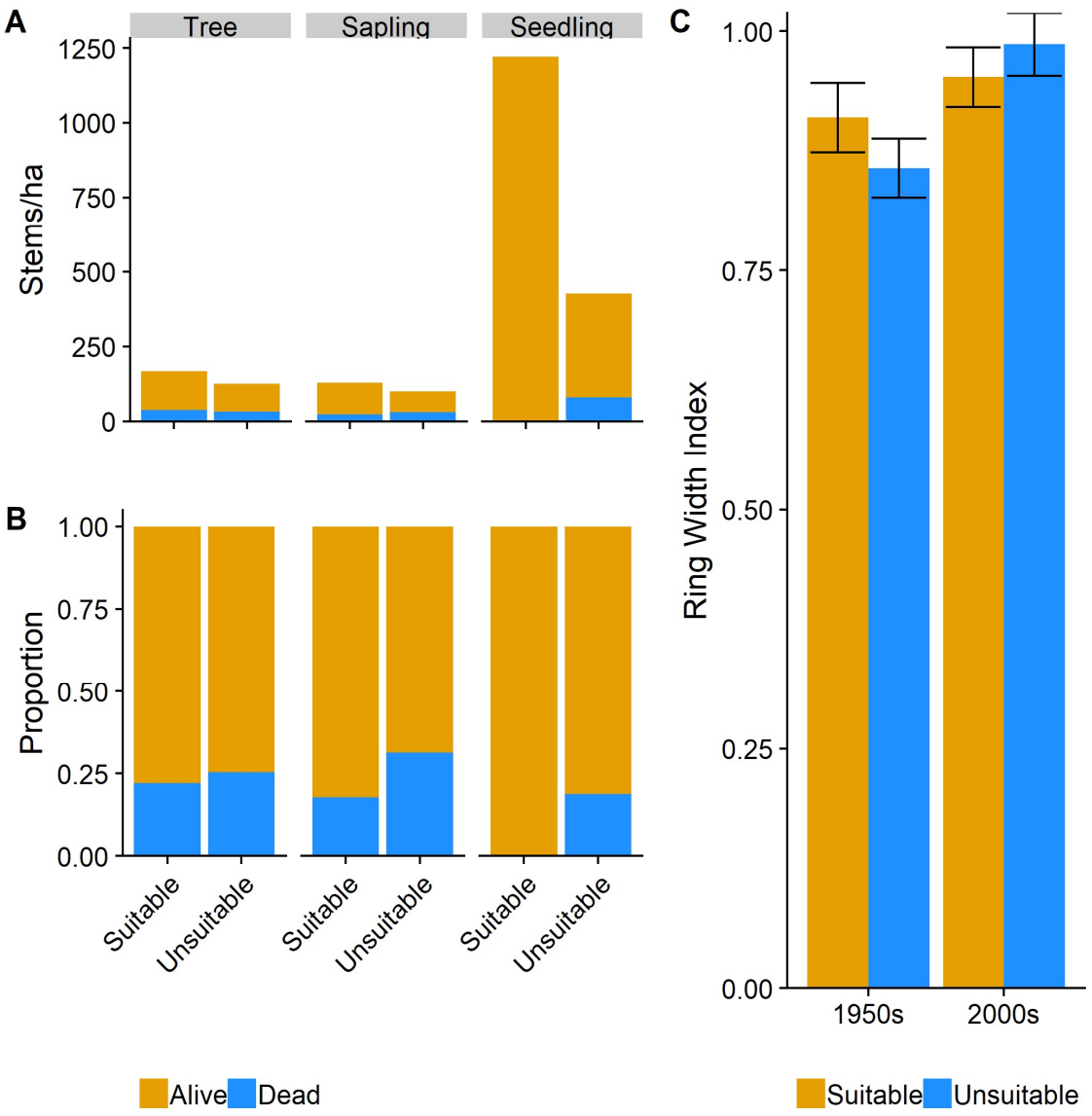

Figure 3: (A) Density of codominant oak stems, by ontogeny. Gold bars represent alive mean stem density, while blue bars represent dead mean stem density. Seedlings density was significantly higher at suitable sites than at unsuitable sites (t-test, p = 0.010), while there was no significant difference for mature trees (p=0.212) or saplings (p=0.564). (B) Proportion of stems by ontogeny, at sites predicted suitable and unsuitable. Stems are grouped by ontogeny (Tree, Sapling, Seedling), and bars for suitable/unsuitable sites are shaded with the proportion alive (gold) or dead (blue). (C) Ring-width index (RWI) was not significantly different based on site prediction for either the 1950s (model training) or 2000s (model projection) ring widths (ANOVA, F = 0.080, p = 0.778). Bar height indicates mean RWI, bar color represents model prediction (blue = predicted unsuitable, gold = predicted suitable). Error bars represent SEM.

DISCUSSION:

Our findings that SDM predictions were supported in the understory—but not in observations of mature trees—serves as a cautionary tale for interpreting SDM projections to future, novel climate scenarios. Predicting suitability in the present-day using known historic occurrence data provided a clear test of SDMs to novel climate space. Here, we built a SDM in the past, projected sixty years forward into the present, and tested model predictions with field observations. While oak seedling and sapling observed mortality were higher at sites predicted to become unsuitable for oak codominance, only seedling density varied significantly based on model predictions (Fig. 3). These findings are supported by research that has shown the earliest life stages are often the most vulnerable in forests to drought-induced mortality (Van Mantgem et al. 2009). Mature trees showed no difference in density, observed mortality, or growth. In long-lived species such as *Quercus*, this indicates that mature canopy trees can be decoupled from perturbations in their climate-envelope, as they have access to deep resource space belowground, and can store vast amounts of carbon and water for use during periods of extreme environmental stress. However, even long-lived oaks (such as the 250+yr individuals cored in this study) must eventually meet their end—and declines in recruitment (e.g., seedling density, survival) could eventually lead to long-term shifts in species distributions.

Extension & Limitations

Some systems are inherently easier to extend this work to than others. We expect that our method would be difficult to apply in systems where observations of occurrence are less complete—oak trees are conspicuous, large, and sessile—making detection and identification of individuals across large areas feasible. Cryptic species may present unique challenges, but datasets existing with any level of occurrence should be considered as opportunities to identify models that can capture change. With vast collections (e.g, herbaria, museums) that are often

georeferenced, the opportunity to put knowledge of species occurrence in the past to work is tempting. When SDMs project range shifts on the order of 50 to 100 years, we should consider the timeframe of occurrence data being used to train models. If older data are identified or available, using a past to present projection (before attempting to predict to an even further, more uncertain future climate space) will provide context to interpret model predictions.

Dusty data

In the early 1990s, advances in computing and digital storage led to an explosion in the digitization of archived scientific data. Eventually, these efforts resulted in the formation of databases to support the organization and access of this data at the global scale. Databases such as the Global Biodiversity Information Facility (GBIF) and the Botanical Information and Ecology Network (BIEN) serve this data, yet many datasets (including the Rice & Penfound dataset used in this study) remain "offline" and are dormant, potentially in dusty filing cabinets of retiring professors. Additionally, spatial biases in online repositories such as GBIF have been shown to reduce the quality of SDM outputs (Beck et al. 2014)—making spatially comprehensive historic datasets such as the present study's invaluable for SDM testing. As precise records of past species distributions, these historic data represent an opportunity to test models of species distribution in an empirical framework. While some studies have asserted that historic observations are likely less accurate in geo-referencing than contemporary, GPS located occurrences (Feng et al. 2019) and historic environmental data (such as the PRISM data used in the present study) is often also less precise (4 km^2). Thus, it is likely that historic occurrences, even if not sub-kilometer accurate, may be of great utility in testing SDMs. Using our method to train SDMs in the recent past, project them to the present day, and field-test their accuracy, dormant data may be enlisted to answer a pressing question of modern day ecology—where will species go, when environment of the present-day range changes?

Framework

Our findings suggest that SDM predictions should be interpreted alongside existing knowledge of resilience, persistence, and community dynamics when considering species distribution changes under future climate scenarios. For example, droughts in recent decades have led to shifts of dominant forest tree distributions, preceded by an absence of recruitment (Allen and Breshears 1998). With much focus on the refinement of modelling future climate and environmental conditions, we advocate for a similar focus on testing how these refinements translate to species distribution prediction utilizing the methods presented in this study. Here, we present a framework for testing SDMs (Fig. 6) that considers species distributions, climate, and disturbance data across past, present, and future conditions.

Since the early 19th century, environmental conditions are known from instrumental records at varying resolutions. Continuous global temperature data derived from instrumental measurement are available from the year 1850 C.E. (Brohan et al. 2006), while reconstructions of temperatures (e.g., tree-ring chronologies, ice-core reconstructions, marine sedimentation) can provide records > 10,000 years in the past (Marcott et al. 2013). Distributions of species during the past are documented through broad collections (e.g., museums, online databases) and also by individual studies that attempted broad-scale measurement (as in Rice and Penfound, 1959). While records of disturbance regimes are less common, evidence of disturbance are recorded in similar records as those for climate, for example by fire scars in the annual rings of trees. Also, disturbance histories have been reconstructed from field notes, journals, management plans, eyewitness interviews, newspaper articles, and other sources (Gimmi *et al*., 2008). In this way, SDMs can be trained in the past using observed data.

In the present, global monitoring of climate is available at finer resolutions than ever before, with modeling techniques providing the ability to interpolate direct measurements at yet finer

scales, with ever increasing accuracy (Felicísimo Pérez and Martín-Tardío 2017, Fick and Hijmans 2017). Similarly, methods for remote sensing of species distributions for conspicuous, immobile species such as trees have recently been developed (Fassnacht et al. 2016). For mobile species, GPS tracking and radio-transmission devices provide more detailed information on the realized niche of broadly distributed organisms than ever before (Coxen *et* al., 2017). Data is available on landscape disturbances in near real-time in the present day, via services such as the Global Fire Atlas and Global Forest Watch (Andela *et* al., 2019; Curtis *et al.,* 2018). In this way, the past and present are rich with data that are either known or observable. In contrast, the future states of environmental conditions, species distributions, and disturbance regimes are as of yet unknown and unobserved—and therefore must be predicted.

Prediction is difficult, but large teams of scientists have developed models of the Earth system that can reproduce many complex interactions to simulate global climate. These models are used to determine what future conditions may be on the planet for a given relative concentration pathway scenario. Of the future data considered, there has been perhaps the greatest effort in the modeling future climate. These models are skillful, as hindcasting with these models provides a means of testing model performance against known data. Disturbances under future conditions also are predicted with skillful models, even for dynamic processes such as wildfire (Turco *et al*., 2018). Species distribution models attempt to build future predictions based on inputs from present and past species occurrence, climate, and disturbance data. Unlike climate models, SDMs presently lack an empirical assessment of skill. Here, we have demonstrated that by building SDMs in the past, projecting to the known present state, and conducting direct field-based observations and measurements of model performance—skill of SDMs can be assessed quantitatively. We encourage future studies to adopt similar methods to provide context for assessing model predictions of future species distributions.

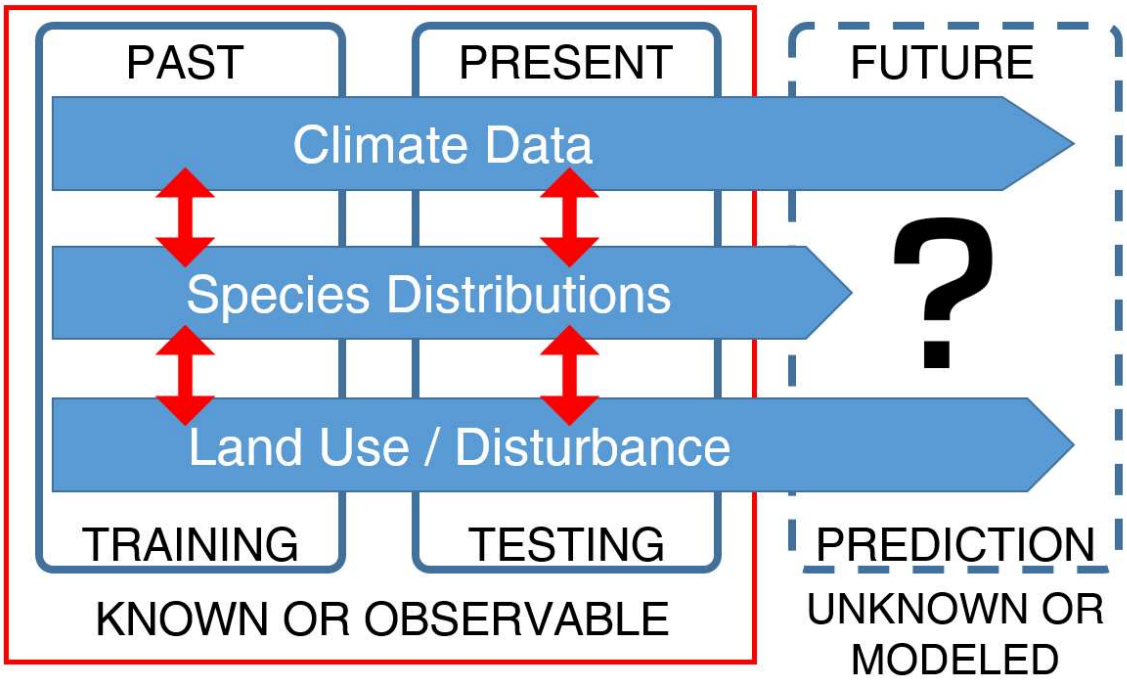

Figure 4: A conceptual diagram for testing species distribution models. Inputs to SDMs (such as Climate Data, and non-climate (e.g., Land Use/Disturbance) are available across past and present timescales. These data are also predicted into future states with models that have been quantitatively assessed for skill. Our past-to-present species distribution modeling method, paired with rigorous field validation, provides the opportunity to similarly assess model skill prior to predicting future species distributions.

Given the model predictions for a 27% reduction in area that is suitable in the present day, a natural conclusion may have been to anticipate broad collapse of oak co-dominance in the Cross Timbers during the years between 1950 and the present day. While field observations agreed with model predictions regarding the ability of these species to establish (e.g., seedlings, saplings) in areas predicted no longer suitable, the lack of response for mature trees is an important nuance that could have otherwise been missed. It is possible that during several favorable years, young trees may become established enough that rare recruitment events prolong the co-dominance of Quercus throughout much of the Cross Timbers. On the other hand, over long timescales it is possible that rare extreme events may lead to conditions that are unfavorable for even mature

trees, and that an absence of recruitment could lead to broad extirpation of *Q. stellata* and *Q. marilandica* from their former co-dominant range.

Conclusion

Predicting species distributions remains a top priority for the field of Ecology. As evidenced by rapid adoption of SDM methods (Fig. 1), interest in this field continues to grow. As projections are made to future climate scenarios, here we have demonstrated that nuance necessary for interpreting SDM results can be gathered through a novel framework that trains models in the past, and projects to a testable present, before making predictions of future species distributions. Our SDM predicted that suitable area would retract by 27% in the Cross Timbers, but field validation results provided context to this prediction—namely, that early life stages were at immediate risk, while mature trees were insensitive to model predictions. Before making management, policy, or other decisions based on SDM outputs—our framework for testing SDMs can provide the necessary context and additional confidence for the many disciplines that have adopted the use of such models.

References

Adams, H. D., G. A. Barron-Gafford, R. L. Minor, A. A. Gardea, L. P. Bentley, D. J. Law, D. D. Breshears, N. G. McDowell and T. E. Huxman (2017). "Temperature response surfaces for mortality risk of tree species with future drought." Environmental Research Letters **12**(11): 115014.

Allen, C. D. and D. D. Breshears (1998). "Drought-induced shift of a forest–woodland ecotone: rapid landscape response to climate variation." Proceedings of the National Academy of Sciences **95**(25): 14839-14842.

Allen, C. D., D. D. Breshears and N. G. McDowell (2015). "On underestimation of global vulnerability to tree mortality and forest die-off from hotter drought in the Anthropocene." Ecosphere **6**(8): art129.

Allen, C. D., A. K. Macalady, H. Chenchouni, D. Bachelet, N. McDowell, M. Vennetier, T. Kitzberger, A. Rigling, D. D. Breshears and E. T. Hogg (2010). "A global overview of drought and heat-induced tree mortality reveals emerging climate change risks for forests." Forest ecology and management **259**(4): 660-684.

Andela, N., Morton, D. C., Giglio, L., Paugam, R., Chen, Y., Hantson, S., ... & Randerson, J. T. (2019). The Global Fire Atlas of individual fire size, duration, speed and direction. Earth System Science Data, 11(2), 529-552.

Araújo, M. B. and A. T. Peterson (2012). "Uses and misuses of bioclimatic envelope modeling." Ecology **93**(7): 1527-1539.

Beck, J., M. Böller, A. Erhardt and W. Schwanghart (2014). "Spatial bias in the GBIF database and its effect on modeling species' geographic distributions." Ecological Informatics **19**: 10-15.

Bertrand, R., V. Perez and J. C. Gégout (2012). "Disregarding the edaphic dimension in species distribution models leads to the omission of crucial spatial information under climate change: the case of Quercus pubescens in France." Global Change Biology **18**(8): 2648-2660.

Box, E. O. (1981). "Predicting physiognomic vegetation types with climate variables." **45**(2): 127-139.

Breshears, D. D., H. D. Adams, D. Eamus, N. G. McDowell, D. J. Law, R. E. Will, A. P. Williams and C. B. Zou (2013). "The critical amplifying role of increasing atmospheric moisture demand on tree mortality and associated regional die-off." **4**.

Brohan, P., J. J. Kennedy, I. Harris, S. F. B. Tett and P. D. Jones (2006). "Uncertainty estimates in regional and global observed temperature changes: A new data set from 1850." Journal of Geophysical Research **111**(D12).

Brown, J. L. (2014). "SDMtoolbox: a python-based GIS toolkit for landscape genetic, biogeographic and species distribution model analyses." Methods in Ecology and Evolution **5**(7): 694-700.

Buck, P. (1983). Distribution and Identification of Woody Plants of Oklahoma in the Winter Condition, Oklahoma Academy of Sciences.

Buckley, T. N. (2019). "How do stomata respond to water status?" New Phytologist **224**(1): 21-36.

Bunn, A. G. J. D. (2008). "A dendrochronology program library in R (dplR)." **26**(2): 115-124.

Coxen, C. L., Frey, J. K., Carleton, S. A., & Collins, D. P. (2017). Species distribution models for a migratory bird based on citizen science and satellite tracking data. Global Ecology and Conservation, 11, 298-311.

Curtis, P. G., Slay, C. M., Harris, N. L., Tyukavina, A., & Hansen, M. C. (2018). Classifying drivers of global forest loss. Science, 361(6407), 1108-1111.

Desantis, R. D., S. W. Hallgren, T. B. Lynch, J. A. Burton and M. W. Palmer (2010). "Long-term directional changes in upland Quercus forests throughout Oklahoma, USA." **21**(3): 606-618.

Dietze, M. C. and P. R. Moorcroft (2011). "Tree mortality in the eastern and central United States: patterns and drivers." **17**(11): 3312-3326.

Dixon, H. H. and J. J. P. T. o. t. R. S. o. L. Joly (1895). "XII. On the ascent of sap." (186): 563-576.

Dormann, C. F., J. Elith, S. Bacher, C. Buchmann, G. Carl, G. Carré, J. R. G. Marquéz, B. Gruber, B. Lafourcade and P. J. Leitão (2013). "Collinearity: a review of methods to deal with it and a simulation study evaluating their performance." Ecography **36**(1): 27-46.

Duck, L. and J. Fletcher (1943). "A game type map of Oklahoma. A survey of the game and furbearing animals of Oklahoma." Oklahoma Department of Wildlife Conservation, Oklaho ma City, Oklahoma.

Elith, J., C. H. Graham, R. P Anderson, M. Dudík, S. Ferrier, A. Guisan, R. J Hijmans, F. Huettmann, J. R Leathwick, A. Lehmann, J. Li and L. G Lohmann (2006). "Novel methods improve prediction of species' distributions from occurrence data." Ecography **29**(2): 129-151.

Elith, J. and J. R. Leathwick (2009). "Species Distribution Models: Ecological Explanation and Prediction Across Space and Time." Annual Review of Ecology, Evolution, and Systematics **40**(1): 677-697.

Elith, J., S. J. Phillips, T. Hastie, M. Dudík, Y. E. Chee and C. J. Yates (2011). "A statistical explanation of MaxEnt for ecologists." Diversity and Distributions **17**(1): 43-57.

ESRI (2011). ArcGIS Desktop: Release 10. Redlands, CA, Environmental Systems Research Institute.

Fassnacht, F. E., H. Latifi, K. Stereńczak, A. Modzelewska, M. Lefsky, L. T. Waser, C. Straub and A. Ghosh (2016). "Review of studies on tree species classification from remotely sensed data." Remote Sensing of Environment **186**: 64-87.

Felicísimo Pérez, Á. M. and M. Á. Martín-Tardío (2017). "A method of downscaling temperature maps based on analytical hillshading for use in species distribution modelling." Cartography and Geographic Information Science: 1-10.

Feng, X., D. S. Park, C. Walker, A. T. Peterson, C. Merow and M. Papeş (2019). "A checklist for maximizing reproducibility of ecological niche models." Nature ecology & evolution **3**(10): 1382-1395.

Fettig, C. J., L. A. Mortenson, B. M. Bulaon and P. B. Foulk (2019). "Tree mortality following drought in the central and southern Sierra Nevada, California, U.S." Forest Ecology and Management **432**: 164-178.

Fick, S. E. and R. J. Hijmans (2017). "WorldClim 2: new 1-km spatial resolution climate surfaces for global land areas." International Journal of Climatology **37**(12): 4302-4315.

Gimmi, U., Bürgi, M. & Stuber, M. Reconstructing Anthropogenic Disturbance Regimes in Forest Ecosystems: A Case Study from the Swiss Rhone Valley. Ecosystems 11, 113–124 (2008).

Hall, S. A. J. Q. R. (1982). "Late Holocene paleoecology of the southern plains." **17**(3): 391-407.

Hijmans, R. J., S. E. Cameron, J. L. Parra, P. G. Jones and A. Jarvis (2005). "Very high resolution interpolated climate surfaces for global land areas." International Journal of Climatology **25**(15): 1965-1978.

Hill, R. T. (1887). "The topography and geology of the Cross Timbers and surrounding regions in northern Texas." American Journal of Science(196): 291-303.

Hoagland, B. W., I. H. Butler, F. L. Johnson and S. Glenn (1999). The Cross Timbers. Savannas, barrens, and rock outcrop plant communities of North America. R. C. Anderson, Fralish, J.S. & Baskin, J.M. Cambridge, UK., Cambridge University Press**:** 231-235.

IPCC (2014). Climate Change 2014: Impacts, Adaptation, and Vulnerability. Part A: Global and Sectoral Aspects. Contribution of Working Group II to the Fifth Assessment Report of the Intergovernmental Panel on Climate Change [Field, C.B., V.R. Barros, D.J. Dokken, K.J. Mach, M.D. Mastrandrea, T.E. Bilir, M. Chatterjee, K.L. Ebi, Y.O. Estrada, R.C. Genova, B. Girma, E.S. Kissel, A.N. Levy, S. MacCracken, P.R. Mastrandrea, and L.L. White (eds.)]. Cambridge, United Kingdom and New York, NY, USA, Cambridge University Press.

Law, D. J., H. D. Adams, D. D. Breshears, N. S. Cobb, J. B. Bradford, C. B. Zou, J. P. Field, A. A. Gardea, A. P. Williams and T. E. Huxman (2019). "Bioclimatic Envelopes for Individual Demographic Events Driven by Extremes: Plant Mortality from Drought and Warming." International Journal of Plant Sciences **180**(1): 53-62.

Marcott, S. A., J. D. Shakun, P. U. Clark and A. C. Mix (2013). "A Reconstruction of Regional and Global Temperature for the Past 11,300 Years." Science **339**(6124): 1198-1201.

Phillips, S. J., R. P. Anderson and R. E. Schapire (2006). "Maximum entropy modeling of species geographic distributions." Ecological modelling **190**(3): 231-259.

PRISM Climate Group, P. C. G. (1991). PRISM Climate Group, PRISM Climate Group, Oregon State University.

Qiao, H., J. Soberón, A. T. J. M. i. E. Peterson and Evolution (2015). "No silver bullets in correlative ecological niche modelling: insights from testing among many potential algorithms for niche estimation." **6**(10): 1126-1136.

R Core Team (2013). "R: A language and environment for statistical computing."

Rehm, E. M., P. Olivas, J. Stroud and K. J. Feeley (2015). "Losing your edge: climate change and the conservation value of range-edge populations." Ecology and Evolution **5**(19): 4315-4326.

Rice, E. L. and W. T. Penfound (1959). "The upland forests of Oklahoma." Ecology **40**(4): 593-608.

Risser, P. G. (1995). "The status of the science examining ecotones." BioScience **45**(5): 318-325.

Speer, J. H. (2010). Fundamentals of tree-ring research, University of Arizona Press.

Stringer, J. W., T. W. Kimmerer, J. C. Overstreet and J. P. Dunn (1989). "Oak mortality in eastern Kentucky." Southern Journal of Applied Forestry **13**(2): 86-91.

Thomas, C. D., A. Cameron, R. E. Green, M. Bakkenes, L. J. Beaumont, Y. C. Collingham, B. F. N. Erasmus, M. F. De Siqueira, A. Grainger, L. Hannah, L. Hughes, B. Huntley, A. S. Van Jaarsveld, G. F. Midgley, L. Miles, M. A. Ortega-Huerta, A. Townsend Peterson, O. L. Phillips and S. E. Williams (2004). "Extinction risk from climate change." Nature **427**(6970): 145-148.

Trouet, V., J. Esper, N. E. Graham, A. Baker, J. D. Scourse and D. C. Frank (2009). "Persistent Positive North Atlantic Oscillation Mode Dominated the Medieval Climate Anomaly." Science **324**(5923): 78-80.

Turco, M., Jerez, S., Doblas-Reyes, F. J., AghaKouchak, A., Llasat, M. C., & Provenzale, A. (2018). Skilful forecasting of global fire activity using seasonal climate predictions. Nature communications, 9(1), 1-9.

Van Mantgem, P. J., N. L. Stephenson, J. C. Byrne, L. D. Daniels, J. F. Franklin, P. Z. Fule, M. E. Harmon, A. J. Larson, J. M. Smith, A. H. Taylor and T. T. Veblen (2009). "Widespread Increase of Tree Mortality Rates in the Western United States." Science **323**(5913): 521-524.

Veloz, S. D., J. W. Williams, J. L. Blois, F. He, B. Otto-Bliesner and Z. Liu (2012). "No-analog climates and shifting realized niches during the late quaternary: implications for 21st-century predictions by species distribution models." Global Change Biology **18**(5): 1698-1713.

Vessella, F. and B. Schirone (2013). "Predicting potential distribution of Quercus suber in Italy based on ecological niche models: conservation insights and reforestation involvements." Forest Ecology and Management **304**: 150-161.

CHAPTER III

A HOTTER-DROUGHT FINGERPRINT ON EARTH'S FOREST MORTALITY SITES— WARMING ACCELERATES RISKS

William M. Hammond[1], A. Park Williams[2], John T. Abatzoglou[3], Henry D. Adams[4], Tamir Klein[5], Rosana López Rodríguez[6], Cuauhtémoc Sáenz-Romero[7], Henrik Hartmann[8], David D. Breshears[9], Craig D. Allen[10]

[1] Department of Plant Biology, Ecology, and Evolution, Oklahoma State University, Stillwater OK 74074 USA

[2] Lamont-Doherty Earth Observatory, Columbia University, Palisades NY, USA

[3] Management of Complex Systems, University of California, Merced CA, USA

[4] School of the Environment, Washington State University, Pullman WA, USA

[5] Department of Plant and Environmental Sciences, Weizmann Institute of Science, Rehovot, IL

[6] Sistemas Naturales e Historia Forestal, Universidad Politécnica de Madrid, Madrid, ES

[7] Instituto de Investigaciones sobre los Recursos Naturales, Universidad Michoacana de San Nicolás de Hidalgo, Morelia Michoacán, MX

[8] Department of Biogeochemical Processes, Max Planck Institute for Biogeochemistry, Jena, DE

[9] School of Natural Resources and the Environment, University of Arizona, Tucson AZ, USA

[10] U.S. Geological Survey, Fort Collins Sci. Center, New Mexico Landscapes Field Station, Los Alamos, NM 87544 USA

Author's note: This chapter is presently in review at *Nature Climate Change.*

Abstract

Earth's forests face grave challenges in the Anthropocene, including hotter droughts increasingly associated with widespread forest die-off. But despite the vital importance of

forests—especially historical forests—to global ecosystem services, their fates in a warming world remain highly uncertain. Critically missing is quantitative determination of hotter-drought climatic drivers at globally-distributed, ground-based, tree-mortality sites. We established a precisely geo-referenced global database documenting climate-induced mortality events spanning all tree-supporting biomes from 154 studies since 1970. Here we quantify a lethal global hotter-drought fingerprint from these tree-mortality sites across 675 locations encompassing 1,303 database plots. Frequency of these lethal climate conditions accelerates under projected warming, up 140% by +4°C. Our database provides initial footing for further community-developed, quantitative, ground-based monitoring of global tree mortality, immediately enabling critical predictive model validation and improved remote-sensing of mortality. This global fingerprint of lethal hotter-drought confirms many of Earth's forests are increasingly imperiled by further warming.

Main

Earth's forests threatened by hotter drought

Central to global ecosystem services and human economies, forests serve as keystone habitats for life, ecosystem drivers for the cycling of water and carbon, and both structural and economic support for human civilization[1]. Global forests are composed of >60,000 tree species[2], store nearly half of terrestrial carbon and sequester up to a third of anthropogenic annual carbon emissions[3]. Earth's historical forests (large-tree communities with dominants established before *circa* 1880) are disproportionately vital in the cycling of carbon and water, and supporting

biodiversity[4,5]. Anthropogenic change poses many threats to forests—wildfires[6], deforestation, and especially hotter drought (e.g., drought atop chronic and/or acute hotter-than-normal climate conditions[7,8]) are rapidly degrading these giants of ecosystem services on Earth. Understanding the climate conditions under which forests will persist—or die off—is urgent. Identification of a global-scale climate signal of forest mortality would indicate that climatic pressures are potentially overwhelming biome-specific differences among Earth's forests, despite vast forest structural and compositional diversity. Despite the widespread association between hotter-drought and tree mortality events (events when mortality was significantly increased from expected background rates)[9,10], it has not been possible to quantify the climate conditions triggering die-off globally without a more precise record of where and when forest mortality has occurred on Earth. Thus, the fates of forests globally—especially Earth's historical forests, relicts of recruitment under already bygone climate conditions—are uncertain in today's rapidly warming world.

Hotter drought as a climatic driver of tree mortality

Rising temperatures present a triple-threat to tree survival: amplification of atmospheric drought; intensified soil drought; and direct effects of heat stress. As temperatures rise, so too does the vapor pressure deficit (VPD, a measure of atmospheric drought, effectively air's unmet demand for moisture), accelerating water loss from both soils and trees during hotter periods, even when leaf stomata are closed[11,12]. Anthropogenic warming also is increasing the frequency, severity, and intensity of chronic soil droughts[13], and diverse evidence from tree rings to remote sensing[14] documents both antecedent warning signals of[15], and lagged growth and mortality effects from, chronic droughts[16]. Direct effects of soil drought on trees can be observed in their physiological responses—as water becomes scarce, global observations show that trees limit

water loss via stomatal control[17], and deploy diverse (e.g., stomatal, osmotic) adjustments to ameliorate the immediate effects of drought[8]. Mild drought merely reduces growth and impairs physiological functioning, but severe drought can permanently damage plant physiological function and even can become lethal when basic hydration and/or metabolic needs are not met—resulting in plant tissue collapse and eventually, death[18,19]. Although plants have some ability to acclimate to warming during drought stress[20], this acclimation potential can be overwhelmed by either sufficient chronic or acute warming and/or by a drought of sufficient severity[7,8]. Hotter droughts present a deadly dilemma to trees, where using water to ameliorate heat stress via evaporative cooling must draw from the same shrinking pool needed to survive the drought[8,19]. Thus, intensifying atmospheric drought (higher VPD) due to warming is especially costly to trees concomitantly experiencing long-term deficits in soil moisture.

Unfortunately for Earth's forests, the frequency of co-occurring extremes of heat and drought has increased over the last century primarily due to chronic warming[21], the highest-confidence and most globally-pervasive impact of climate change. At some point, chronic warming effects could become so strong that they largely overwhelm biome differences and result in amplified mortality across diverse biomes, becoming detectable with a single set of hotter-drought metrics referred to hereafter as a "global fingerprint" of climate change on tree mortality. Thus the question: is there a global fingerprint of hotter-drought triggered tree mortality, and if so, what climate conditions constitute such a global fingerprint—how hot is too hot, and how dry is too dry, relative to long-term climate? To answer these questions, we aimed to (1) establish a precisely geo-referenced database of on-the-ground tree mortality observations during hotter droughts; (2) use this database to quantify a global hotter-drought fingerprint on Earth's forests to evaluate if hotter-drought extremes are beginning to exceed the range of survivable climate across diverse forested biomes; and (3) determine the frequency of such lethal climate conditions under further warming.

Database of global tree mortality

Here we provide a global database of precisely geo-referenced observations of tree mortality associated with drought and heat (but not fire), from 154 peer-reviewed publications (Table S1) spanning five decades, including research on all of Earth's forested continents (see Methods). Our literature review and data requests resulted in a precisely geo-referenced global database of 1,303 plots where ground-based observations of drought and/or heat-induced tree mortality occurred between 1970 and 2018 (Fig. 1).

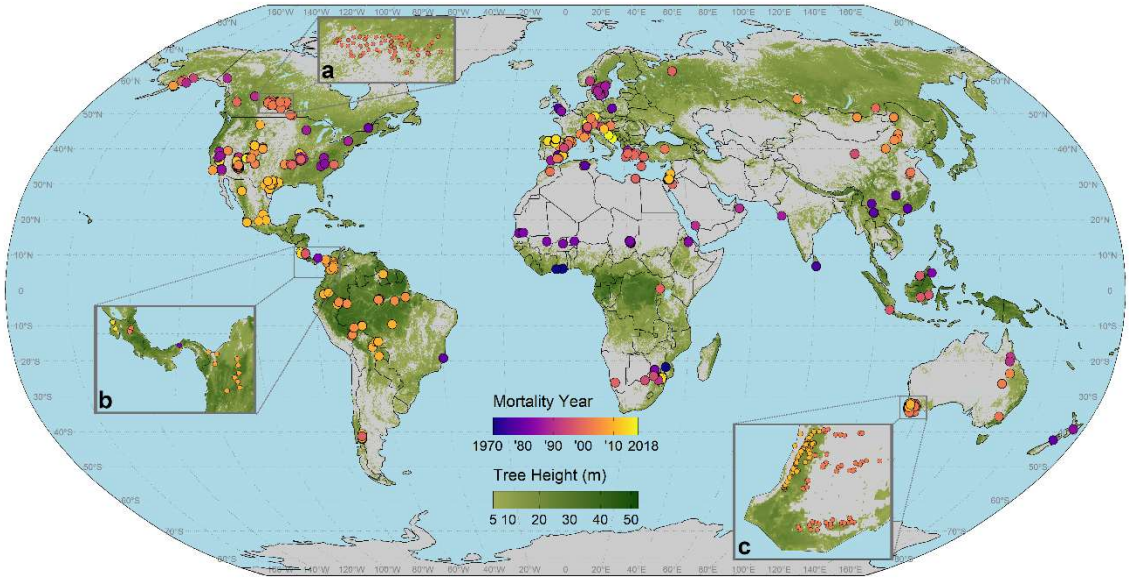

Figure 1: Global distribution of hotter-drought tree mortality plots.

Geo-referenced tree mortality plots (n= 1,303) in the database. Dots are color coded according to the year of mortality. Each point has been precisely georeferenced. Insets show examples of dense plot networks in Canada, Central America, and Southwest Australia. To illustrate the extent of global forests, a background layer in green shows canopy height[51], with darker green shading indicating taller forests. Inset (a) shows a broad plot network from aspen die-off during drought in Canada. Inset (b) shows dense plot networks in Costa Rica, Panama, and Colombia. Inset (c) shows plots in the Jarrah and Wandoo forests of Southwest Australia.

Every global biome with trees is represented by at least three plots of climate-driven tree die-off in our database (Fig. 2). Notably, an annual precipitation gradient of over 4 meters and an annual average temperature gradient of over 30 °C bounds our observations of tree mortality events. By Whittaker biome[22], woodland/shrubland accounted for 49% of plots (n=638), but it is important to note that these coarse climate-based Whittaker biomes (a useful simplification for our global approach) obscures heterogeneous forest types within single biomes; in particular, the woodland/shrubland Whittaker biome has the largest climate envelope and actually is dominated in our database by diverse closed-canopy forest types, including those composed of conifer species, aspen, oaks, and eucalypts. Temperate seasonal forest plots represented 14% of the database, followed by subtropical desert (13%), temperate grassland/desert (12%), and tropical seasonal forest/savanna (8%). Tropical rainforest, temperate rainforest, and boreal forest biomes combined contained just 4% of plots. The remainder (4 plots) fell outside of Whittaker biome space. Multiple biomes experienced mortality in 78% of the mortality years covered by our database (Fig. S5). Mortality spanned elevations from sea level to 3,488m (Fig. 2).

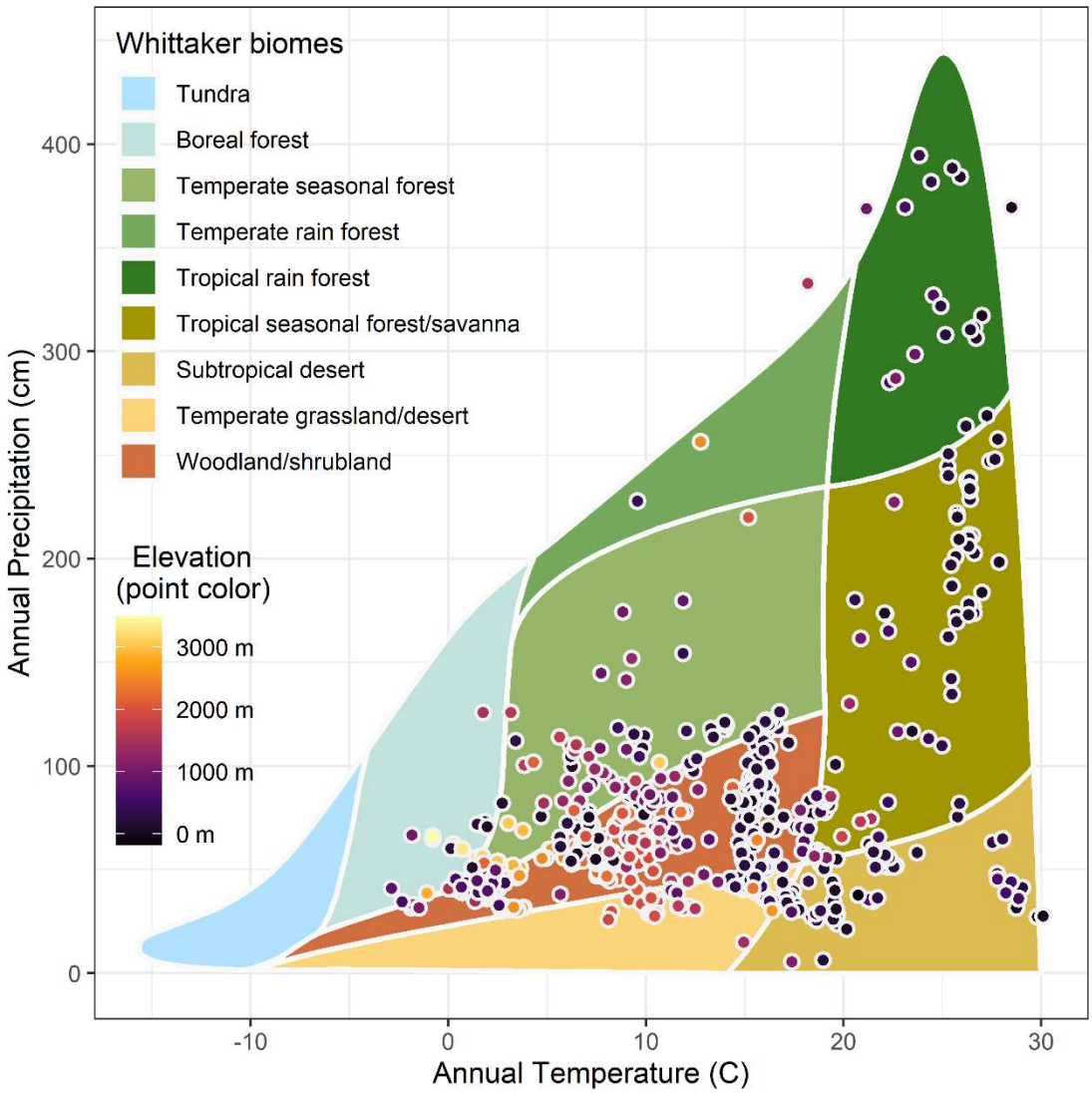

Figure 2: Biomes of global tree mortality plots.

Whittaker biome plot of database locations, showing the mean annual temperature (°C) and mean annual precipitation (cm) for all 1,303 database plots. Each point represents a plot from the global database where climate induced tree mortality happened. Notably, these mortality locations have occurred in all forested biomes, across a range of 30 °C of mean annual temperatures, and a four-meter annual precipitation gradient. Point color represents elevation, which ranged from sea level to 3,488m. Climate data for mean annual precipitation and mean annual temperature are taken from TerraClimate[23], and represent the average over 1970-2000. These data illustrate that whether a site is typically cool, warm, dry, or wet—eventually, a locally-extreme hot drought can lead to tree mortality.

Quantifying a hotter-drought fingerprint on Earth's forest mortality sites

We included 6 climate metrics related to hotter drought from TerraClimate[23], a globally gridded climate and hydroclimate product in our analysis: monthly average maximum temperature (TMAX), vapor pressure deficit (VPD), climatic water deficit (CWD), soil moisture (SOIL M), precipitation (PPT), and the Palmer Drought Severity Index (PDSI). Our 1,303 plots were encompassed within 675 locations at the spatial resolution (1/24°) of TerraClimate. To quantify climate conditions associated with heat- and drought-induced tree mortality, we identified the typically warmest and driest months (e.g. months with the highest TMAX, VPD, CWD, and lowest SOIL M, PPT, PDSI) for each variable at each location during the 71 years of available climate data (1958-2019). We calculated monthly z-scores of these climate metrics relative to the period of record (1958-2019) to facilitate comparison across the diverse climates at database sites during the years bounding mortality events (± 4 years from onset of mortality). Across the global database, climate conditions in the year of tree mortality (defined as the year mortality began, as determined from source papers or data requests) for every metric we assessed were significantly warmer and drier than the long-term mean (Fig. 3). Specifically, during the mortality year, we identified a global hotter drought fingerprint when typically warmest/driest months for TMAX, VPD, and CWD z-scores were significantly higher than the long-term average by 0.37 $\sigma \pm 0.04$, 0.30 $\sigma \pm .04$, and 0.49 $\sigma \pm .04$ SE, respectively while PPT, and with SOIL M z-scores below average by -0.21 $\sigma \pm .03$, and -0.39 $\sigma \pm 0.03$ SE, respectively. The drought index PDSI, which includes memory of water balance anomalies over several months, had the largest z-score magnitude of all variables and was significantly negative (drier), -0.73 $\sigma \pm$ 0.04 (as were 3-, 6-, 12-, and 24-month Standardized Precipitation-Evapotranspiration Index, SPEI, z-scores, a comparable climatological drought index, see Fig. S1). Mortality year TMAX anomaly was 0.55

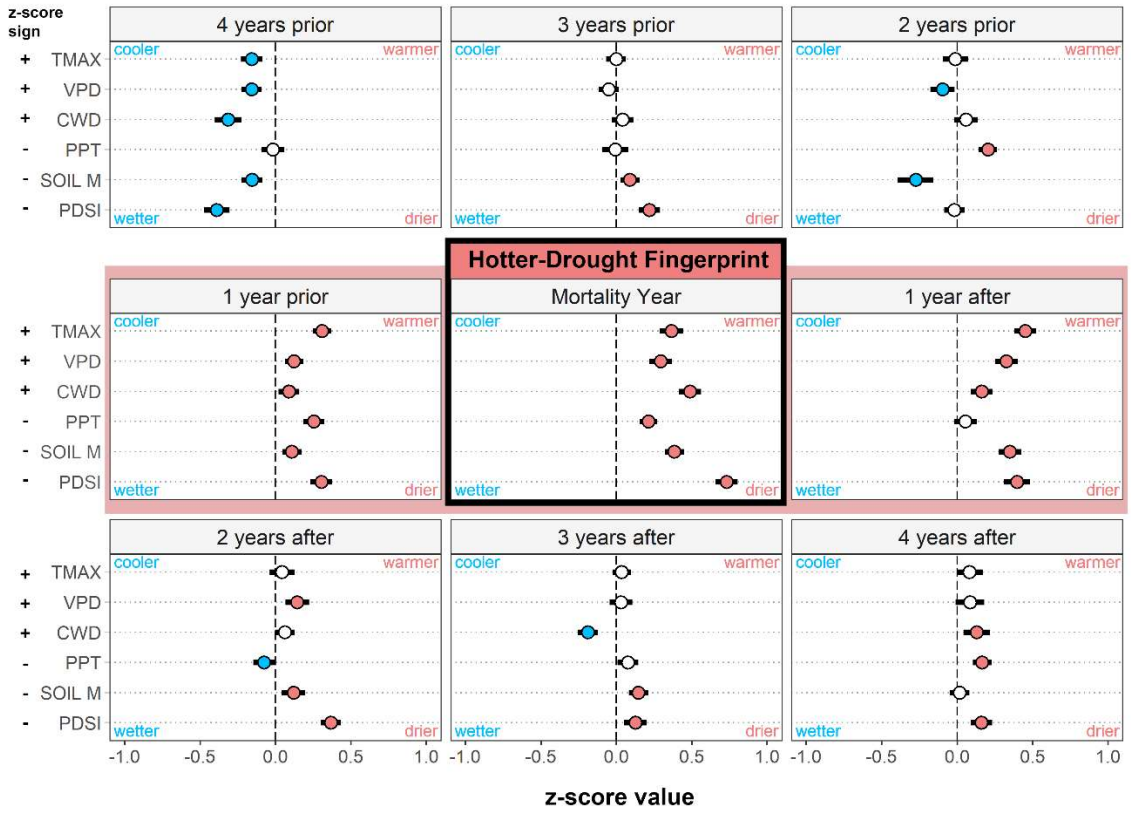

Figure 3: Hotter-drought fingerprint of global tree mortality.

The z-scores of climate variables during typically warmest/driest months (as described in text) for the 4 years preceding, 4 years following, and during the onset of tree mortality events. For each variable, circles indicate the mean z-score of all sites, while whiskers represent the 95% confidence interval of that mean. Panels are arranged chronologically from left-to-right, top-to-bottom, from 4 years before mortality began through 4 years after. During the year of onset of mortality, a *hotter-drought fingerprint* on forest mortality events was revealed as the mean of plot z-scores for all climate variables significantly shifted toward values characteristic of warmer and drier conditions, with the year prior and year following mortality showing similar, but weaker, tendencies (this three-year window, centered on the year mortality began, is outlined in red). The z-scores for TMAX, VPD, and CWD are shown with their original sign, while the sign of z-scores for PPT, SOIL M, and PDSI were flipped such that positive indicates warm/dry, and negative indicates cool/wet across all variables. Point color represents the variable condition relative to long-term (1958-2019) climate: white indicates no difference, blue is significantly wetter/cooler, and red is significantly warmer/drier.

°C (+/- 0.05 °C SE) warmer than the long-term trend. The year preceding the onset of mortality was also significantly warmer and drier for all variables, although less so than the year mortality began; the year following the onset of mortality also tended toward hotter and drier than the local 71-year average. In contrast, years preceding or following this 3-year window—centered on the

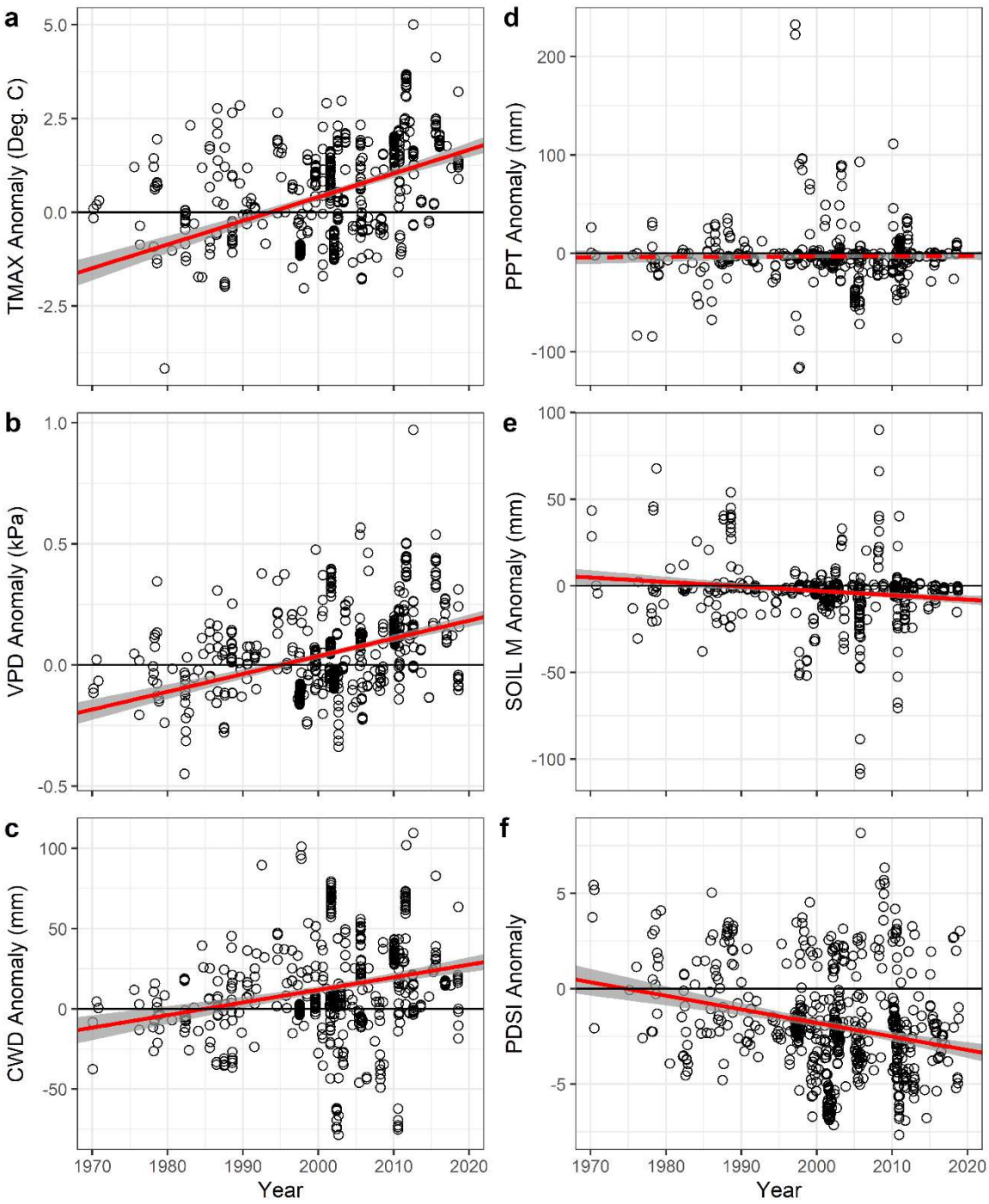

<u>Figure 4:</u> Mortality year conditions trending hotter and drier.

Trends for the six climate variables (a-f) that comprise the hotter-drought fingerprint during the typically hottest/driest months of the mortality year across all site locations. Points represent a single site's mortality year anomaly for each climate variable from the long-term (1958-2019) climate average. Trendlines shown in red are linear model fits, with grey shading representing model standard error; all regressions are significant except for precipitation (a dashed red line). In years when mortality occurred, the typically warmest and driest months' climate variables which depend on temperature have increasingly become hotter and/or drier through time.

year mortality began—had smaller differences from the long-term (1958-2019) climate (Fig. 3). This finding indicates that long-term trends (e.g., chronic warming, for further evidence see Fig. S3 and Fig. S6) are not responsible for the anomalous mortality year hotter-drought fingerprint signal (Fig. 3, center panel), as z-scores return to relatively typical long-term values two years following the onset of mortality. Importantly, this hotter-drought fingerprint was also detected in a separate biome-specific analysis, across all biomes except the tropical rain forest (see Fig. S7), where our sample of known mortality events is limited and sparse climatological instrumental records may result in higher uncertainty for the spatially interpolated global climate data used in our analysis.

Since 1970, many conditions during mortality years became warmer and drier in the study plots. In particular, TMAX, VPD, and CWD have all trended positively (Fig. 4a, b, c), while mean dry-month precipitation anomalies at the sites represented in our database have not significantly changed (Fig. 4d)—which may be partly due to the large proportion of sites which receive zero precipitation during their typically driest month. At the same time, SOIL M and PDSI have trended toward drier values over these years (Fig. 4e, f).

A hotter-drought fingerprint forewarns that tree mortality risk accelerates with warming

Under the two warming scenarios (+2 °C, +4 °C), superposed on observed climate (+0.7 °C, 1985-2015) for comparison[24], conditions are projected to become drier (more negative PDSI) and more arid (higher VPD) relative to observed climate (Fig 5a-c). We determined the number of years when each of the six variables exceeded their site-specific mortality-year heat and aridity thresholds—the local, site-specific hotter-drought fingerprint. As a result, the frequency of mortality-triggering environmental conditions increases nonlinearly with warming (Fig. 5D).

Under the observed (1985-2015) climate, which represents warming of ~0.7 ℃ above pre-industrial (1850-1879) climate levels, mortality-year conditions occurred on average 1.62 years per decade (+/- .08 SE) at sites in our analysis. Under +2 ℃ and +4 ℃ warming, mortality-year frequencies increase by 22% and 140% (1.97 +/- .07, 3.88 +/- .10 years per decade), respectively. The rate of increase in die-off conditions is best fit with an exponential curve, indicating an acceleration in mortality condition frequency with climate warming (Fig. 5D).

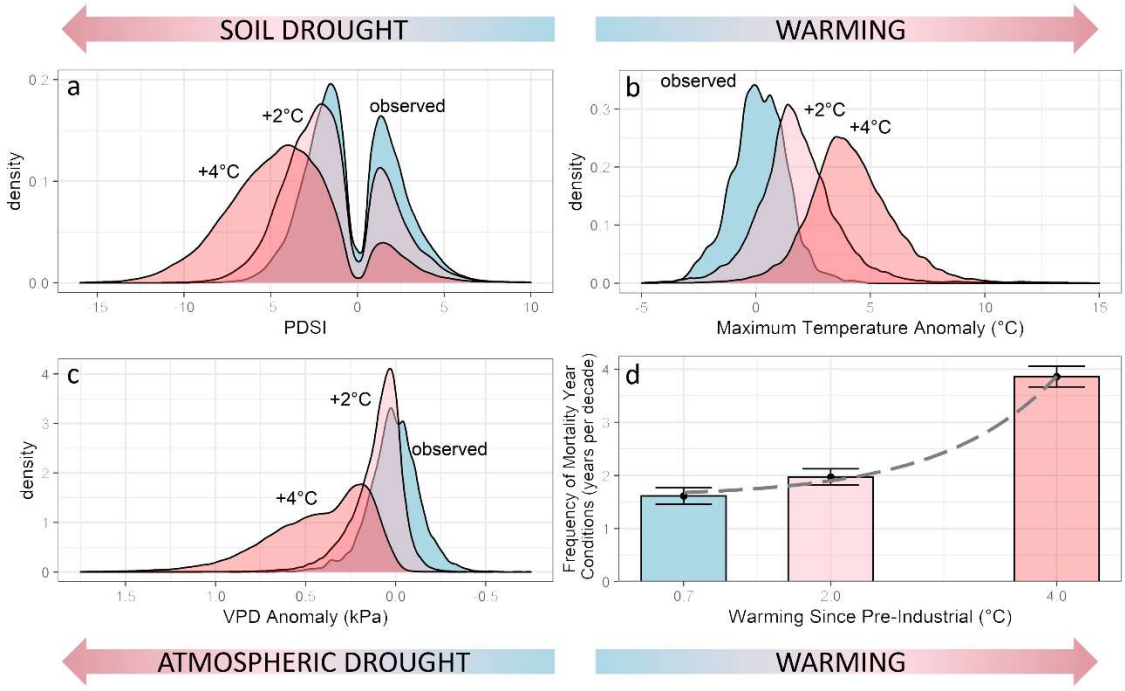

Figure 5: Warming triple-threat accelerates mortality risks.

Under two warming scenarios, leading indicators of tree mortality representing the triple-threat that warming poses to tree survival at the plots in our analysis departed from recent values toward drier (PDSI, panel a, VPD, panel c) and warmer (TMAX values, panel b) indicating further warming will shift climatic space toward that recently associated with mortality events. In panels a-c, the density distributions of PDSI, TMAX, and VPD during observed (+0.7 ℃, light blue) and warmed +2 ℃ (pink) and +4 ℃ (red) climate scenarios are shown. In panel D, barplots show the mean frequency of mortality year hotter-drought fingerprint conditions (when for a particular location, all six monthly variables met or exceeded the local hotter-drought fingerprint conditions of the mortality year), while the x-axis represents the mean warming since pre-industrial (1850-1879) climate. Error bars represent 95% confidence interval, and dashed grey line is an exponential fit.

Earth's forests imperiled by further warming

We found that Earth's forests are increasingly imperiled by further warming and drought, as the frequency of lethal climate conditions observed with recently documented global mortality events will accelerate with further warming (Fig. 5d). We quantified a global-scale hotter-drought fingerprint, representing a global climate signal for years with documented site-specific tree mortality. Climate-induced tree mortality in recent decades under hotter-drought conditions has been documented across forests from a diverse array of boundary conditions, spanning from the tropics to the boreal, from sea level to 3,500 m, and across a four-meter precipitation gradient and 30 °C of mean annual temperature. The result that the hotter-drought fingerprint is similarly evident in the year prior to reported mortality onset (Fig. 3), as well as largely echoed in the year after, may be due in part to the imprecise nature of identifying the 'onset' and duration of mortality (e.g., visual indications of mortality may lag significantly behind environmental drivers[18]). In addition, chronic drought conditions commonly span multiple years, cumulatively predisposing eventual, lagged mortality events[14–16]—consistent with our observed 'three-year hotter-drier window', centered on the nominal mortality year (Fig. 3, red shading). Although our approach does not reveal detailed mechanistic ecophysiological responses driving mortality, it exemplifies the powerful utility and practical potential of empirical approaches that tightly link direct observations of tree stress and mortality to observed climate drivers. While multiple emerging lines of evidence indicate that warming puts trees at greater risk under drought conditions[8,12,20,25–27], the quantitative hotter-drought fingerprint we identified provides robust confirmation using extensive ground-based global observations of mortality that further warming will accelerate global forest die-off. Importantly, despite the structural, compositional, and biome diversity of forests analyzed together, a global hotter-drought fingerprint emerged.

The impact of this hotter-drought fingerprint is reflected in how Earth's forests are rapidly changing already, with nearly half a billion trees having died in Texas and California alone since 2010[28,29]. Hotter central-European drought starting in 2018 has led to extensive dieback of forests that is ongoing—and of yet undetermined extent—which could lead to significant ecological transitions[30]. Other notable global tree mortality events during hotter-drought episodes include pulses of large-tree mortality since 2005 across Amazon basin tropical forests[31,32], and historically-unprecedented hotter-drought triggered dieback in Jarrah forests of SW Australia in 2011[7,27].

Although these changing forest ecosystems may benefit in various ways (e.g., increased water-use efficiency, stored non-structural carbon, etc.) from productivity gains under elevated atmospheric CO_2[33]—when soil nutrients and water are not limiting—the net effects of increasing CO_2 on the mortality of global forests during hotter drought are uncertain[8,25,34]. In particular, during hotter-drought events plant uptake of CO_2 is limited by initial closing of stomata, with CO_2 uptake eventually blocked as leaves lose turgor, followed by failure of the coupled plant water:carbon transport system which may ultimately result in death[17,19]. Thus potential amelioration of mortality risk by the ~85ppm CO_2 increase during mortality-event years in our database (1970-2018) might have been overwhelmed by the concurrent increases in TMAX anomalies observed during mortality-event years (Fig. 4), intensifying the warming triple-threat to tree survival (soil drought, atmospheric drought, and heat stress)—consistent with experimental findings combining drought, warming, and elevated CO_2[35,36]. Recent empirically based global-to-subcontinental studies have found that eCO2 acclimation in some systems may have been exhausted for decades already, with remaining ecosystems soon to follow[33,37-39]. Also, while carbon gains from increased CO_2 prior to drought may prolong plant survival by preventing carbon reserve exhaustion, an empirical global synthesis found that trees dying during drought are rarely starved of carbon[40]. Finally, evidence suggests that productivity gains from CO_2

enrichment in non-drought years also may be offset by shortening of tree lifespans from hotter-drought-amplified mortality, driving decreases in both forest carbon residence time and total storage[33,41].

Earth's historical forests are especially vulnerable

As the longest-lived organisms on Earth, trees routinely are imbued with historical and cultural significance by human societies, while also persistently sequestering carbon and amplifying local biodiversity for centuries, sometimes millennia. In contrast, extreme climate stress events occur on the scale of days to months to just a few years, and in these relatively brief periods, large old trees—exemplars of Earth's historical forests[5]—can be especially susceptible to mortality[4,42–45]. Forests will certainly persist and thrive over large areas into Earth's future, but increasingly they will have to rapidly shift in physiological function, morphology, genetics, species composition, structure, and geographic distribution in response to anticipated climate changes. Where the pace of climate change outruns the adaptive or acclimation capacities of historically-dominant tree individuals and species, additional die-off events will occur and some forests may cease to exist. In particular, the current tree communities of Earth's historical forests—which took centuries to grow to structural dominance under locally vanished climate conditions—may continue to often be most negatively affected by continued warming and drying[34,44], as novel hotter-drought extremes increasingly exceed the range of survivable climate across diverse forested biomes The expected near-term outcome is simplified tree communities, where more drought- and heat-tolerant species survive, and less tolerant species diminish or perish. In many cases, this may lead to lasting changes in vegetation composition, stature, and

spacing, where surviving woody plants in these communities do not maintain or develop the canopy structure typical of historical old-growth forests[8,25,34,46].

Underestimation of tree mortality from hotter droughts

While our projections for an increase in the frequency of climate conditions associated with historical forest die-off by up to 140% under +4 ℃ may seem severe, they are modest in comparison to some recent empirical and mechanistic process-based model predictions for catastrophic forest die-off at continental scales under hotter droughts44. We believe our projections of increasingly frequent, historically lethal climate conditions for Earth's forests may be conservative for several reasons. First, requiring that all six climate variables meet or exceed mortality year conditions, concurrently in the same year, is an exceptionally strong filter. For example, TMAX, VPD, and PDSI independently exceed mortality-year conditions under +4 ℃ in about 4 out of every 5 years (Fig. S2), whereas under the same warming scenario, all six metrics exceeded the hotter-drought fingerprint only half as often. Second, tree mortality is complex and many forest disturbance agents amplify forest die-off in the presence of global warming and hotter droughts,[25,34] including insects[45,48], pathogens[49], wind[32,50], and lightning[51]. Additionally, anthropogenic warming promotes greater wildfire activity, particularly fire extent and severity in many forests worldwide[6,52], driving further declines in Earth's forests. We also have not considered disturbance interactions among these many amplifying and synergistic agents of tree mortality[50,53], but conversely we also acknowledge that thinning from either climate-triggered mortality, or that associated with these synergistic agents, may partially buffer against future losses. Third, our findings indicate that climate anomalies of mortality years are trending towards

even hotter and drier conditions (Fig. 4, but see also that mortality-year warming outpaces the all-years warming trend, Fig. S3), concurrent with any ongoing acclimation to temperature and/or CO2 fertilization. Yet the potential for tree species to acclimate to ongoing climate warming, even with increasing atmospheric CO2 concentrations, is not unlimited—and when exhausted—forest die-off may rapidly accelerate[8,37]. Recent empirical studies using regional to global observations of vegetation suggest further acclimation may be locally exhausted, and globally limited in as soon as a decade[37,38]. Since projected warmer climate conditions include unprecedented extremes of hotter drought for which there are no observed analogs, the potential for crossing historically unknown tipping-point climatic stress thresholds may increase, further amplifying tree mortality[25]. Fourth, our analysis of mortality-year frequency uses monthly climate data, yet important drivers can occur on longer (e.g., drought[15]), and shorter (e.g., heatwave[7,27]) timescales. For example, the four-year-prior signal of cooler/wetter climate (Fig. 3) may reflect favorable pre-drought conditions promoting structural overshoot of trees, which could amplify dieback and mortality risk during subsequent years of hotter-drought[46].

Roadmap for research enabled by a quantitative ground-based global database

Our hotter-drought fingerprint was consistent across all biomes except the tropical rain forest (Fig. S7) — despite published direct observations of hotter drought as a driver of tree mortality at these tropical rainforest sites[31,32], perhaps because both mortality events and climatic instrumental observations are sparse in this biome, inflating uncertainty. This global coherence of our empirically quantified hotter-drought fingerprint may provide immediate improvements for representing tree mortality in models of the Earth system, while also enabling diverse future analyses. Although global in geographic extent, our database is limited by the availability of peer-

reviewed, ground-based empirical studies of climate-induced tree mortality, and thus only sparsely covers some regions, particularly large portions of boreal and tropical forests. Despite this and some other limitations, our database represents the first globally-distributed dataset with precisely geo-referenced sites where ground-based heat- and drought-induced tree mortality has been documented. Importantly, our use of this database to quantify a global hotter-drought fingerprint of tree mortality illustrates the potential for rapid progress in empirical modeling of forest mortality drivers and thresholds at spatial scales from local to global, where direct observations of forest responses to climate stress can help identify and quantify mortality drivers. Toward the goal of fostering further rapid community development of many more such direct observations of climate-induced forest stress and tree mortality world-wide—with methods ranging from local ground-based sites to synoptic remote-sensing—this database immediately will be served as an open-access resource at *tree-mortality.net*, a website associated with the International Union of Forest Research Organizations (IUFRO) task force on monitoring global tree mortality patterns and trends (https://www.iufro.org/science/task-forces/tree-mortality-patterns). The complete database—along with an interactive version of Figure 1 from this paper—will allow users to zoom in on dense plot networks, with direct links to the supporting literature for each point. This online database includes the reference for each plot, its precise coordinates, dominant species, associated biotic agents, and the year of mortality onset. To further update and rapidly increase the quantity and spatial representativeness of global tree mortality observations, ongoing on-line contributions from diverse observer groups, ranging from practicing foresters and field ecologists to remote-sensing scientists, can be integrated into the website in near-real-time via a user-friendly entry form.

As the largest set of ground-truthed observations of drought- and heat-induced tree mortality, this database can immediately aid in validating remote-sensing technologies for eventual synoptic monitoring in near-real-time of tree mortality (which could then feed back into the database).

Additional groups to benefit from the database are those interested in climate and physiological mechanisms of tree mortality, including the connected fates of all forest-dependent life[4,27], with an aim toward improving the representation of climate-induced tree mortality representations in Earth system models. Related future research opportunities associated with this initial online database include:

(1) identify additional chronic (e.g., seasonal to decadal) and acute (daily to weekly) climatic signals of tree mortality, including through analyses which quantitatively consider antecedent and lagging factors, and duration of drought stress;

(2) synthesize mortality observations from extensive forestry plot inventory networks, to increase spatial representation for the global climate signal of tree mortality;

(3) apply remote-sensing approaches to mortality detection using this spatially precise (and sometimes plot-dense) database for ground-truthing, to determine the full spatial extent of known mortality events, and aid in ongoing monitoring of forest stress and tree mortality events in near-real-time;

(4) benchmark state-of-the-art Earth system models via hindcasting, to assess accuracy of tree mortality event representation— and importantly also across spatial resolutions (as in Fig. S4) at which these planetary models operate;

(5) develop approaches to understand potentially unique features and drivers of hotter-drought mortality in tropical rain forests, the single biome in which our global approach did not reveal a strong hotter-drought fingerprint; and

(6) investigate how the severity of forest die-off events will respond to further warming.

Future challenges for Earth's forests and societies under hotter drought

In conclusion, our findings reveal the emergence of a global acceleration of lethal climate conditions, associated with recent forest mortality events under further warming. Earth's historical forests in particular face a challenging future, including dramatic changes in the extent, composition, age, and structure of these unique forests, with planetary-scale consequences for biodiversity and the cycling of water and carbon. Although forests often are invoked as an important part of the solution to the present global climate crisis, their role as carbon sinks in mitigating climate change depends upon their ability to survive further warming[9,33,53]—which our global hotter-drought fingerprint identifies as an imminent threat. Importantly, our findings show that limiting warming to +2 ℃ over pre-industrial levels could reduce the frequency of these lethal climate conditions associated with observed tree mortality events to less than half that predicted at +4 ℃. Efforts to protect the world's climate from excessive warming likely will be decisive in determining the future of many of Earth's forests.

Methods:

Literature review methods

We reviewed the references from four recent progressively updated reviews of drought and heat-induced tree mortality[1,9,10,25] which included references to 209 peer-reviewed studies documenting drought and heat induced tree mortality. Additionally, we reviewed 21 recent peer-reviewed studies not included in those prior reviews. Studies were included in the database when they met the following conditions: 1) the study had on-the-ground observations of pulses of tree mortality (e.g., events where mortality was significantly increased from expected background rates). 2) the study attributed the mortality to a climatic driver of heat, drought, or their combination. 3) the study contained either precise coordinates (within a kilometer) or a site description, map, or other means of accurate geolocation. To identify the year that significant tree mortality began for a site, we used the authors' assessment (as described in their paper, or communicated during data request). Of the 230 papers, 154 met our criteria and were included in the global database (Table S1).

Precise Georeferencing

Georeferencing was done in one of two ways: either a paper contained precise coordinates for the location of plots with dead trees, or we submitted a data request to the paper's author seeking coordinates, plot descriptions, and accompanying mortality data. Of the 1,303 plots included in

our database, 248 had precise location information listed in the publication (or associated supplemental materials) while 1,055 locations were obtained via e-mailed data requests to authors of the studies. When mortality was reported as a percentage, we determined 'higher-than-expected' mortality based on authors' expertise of their study system. Often, "standing dead" of 15% or greater was used, as 2-3% annual background mortality rates accumulated for up to five years would not be expected to exceed this threshold. Of the 76 excluded studies, most were remote-sensing studies (e.g., aerial photographs, aerial observer mapping, satellite or airplane-borne multispectral sensors) or extensive forestry plot inventory networks (e.g., USFS FIA, EU NFIs), where precise geolocation and attribution of mortality to drought and/or heat were not possible. To place these broadly distributed mortality sites in the context of global forests, we plotted our database (in Fig. 1) along with global canopy cover of 5 m or higher [54].

Historical Climate data

Climate data for our study came from TerraClimate, a globally gridded (1/24-degree, or ~4 km) product of climate and hydroclimate[23]. As the spatial resolution of the climate data was more coarse than the spatial resolution of our database, we filtered our 1,303 plots with a spatial grid of TerraClimate's resolution, such that 675 unique locations were included in the final analysis, to avoid over-representation of dense plot networks in our analysis. We considered 6 monthly TerraClimate variables from 1958 through 2019: mean daily maximum temperature (TMAX), vapor pressure deficit (VPD), climatic water deficit (CWD), soil moisture (SOIL M), precipitation (PPT), and the Palmer Drought Severity Index (PDSI). We additionally considered the 12-month Standardised Precipitation-Evapotranspiration Index (SPEI), calculated from reference evapotranspiration (PET) calculated using the Penman-Monteith approach and PPT[55].

Additionally, we used mean annual precipitation and mean annual temperature data from TerraClimate, from the period 1970-2000, to calculate the Whittaker biome classification [22] of all 1,303 plots in our database using R package 'plotbiomes'[56]. We acquired elevation data using R package 'elevatr'[57].

Climate warming data

We also considered projected climate for two pseudo-global warming scenarios that perturb TerraClimate data for 1985-2015 with projections commensurate with global mean temperature +2 ℃ and +4 ℃ above pre-industrial (1850-1879) levels[24]. Briefly, these warming scenarios use a pattern-scaling approach that scales local changes and variance in monthly climate relative to changes in global mean temperature. These changes are then superposed to 1985-2015 data to provide time series data comparable with the observational record; we additionally apply an empirical correction to PET calculations that account for enhanced water use efficiency and enhanced surface resistance to transpiration losses[58].

Statistical methods for historical data

For each climate variable (TMAX, VPD, CWD, SOIL M, PPT, PDSI, we calculated the anomaly (for example, TMAX of the warmest month in the year of mortality - TMAX average for the 71 values of the same month). To provide cross-comparison between metrics with different scales and across disparate climates, anomalies were standardized into z-scores, such

that time series had a mean of 0 and a standard deviation of 1 based on using the entire period of record 1958-2019.

We quantified the global signal of mortality by calculating the mean and 95% confidence interval of z-scores for all 675 sites during the year of mortality. To assess the antecedent and lagging conditions for this climate signal, we calculated anomalies and z-scores for the 4 years prior and 4 years following mortality for each plot, and calculated mean and 95% CI's as during the mortality year. We expected this nine-year period, centered on the mortality year (the response for which provides the hotter-drought fingerprint), to include conditions sufficiently prior to mortality (4 years before) to represent normal conditions. As we could only identify the initial year of mortality (studies rarely persist for the years required to determine if elevated mortality has ceased), we investigated the lagging years to see if the climatic signal of tree mortality persisted beyond the mortality year, as legacy effects have been reported following intense droughts[16]. We conducted linear regressions for the year of mortality and each variable's anomaly to determine if anomalies during extreme conditions the year of mortality were increasing, decreasing, or remained unchanged through time

Statistical methods for warming scenarios

We first calculated for each site the number of years during observed (1985-2015) climate in which the local mortality-year threshold conditions (that is, years when all six climate variables met or exceeded the mortality year conditions during that site's typically warmest/driest months). We repeated this with +2 °C and +4 °C warming scenarios. We summarized the frequency of annually concurrent threshold conditions per decade for all sites under historic, +2 °C, and +4 °C climate conditions (Fig. 5D).

Acknowledgements

We wish to thank Amanda Schwantes, Ted Hogg, Niels Brouwers, George Matusick, Kenneth Feeley, Nate Stephenson, Adrian Das, Joseph Ganey, Maxime Cailleret, Timothy Assal, Patrick Gonzalez, Ted Feldpausch, Erika Gómez-Pineda, and Oscar Trejo-Ramírez for substantial database contributions and assistance in identifying plots suitable for addition to the database. Additionally we extend our gratitude to the RAINFOR and ForestPlots.net team for their contributions. W.M.H. was supported by NSF GRFP #1-653428. H.D.A. was supported by the NSF Division of Integrative Organismal Systems, Integrative Ecological Physiology Program (IOS-1755345), and USDA National Institute of Food and Agriculture (NIFA), McIntire Stennis project WNP00009. C.S.R. was supported by the Coordinación de la Investigación Científica, Universidad Michoacana de San Nicolás de Hidalgo, and the Monarch Butterfly Fund (Madison, WI, USA). D.D.B. was supported by NSF (DEB-1550756, DEB-1824796, DEB-1925837), USGS SW Climate Adaptation Science Center (G18AC00320) USDA NIFA McIntire Stennis ARZT-1390130-M12-222, and a Murdoch University Distinguished Visiting Scholar award. C.D.A. was supported by the U.S. Geological Survey's Ecosystems mission area and Land Resources Research & Development program.

Author contributions

W.M.H. and C.D.A. designed and collected the data for the georeferenced database. W.M.H. conceived and conducted the climate analysis, with C.D.A, A.P.W., H.D.A., and J.T.A. providing substantial input. C.D.A., R.L.R., C.S.R., H.H., and T.K. all contributed significant data directly to the database. W.M.H., D.D.B., and C.D.A. wrote the manuscript, with significant input and contribution from all coauthors.

References

1. IPCC. Climate Change 2014: Impacts, Adaptation, and Vulnerability. Part A: Global and Sectoral Aspects. Contribution of Working Group II to the Fifth Assessment Report of the Intergovernmental Panel on Climate Change [Field, C.B., V.R. Barros, D.J. Dokken, K.J. Mach, M.D. Mastrandrea, T.E. Bilir, M. Chatterjee, K.L. Ebi, Y.O. Estrada, R.C. Genova, B. Girma, E.S. Kissel, A.N. Levy, S. MacCracken, P.R. Mastrandrea, and L.L. White (eds.)]. (Cambridge University Press, 2014).
2. Beech, E., Rivers, M., Oldfield, S. & Smith, P. P. GlobalTreeSearch: The first complete global database of tree species and country distributions. J. Sustain. For. **36**, 454–489 (2017).
3. Pan, Y. et al. A Large and Persistent Carbon Sink in the World's Forests. Science **333**, 988–993 (2011).
4. Lindenmayer, D. B. & Laurance, W. F. The ecology, distribution, conservation and management of large old trees: Ecology and management of large old trees. Biol. Rev. **92**, 1434–1458 (2017).
5. Lutz, J. A. et al. Global importance of large-diameter trees. Glob. Ecol. Biogeogr. **27**, 849–864 (2018).
6. Bowman, D. M. et al. Vegetation fires in the Anthropocene. Nat. Rev. Earth Environ. 1–16 (2020).
7. Matusick, G. et al. Chronic historical drought legacy exacerbates tree mortality and crown dieback during acute heatwave-compounded drought. Environ. Res. Lett. **13**, 095002 (2018).
8. Brodribb, T. J., Powers, J., Cochard, H. & Choat, B. Hanging by a thread? Forests and drought. Science **368**, 261–266 (2020).
9. Allen, C. D. et al. A global overview of drought and heat-induced tree mortality reveals emerging climate change risks for forests. For. Ecol. Manag. **259**, 660–684 (2010).
10. Hartmann, H. et al. Research frontiers for improving our understanding of drought-induced tree and forest mortality. New Phytol. **218**, 15–28 (2018).
11. Breshears, D. D. et al. The critical amplifying role of increasing atmospheric moisture demand on tree mortality and associated regional die-off. **4**, (2013).
12. Williams, A. P. et al. Temperature as a potent driver of regional forest drought stress and tree mortality. Nat. Clim. Change **3**, 292–297 (2013).
13. Cook, B. I. et al. Twenty-First Century Drought Projections in the CMIP6 Forcing Scenarios. Earths Future **8**, (2020).
14. Kannenberg, S. A., Schwalm, C. R. & Anderegg, W. R. L. Ghosts of the past: how drought legacy effects shape forest functioning and carbon cycling. Ecol. Lett. **23**, 891–901 (2020).
15. Cailleret, M. et al. Early-Warning Signals of Individual Tree Mortality Based on Annual Radial Growth. Front. Plant Sci. **9**, (2019).
16. Trugman, A. T. et al. Tree carbon allocation explains forest drought-kill and recovery patterns. Ecol. Lett. **21**, 1552–1560 (2018).

17. Martin-StPaul, N., Delzon, S. & Cochard, H. Plant resistance to drought depends on timely stomatal closure. Ecol. Lett. **20**, 1437–1447 (2017).

18. Hammond, W. M. et al. Dead or dying? Quantifying the point of no return from hydraulic failure in drought-induced tree mortality. New Phytol. (2019) doi:10.1111/nph.15922.

19. Martinez-Vilalta, J., Anderegg, W. R. L., Sapes, G. & Sala, A. Greater focus on water pools may improve our ability to understand and anticipate drought-induced mortality in plants. New Phytol. **223**, 22–32 (2019).

20. Teskey, R. et al. Responses of tree species to heat waves and extreme heat events. Plant Cell Environ. **38**, 1699–1712 (2015).

21. Zscheischler, J. & Seneviratne, S. I. Dependence of drivers affects risks associated with compound events. Sci. Adv. **3**, e1700263 (2017).

22. Whittaker, R. H. Communities and ecosystems. Communities Ecosyst. (1970).

23. Abatzoglou, J. T., Dobrowski, S. Z., Parks, S. A. & Hegewisch, K. C. TerraClimate, a high-resolution global dataset of monthly climate and climatic water balance from 1958–2015. Sci. Data **5**, 170191 (2018).

24. Qin, Y. et al. Agricultural risks from changing snowmelt. Nat. Clim. Change **10**, 459–465 (2020).

25. Allen, C. D., Breshears, D. D. & McDowell, N. G. On underestimation of global vulnerability to tree mortality and forest die-off from hotter drought in the Anthropocene. Ecosphere **6**, art129 (2015).

26. Adams, H. D. et al. Temperature response surfaces for mortality risk of tree species with future drought. Environ. Res. Lett. **12**, 115014 (2017).

27. Ruthrof, K. X. et al. Subcontinental heat wave triggers terrestrial and marine, multi-taxa responses. Sci. Rep. **8**, (2018).

28. Moore, G. W. et al. Tree mortality from an exceptional drought spanning mesic to semiarid ecoregions. **26**, 602–611 (2016).

29. Fettig, C. J., Mortenson, L. A., Bulaon, B. M. & Foulk, P. B. Tree mortality following drought in the central and southern Sierra Nevada, California, U.S. For. Ecol. Manag. **432**, 164–178 (2019).

30. Schuldt, B. et al. A first assessment of the impact of the extreme 2018 summer drought on Central European forests. Basic Appl. Ecol. **45**, 86–103 (2020).

31. Feldpausch, T. R. et al. Amazon forest response to repeated droughts: AMAZON FOREST RESPONSE TO DROUGHTS. Glob. Biogeochem. Cycles **30**, 964–982 (2016).

32. Esquivel-Muelbert, A. et al. Tree mode of death and mortality risk factors across Amazon forests. Nat. Commun. **11**, (2020).

33. Walker, A. P. et al. Integrating the evidence for a terrestrial carbon sink caused by increasing atmospheric CO 2. New Phytol. (2020) doi:10.1111/nph.16866.

34. McDowell, N. G. et al. Pervasive shifts in forest dynamics in a changing world. Science **368**, eaaz9463 (2020).

35. Duan, H. et al. Elevated CO_2 does not ameliorate the negative effects of elevated temperature on drought-induced mortality in Eucalyptus radiata seedlings: Mortality under rising CO_2 and temperature. Plant Cell Environ. **37**, 1598–1613 (2014).

36. Birami, B. et al. Hot drought reduces the effects of elevated CO_2 on tree water-use efficiency and carbon metabolism. New Phytol. **226**, 1607–1621 (2020).

37. Duffy, K. A. et al. How close are we to the temperature tipping point of the terrestrial biosphere? Sci. Adv. 7, eaay1052 (2021).

38. Belmecheri, S. et al. Precipitation alters the CO 2 effect on water-use efficiency of temperate forests. Glob. Change Biol. gcb.15491 (2021) doi:10.1111/gcb.15491.

39. Peñuelas, J. et al. Shifting from a fertilization-dominated to a warming-dominated period. Nat. Ecol. Evol. 1, 1438–1445 (2017).

40. Adams, H. D. et al. A multi-species synthesis of physiological mechanisms in drought-induced tree mortality. Nat. Ecol. Evol. **1**, 1285–1291 (2017).

41. Yu, K. et al. Pervasive decreases in living vegetation carbon turnover time across forest climate zones. 6 (2019).

42. Mcdowell, N. G. & Allen, C. D. Darcy's law predicts widespread forest mortality under climate warming. Nat. Clim. Change **5**, 669–672 (2015).

43. Rowland, L. et al. Death from drought in tropical forests is triggered by hydraulics not carbon starvation. Nature **528**, 119–122 (2015).

44. Bennett, A. C., McDowell, N. G., Allen, C. D. & Anderson-Teixeira, K. J. Larger trees suffer most during drought in forests worldwide. Nat. Plants **1**, 15139 (2015).

45. Stephenson, N. L., Das, A. J., Ampersee, N. J., Bulaon, B. M. & Yee, J. L. Which trees die during drought? The key role of insect host-tree selection. J. Ecol. **107**, 2383–2401 (2019).

46. Jump, A. S. et al. Structural overshoot of tree growth with climate variability and the global spectrum of drought-induced forest dieback. Glob. Change Biol. **23**, 3742–3757 (2017).

47. McDowell, N. G. et al. Multi-scale predictions of massive conifer mortality due to chronic temperature rise. Nat. Clim. Change **6**, 295 (2016).

48. Anderegg, W. R. et al. Tree mortality from drought, insects, and their interactions in a changing climate. New Phytol. **208**, 674–683 (2015).

49. Oliva, J., Stenlid, J. & Martínez-Vilalta, J. The effect of fungal pathogens on the water and carbon economy of trees: implications for drought-induced mortality. New Phytol. **203**, 1028–1035 (2014).

50. Seidl, R. et al. Forest disturbances under climate change. Nat. Clim. Change **7**, 395–402 (2017).

51. Yanoviak, S. P. et al. Lightning is a major cause of large tree mortality in a lowland neotropical forest. New Phytol. **225**, 1936–1944 (2020).

52. Higuera, P. E. & Abatzoglou, J. T. Record-setting climate enabled the extraordinary 2020 fire season in the western United States. Glob. Change Biol. (2020) doi:10.1111/gcb.15388.

53. Anderegg, W. R. L. et al. Climate-driven risks to the climate mitigation potential of forests. Science **368**, eaaz7005 (2020).

54. Simard, M., Pinto, N., Fisher, J. B. & Baccini, A. Mapping forest canopy height globally with spaceborne lidar. J. Geophys. Res. **116**, G04021 (2011).

55. Beguería, S., Vicente-Serrano, S. M. & Beguería, M. S. Package 'SPEI'. (2017).

56. Valentin, S. & Levin, S. plotbiomes: Plot Whittaker biomes with ggplot2. R package version 0.0.0.9001. (2020).

57. Hollister, J. & Shah, T. elevatr: Access elevation data from various APIs. Retrieved Httpgithub Comusepaelevatr (2017).

58. Kruijt, B., Witte, J.-P. M., Jacobs, C. M. J. & Kroon, T. Effects of rising atmospheric CO2 on evapotranspiration and soil moisture: A practical approach for the Netherlands. **349**, 257–267 (2008).

CHAPTER IV

DEAD OR DYING? QUANTIFYING THE POINT OF NO RETURN FROM HYDRUALIC FAILURE IN DROUGHT-INDUCED TREE MORTALITY.

Hammond, William M. [1], Yu, Kailiang.L. [2], Wilson, Luke A. [1,3], Will, Rodney E. [3], Anderegg, William R.L. [2], and Adams, Henry D[1].

[1]Plant Biology, Ecology and Evolution, Oklahoma State University, Stillwater, OK
[2]School of Biological Sciences, University of Utah, Salt Lake City, UT
[3]Department of Natural Resource Ecology and Management, Oklahoma State University, Stillwater, OK

Author's note: This chapter was published in *New Phytologist* May, 2019. doi: 10.1111/nph.15922.

Abstract

Determining physiological mechanisms and thresholds for climate-driven tree die-off could help improve global predictions of future terrestrial carbon sinks. We directly tested for the lethal threshold in hydraulic failure—an inability to move water due to drought-induced xylem embolism—in a pine sapling experiment.

In a greenhouse experiment, we exposed loblolly pine (Pinus taeda) saplings (n=83) to drought-induced water stress ranging from mild to lethal. Before re-watering to relieve drought stress, we measured native hydraulic conductivity and foliar color change. We monitored all measured individuals for survival or mortality.

We found a lethal threshold at 80% loss of hydraulic conductivity—a point of hydraulic failure beyond which it is more likely trees will die, than survive, and describe mortality risk across all levels of water stress. Foliar color changes lag hydraulic failure—best predicting when trees have been dead for some time, rather than when they are dying.

Our direct measurement of native conductivity, while monitoring the same individuals for survival or mortality, quantifies a continuous probability of mortality risk from hydraulic failure. Predicting tree die-off events and understanding mechanism requires knowledge not only of when trees are dead, but when they begin dying—having passed the point of no return.

Introduction

Earth is undergoing rapid shifts in ecosystem structure and composition due to an unprecedented rate of warming accompanied by increased variability in precipitation driven by anthropogenic climate change (IPCC, 2014). Forests in many regions around the world have experienced elevated rates of tree mortality and episodes of widespread, regional forest die-off (Allen *et al.*, 2010). Trees provide important ecosystem services, including erosion prevention, hydrologic balance, and maintaining biodiversity (Anderegg *et al.*, 2013; Hartmann *et al.*, 2018a; Morillas *et al.*, 2017), and also dominate terrestrial carbon sequestration, contributing more to carbon sink strength per land area than any other vegetation type (Bonan, 2008). The fate of feedbacks in carbon exchange between forests and the atmosphere under a changing climate remains one of the largest uncertainties in projecting future climate change (Friedlingstein *et al.*, 2006; Friedlingstein *et al.*, 2014; Friend *et al.*, 2014) . Despite the importance of forest die-off, predicting when and where it will occur in response to climate remains a challenge for vegetation modeling. Development of process-based models that simulate physiological mechanisms of

stress and mortality may be the best solution for prediction of rapid, non-linear tree mortality events under future climate scenarios that are not analogous to current climate conditions (Allen *et al.*, 2010; McDowell *et al.*, 2011).

Process-based prediction of forest mortality requires identifying the physiological causes of tree death. Two interrelated physiological mechanisms for tree mortality from drought have been proposed: hydraulic failure and carbon starvation (McDowell *et al.*, 2008). Hydraulic failure occurs during drought-induced water stress when xylem tensions become high enough to cause air-seeded embolism that occludes water transport beyond a threshold for survival (Cochard *et al.*, 1992; Sperry & Tyree, 1988). Carbon starvation during drought is proposed to occur after stomatal closure when maintenance respiration demands exceed stored non-structural carbohydrate (NSC) reserves via reserve exhaustion or though immobilization if reserves are inaccessible (McDowell *et al.*, 2011; Sala *et al.*, 2010; Sevanto *et al.*, 2014).

While hydraulic failure and carbon starvation are likely highly interactive during tree mortality—and clearly not mutually exclusive mechanisms (McDowell *et al.*, 2011)—observations have demonstrated that hydraulic failure is a ubiquitous factor in tree death from drought in experiments and natural settings (Adams *et al.*, 2017). In the global synthesis of Adams *et al*., hydraulic failure was > 60 PLC (percent loss of xylem conductivity) in all cases where trees died. In contrast, reductions in NSC (compared to control groups) were observed in only 48% of cases. Resistance to hydraulic failure has also been found predictive of tree species' mortality rates during drought around the world (Anderegg *et al.*, 2016; Martin-StPaul *et al.*, 2017). Carbon starvation has been observed to interact with hydraulic failure in causing tree death (O'Brien *et al.*, 2014), but may only prove directly lethal on its own in the case of extreme light limitation (Sevanto *et al.*, 2014; Wiley *et al.*, 2017). In a shade-mortality experiment, Wiley et al. found that NSC reserves in roots could be nearly exhausted (<1% dry weight) at whole-plant death, levels rarely observed in field or greenhouse studies of drought-induced mortality (Adams

et al., 2017). Although carbon starvation can occur in the absence of drought-induced hydraulic failure (Wiley *et al.*, 2017), it seems unlikely that any level of hydraulic failure can occur without some amount of carbon immobilization. In the present study, we quantify only hydraulic failure as a risk factor for drought-induced tree mortality, but acknowledge a secondary effect of hydraulic failure is immobilization of some carbon stores (Sala *et al.*, 2010) and thus, measures such as PLC could be integrative of both water and carbon stress.

While previous work has often focused on comparisons between trees which are dead or likely committed to death (i.e., past the point of no return), and those which survive, we still lack an understanding of the transition space between life and death. Most importantly, we do not yet know when trees begin dying during drought stress—passing a point of no return—such that they will fail to recover and eventually die, even if drought stress is relieved. For example, measurement of hydraulic failure in studies summarized by Adams *et al*. (2017) likely occurred long after trees passed the point of no return in hydraulic function. In order to advance our ability to predict tree mortality, we need to pivot from describing the symptoms in trees that are already dead (i.e. past the "point of no return") to quantify the risk factors that distinguish dying trees from those which will survive (Hartmann *et al.*, 2018a; Martínez-Vilalta *et al.*, 2018). For hydraulic failure during prolonged drought stress, embolism continues to accrue until no xylem remains functional as tree tissues become desiccated. However, it is unlikely that complete loss of xylem conductivity is necessary to cause mortality. Trees can die when some portion of the xylem is still functional but conductivity has been reduced below a threshold sufficient for survival, such that trees will die even if water becomes available (Adams *et al.*, 2017; Hartmann *et al.*, 2018a).

Quantifying this threshold, the point of no return for hydraulic failure beyond which it is expected that the majority of trees in a population will die, is a current priority for understanding mechanisms causing tree mortality (Adams *et al.*, 2017; Martínez-Vilalta *et al.*, 2018; McDowell

et al., 2011). Supply-demand hydraulic theory, based on the hydraulic constraints on water transport through plants from atmospheric demand and soil water supply, posits that exceeding some substantial level of hydraulic loss, perhaps 60 PLC, results in an increased likelihood of mortality (Sperry & Love, 2015). Model hindcasting of drought-induced tree mortality found that a threshold in hydraulic function associated with a chronic PLC > 50 successfully predicted landscape-scale patterns of aspen (*Populus tremuloides* Michx.) mortality (Anderegg *et al.*, 2015). Results from several drought experiments were used to infer a lethal threshold near or above 60 PLC following post-drought re-watering from either the timing of gas exchange recovery (Brodribb *et al.*, 2010; Brodribb & Cochard, 2009; Urli *et al.*, 2013) or from thresholds in water potential as related to PLC via hydraulic vulnerability curves (Li *et al.*, 2015). Although experiments, landscape-level modeling, and theory have indicated that ~60 PLC might be a useful predictor of drought-induced tree mortality, hydraulic failure thresholds have not been experimentally determined with direct measurement of PLC just before relieving drought and monitoring for survival or mortality of measured individuals.

Canopy color is available from many remote sensing products and may be a useful indicator of drought-induced tree death to facilitate detecting and monitoring widespread drought-induced tree die-off (Hartmann *et al.*, 2018a). Changes in foliar color have been used often in previous studies to determine whether trees are dead or alive, with a common definition of death including foliar browning (see table S3 in Adams *et al*., 2017 for a recent review; Adams *et al.*, 2009; Anderegg *et al.*, 2012). However, it remains unknown whether foliar color changes (including browning) occur before, during, or after the point of no return from hydraulic failure.

Here we focus on directly testing the lethal limit for hydraulic failure with a point of no return drought experiment on loblolly pine (*Pinus taeda* L.). We exposed a population of saplings (n=83) to variable levels of water stress, ranging from mild to severe, before re-watering saplings once pre-assigned targets in pre-dawn water potential for each treatment had been reached. Prior

to re-watering, we directly measured PLC in stem segments from each sapling. Our objective was to characterize the risk of tree mortality associated with hydraulic failure. We hypothesized that the lethal threshold for hydraulic failure, beyond which 50% of trees would die, would be near 60 PLC, the threshold supported by theoretical, observational, and inferential studies (Anderegg *et al.*, 2015; Brodribb *et al.*, 2010; Brodribb & Cochard, 2009; Sperry & Love, 2015). A second objective of our study was to characterize the changes in foliar color of saplings during the experiment to determine if foliar color at re-watering was predictive of death or survival. We hypothesized that foliar color change between initial (unstressed) measurements and re-watering (relief of drought stress) for trees which died would be greater than foliar color change of trees which survived.

Materials and Methods

We obtained two-year-old loblolly pine saplings (n = 83) from a local nursery (Cedar Valley Nurseries, Ada, OK, USA), grown from seeds sourced in Louisiana, USA. We transplanted saplings to 37.8 L pots with a soil consisting of 2:1:1 mixture of peat moss (Peat Grower Black Bale, Berger, Quebec, Canada), Turface clay (MVP, Profile Products LLC, Illinois, U.S.A.), and vermiculite (Ambient Minerals, Arkansas, USA) in June of 2016. We chose this mixture to create a slow, steady drying from a high initial moisture content, as this soil has a more gradual slope in the relationship between soil moisture and soil water potential, than many other soils or potting mixes (Kulbaba, 2014). When transplanting, we carefully removed the nursery soil under water, such that loblolly pine saplings were planted with bare roots in our mixed soil. After transplant, all trees were kept well-watered, received a complete fertilizer mix, (18-18-21 NPK, plus micronutrients, Miracle-Gro, Scotts Miracle-Gro Company, Marysville, OH, USA) supplemented

with iron (Liquid Iron, Bonide, Oriskany, NY, USA) and grown for 215 days to allow acclimation in the greenhouse before we began the experiment. No trees died after transplanting. In order to enable trees to better acclimate to drought conditions and avoid conducting our experiment on tree saplings that had never experienced water stress, we exposed all trees, including the watered controls, to a pre-experimental drought treatment by withholding water until stomatal closure occurred. We verified stomatal closure (> 90% reduction in stomatal conductance from well-watered measurements) in a random subsample of the population (n=36), as confirmed by measurement with an LI-6400 infrared gas analyzer (LI-COR Biosciences, Lincoln, Nebraska, USA) and a mean pre-dawn water potential of -2.3 (± 0.25 SD) MPa. No tree died as a result of this acclimation drought. Following this pre-experimental drought, which lasted for 43 days, trees were again well-watered from 35 days before the experiment began. In January 2017, at the start of the drought experiment, mean sapling height was 2.02 ± 0.12 m SD, and mean stem diameter at the root collar (soil level) was 3.01 ± 0.24 cm SD. We conducted a branch census before and after the experiment and estimated that less than 10% of shoot biomass was harvested for measurements during the study.

To identify re-watering targets representing a range of hydraulic failure, we constructed a vulnerability curve using 6 additional saplings, acquired at the same time as the 83 in our study, potted and grown in the same manner as experimental trees. First, we excised 18 branches (3 each from the 6 individual saplings), from the most recent year's growth, 0.5 – 0.75m in length, at pre-dawn. Whole branches were re-cut underwater in the laboratory, allowing xylem tension to relax. Branches were then wrapped in damp paper towels, sealed in three layers of plastic bags, and shipped overnight to the University of Utah, where centrifuge measurements were conducted on stem segments. Stem segments 5–7 mm in diameter were prepared by cutting and trimming them from longer branches underwater to the desired length (~10 cm). These segments were then vacuum infiltrated at 100 kPa for 1 h with degassed and filtered 20 mM KCl solution and were

used to measure maximum hydraulic conductivity (Sperry *et al.*, 2012). We then spun stems in a centrifuge to induce negative pressure at target values, which were -1, -2, -2.5, -3, -3.5, -4, -5 MPa in the xylem sap. Hydraulic conductivity at each pressure stop was then determined using a conductivity apparatus as described previously (Sperry *et al.*, 2012). We used a Weibull function to fit the hydraulic vulnerability curve results (Fig. S1).

To identify the lethal threshold of hydraulic failure, we designed our drought experiments such that trees would be re-watered at a wide range of levels of water stress. Using our centrifuge-generated vulnerability curve as a guide (Fig. S1) and informed from a prior pilot study on a few individuals (data not included in this study), we chose specific targets at which to re-water trees and subsequently monitor for survival or mortality. We determined drought-stress treatment groups by water potential ranges from our vulnerability curve, to ensure trees were re-watered along the entire potentially lethal drought-stress gradient, from stomatal closure (-2.1 MPa, 20 PLC) until complete hydraulic failure (-6.0 MPa, 100 PLC). Targets for groups between these points included water potential associated with 60 (-3.3 MPa), 80 (-3.7 MPa), and 90 (-4.1 MPa) PLC. An additional group of control trees (n=6) remained well watered throughout the experiment with weekly irrigation to field capacity. We measured pre-dawn water potential of distal stems (twigs) using a Scholander-type pressure-bomb (model 1505-D, PMS Instruments, Albany, OR, USA) at least weekly, and often more frequently for trees approaching re-watering targets.

At the start of the experiment, we completely withheld water from all trees except the well-watered controls. As each tree under drought reached its assigned water potential re-watering target, we excised a branch for measurement of PLC. After sampling, each tree was re-watered to field capacity and watered weekly to monitor for survival (or death). Initial excisions of stem segments, all over 20 cm in length, were made in air, and were immediately placed in filtered (0.2 μm) 100mM KCl and transported to the laboratory for measurement of hydraulic conductivity. In

the laboratory, we re-cut stems under filtered solution by removing at least 2 cm from the cut end in two successive ≥ 1 cm cuts, allowing time for relaxation of the xylem tension, and then we immediately excised a segment of interest once tension was relaxed to prevent refilling of native embolism (Torres-Ruiz *et al.*, 2015). Immediately before measurement of hydraulic conductivity, we removed ~0.5 cm of bark from each end, exposing the xylem for measurement of diameter, and shaved the ends of each segment (while underwater) with a fresh razor blade. After determining conductivity, we measured segment length and perpendicular diameters of each end using digital calipers (VWR, U.S.A.) in order to correct measurements to area for specific conductivity. All measured segments collected were from the most recent year's growth, and mean diameter was 3.91 ± 0.60 mm SD, and mean length was 62.68 ± 10.06 mm SD. We also measured conductivity of the well-watered control trees at the end of the experiment.

We measured native conductivity (K_s) using a Sperry apparatus with a 50 cm height gravity-fed pressure head (Sperry *et al.*, 1988). We filtered DI water (0.2µm), mixed to a concentration of 100 mM KCl, and then degassed this perfusing solution using a membrane contactor (LiquiCell micro module, 3M, St. Paul, Minnesota, USA) connected to a vacuum pump following best practices (Cochard *et al.*, 2013; Venturas *et al.*, 2015). We then placed stem segments in perfusing solution overnight under vacuum, infiltrating them to their maximum conductivity (K_{max}), which was verified with active xylem staining using 0.1% safranin solution after the K_{max} measurement was complete. We measured K_{max} using the same methods as K_s, corrected all conductivity measurements to sample dimensions, including length (Sperry *et al.*, 1988), and calculated the percent loss of conductivity:

$$PLC = 100[1 - \left(\frac{Ks}{Kmax}\right)]$$

Monitoring for survival or mortality occurred during the growing season, and we determined that a tree had survived drought if we observed new growth after re-watering. The last re-

watering treatment occurred on May 15, 2017, after 125 days of drought. We analyzed the effect of PLC and K_s on mortality using logistic regression, a method appropriate for binary outcomes such as life or death (Menard, 2002), using program R version 3.3.3 (R Core Team, 2013). Logistic models have been widely used for describing and predicting tree mortality and survival in response to environmental (Van Mantgem *et al.*, 2009), tree growth (Cailleret *et al.*, 2016), or ecophysiological conditions (Anderegg *et al.*, 2013; Bolte *et al.*, 2016; Kursar *et al.*, 2009; Venturas *et al.*, 2018). We assessed fit of logistic regressions using a Nagelkerke R^2, a pseudo R^2 metric. Additionally, we conducted further active xylem staining on surviving trees to assess where in stems xylem remained functional after recovery.

We assessed foliar color using a Munsell plant tissue color book (Munsell Color, Grand Rapids, Michigan, USA) during three discrete stages of each tree's progression through the experiment. To measure foliar color, a representative fascicle of needles was removed from the upper third of each tree's canopy, and compared to the plant tissue color book for color matching (Tucker *et al.*, 1991). Initial color was documented before water was withheld to initiate drought-induced water stress, another measurement was taken at the re-watering treatment, and a final measurement was taken 60 days post-re-watering. We transformed all color values from Munsell Hue / Value / Chroma into sRGB using the R package 'aqp' (Beaudette *et al.*, 2018). We chose this color space because it is accurately represented on most digital devices, and allowed for comparison between trees that survived, and those that died, in color space. We used a Euclidean distance equation to calculate the Euclidean color distance between red (*R*), green (*G*), and blue (*B*) foliar color values at the initial (*i*, pre-drought), and re-watering (*f*, final) stages:

$$\sqrt{\left(R_f - R_i\right)^2 + \left(G_f - G_i\right)^2 + \left(B_f - B_i\right)^2}$$

We tested for differences in Euclidean color distance (from initial to re-watered canopy foliar color) between watered controls, trees that survived, and those that died using ANOVA, with post-hoc testing using Fisher's LSD, in program R.

Results

Our drought followed by re-watering treatments at variable water potential targets in 77 saplings provided the intended wide variation in PLC at re-watering that ranged from 35.4 to 100.0 PLC (Table S1). After allowing at least 60 days for recovery following re-watering, we determined whether trees resumed growth (survived) or had complete canopy desiccation and browning (died). We found that 57 trees died, and 20 survived. From measurements taken the day drought stress was relieved, the mean PLC of trees that eventually recovered was 77.2 (± 19.7 SD), while trees that would die averaged 94.5 PLC (± 6.9 SD; Fig. 1). All trees which died had a PLC > 72 at re-watering. Control trees which were watered weekly during the experiment (n=6) had a mean PLC of 27.5 (± 9.7 SD). Median values for the three groups (control, survived drought, died) were significantly different (Kruskal-Wallis test, $p < 0.001$, Fig. 1).

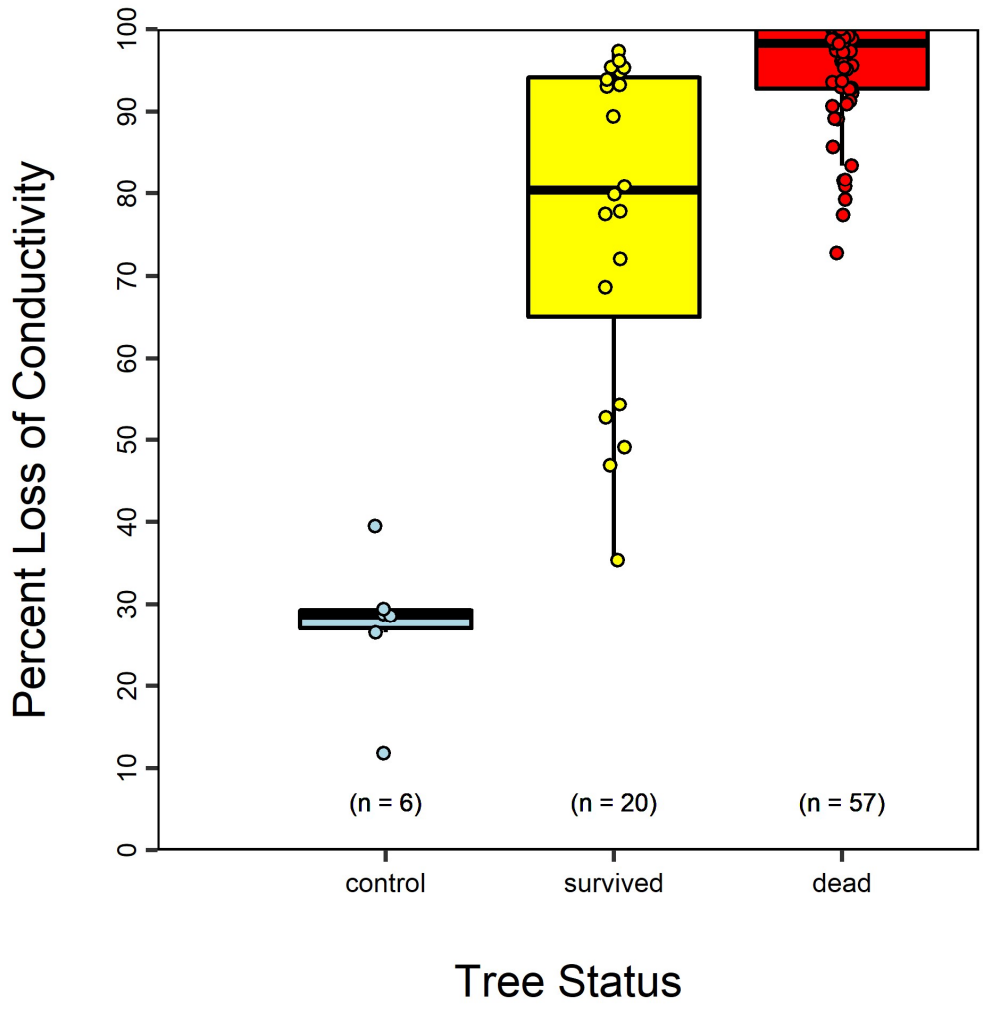

Figure 1. Native (directly measured) percent loss of hydraulic conductivity (PLC) in *Pinus taeda* that died or survived drought, or were watered throughout the experiment (control). PLC values shown for drought trees were measured just prior to re-watering. Watered control PLC measurements were taken at the end of the experiment. All trees that died had a directly measured PLC exceeding 70. Central bars indicate median values, boxes represent the interquartile range (IQR), and whiskers extend to the maximum and minimum data value within 1.5 * IQR. Data points are jittered to reveal overlapping points. Median values are significantly different from each other for all three groups (Kruskal-Wallis test, $p < 0.001$)

Using logistic regression, we determined the lethal threshold for hydraulic failure, at which 50% of trees would die (LD50), to be 80.2 PLC (Nagelkerke $R^2 = 0.53$, Fig. 2). A Wald 95% confidence interval (CI) for our logistic regression predicting mean probability of mortality

contained a minimum of 67.1 PLC and a maximum of 85.5 PLC, but did not include PLC 60, the hypothesized

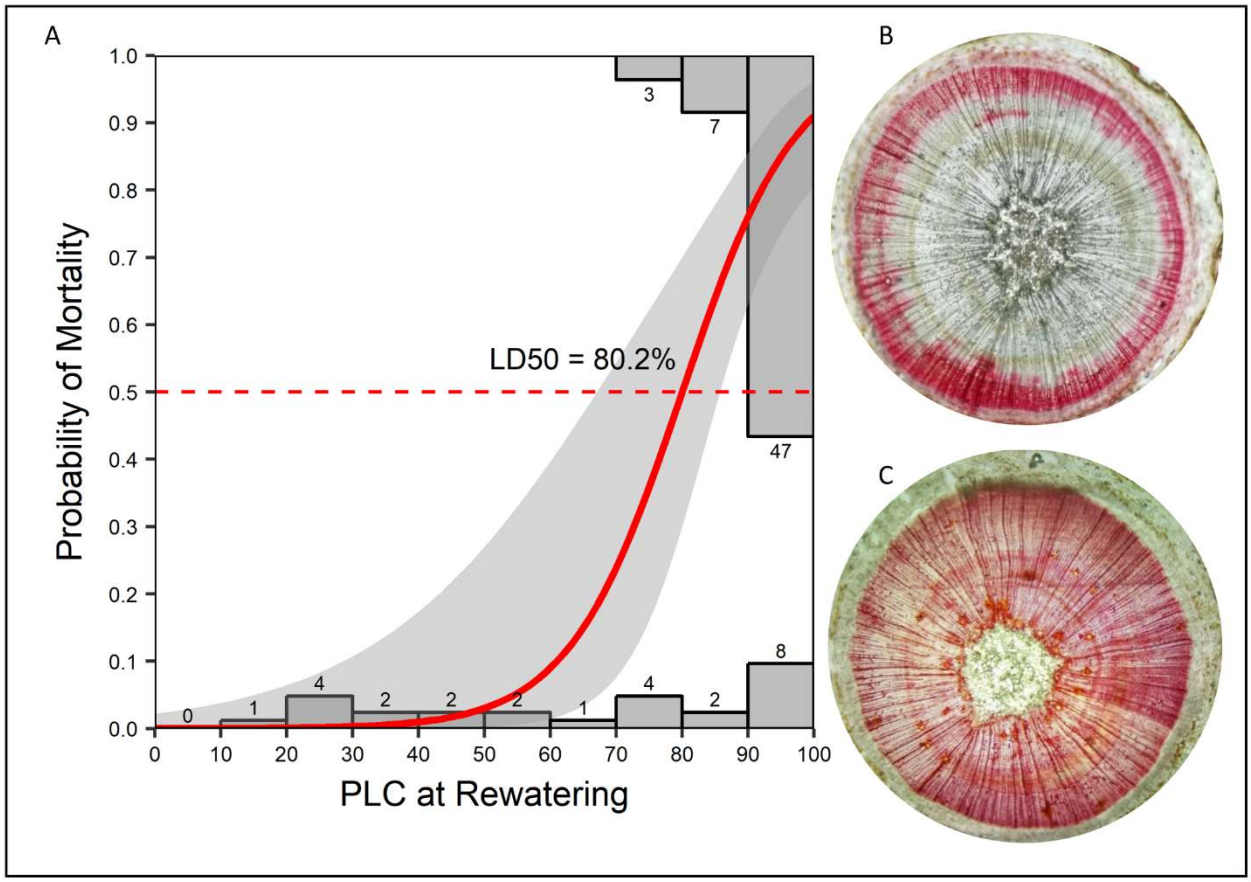

Figure 2. A logistic regression to determine the 50% lethal dose (LD50, dashed red line) of percent loss of hydraulic conductivity (PLC) during drought, which was 80.2 (95% Wald Confidence for probability of mortality had a minimum PLC = 67.1 and maximum PLC = 85.5 at LD50; panel A). Bars represent the proportion of all trees in each 10% PLC bin, scaled to the height of the y-axis, with count of trees per bin labeling each bar. The solid red line is the logistic regression fit, with shaded grey area representing a Wald 95% confidence interval for the logistic regression. The predicted lethal threshold for hydraulic failure, PLC = 60, was not contained in this interval at LD50 (dashed red line). The majority of trees which died (n=47) did so with a PLC > 90. Panels B and C are stem cross sections of Pinus taeda with functional xylem stained red using 0.1% safranin. Panel B shows the stem of a tree at 83.4 PLC, past the hydraulic failure point of no return, which died following re-watering. Panel C is a well-watered control tree, with all xylem functional.

PLC at 50% probability of mortality. Probabilities for mortality were 0.03 (95% CI: 0.00 – 0.27) for 50 PLC, 0.09 (95% CI: 0.01 – 0.39) for 60 PLC, 0.24 (95% CI: 0.08 – 0.54) for 70 PLC,

and 0.76 (95% CI: 0.63 – 0.86) for 90 PLC. Specific native conductivity of stems (K_s) measured immediately before re-watering ranged from 0.37 kg m^{-1} MPa^{-1} s^{-1} to 0 (no flow), and using logistic regression we determined LD50 in K_s of 0.06 kg m^{-1} MPa^{-1} s^{-1} (Nagelkerke $R^2 = 0.51$, Fig. S3), which was an 83.8% loss of the maximum observed Ks (Fig. S3). We provide our fitted probability functions for mortality from PLC and K_s, and the confidence intervals for both in Table S1.

Euclidean color distance between initial canopy foliar color and canopy foliar color at re-watering was significantly higher for trees that died, compared to those that either survived drought, or did not experience drought (ANOVA, $F(2,80)=4.737$, $p = 0.0114$, post-hoc Fisher's LSD, Fig. 3D). The general trend for trees that died was a change from green to a more yellow or brown foliar color (Fig. 3A, 3B). Sixty days after re-watering, foliar color had returned to a deep green for trees that survived, and trees that died had complete foliar browning (Fig. 3C). Observations from active xylem stains of stems from recovered trees revealed that embolism remained in tissues which experienced the drought treatment, but that surviving trees had active xylem near the vascular cambium when drought was relieved, which remained functional during our stains (Figure 4). Additionally, embolism from the drought remained in the interior of the stems when sections were made, 90 days after relief of drought (Figure 4).

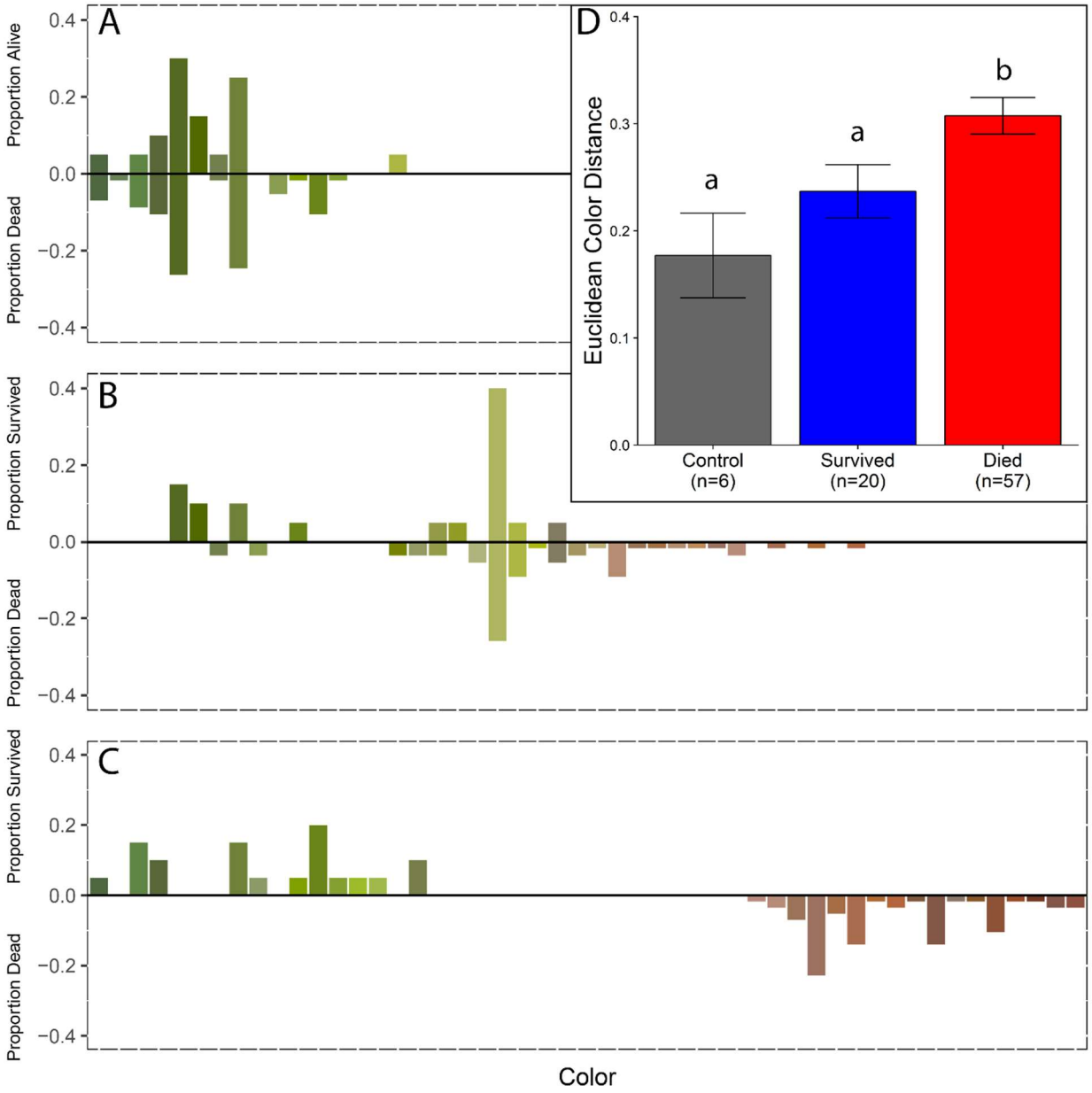

Figure 3. Observed canopy color, arranged from darkest green to deepest red-brown. Bar height indicates the proportion of trees that survived (positive proportion) or of trees that died (negative proportion) at a given color. Bars are filled with the same color we observed in the tree foliage. Panel A shows canopy foliar color at the beginning of the experiment, before drought, and foliar color of all trees was a deep green. Panel B shows canopy foliar color at re-watering, with trees that survived tending toward green, while trees that died tended toward yellow/brown colors. Panel C shows canopy foliar color 60 days after re-watering, where trees that survived have returned nearer to initial foliar color positions and trees that died all experienced browning of foliage. Data in panels A, B, and C are for trees exposed to drought that either survived or died, analogous data for the watered control trees are shown in Fig. S4. Panel D shows the Euclidean color distance, a calculation of the change in color between pre-drought (panel A) and re-watering (panel B) for control trees (grey) and trees that experienced drought and survived (blue) or died (red). Trees that died during drought stress had a significantly greater Euclidean color distance than trees which survived (whether they experienced drought, or were a watered control; ANOVA, $F(2,80)=4.737$, $p = 0.0114$, post-hoc Fisher's LSD). Letters above bars in panel D indicate significant differences and error bars are standard error of the mean.

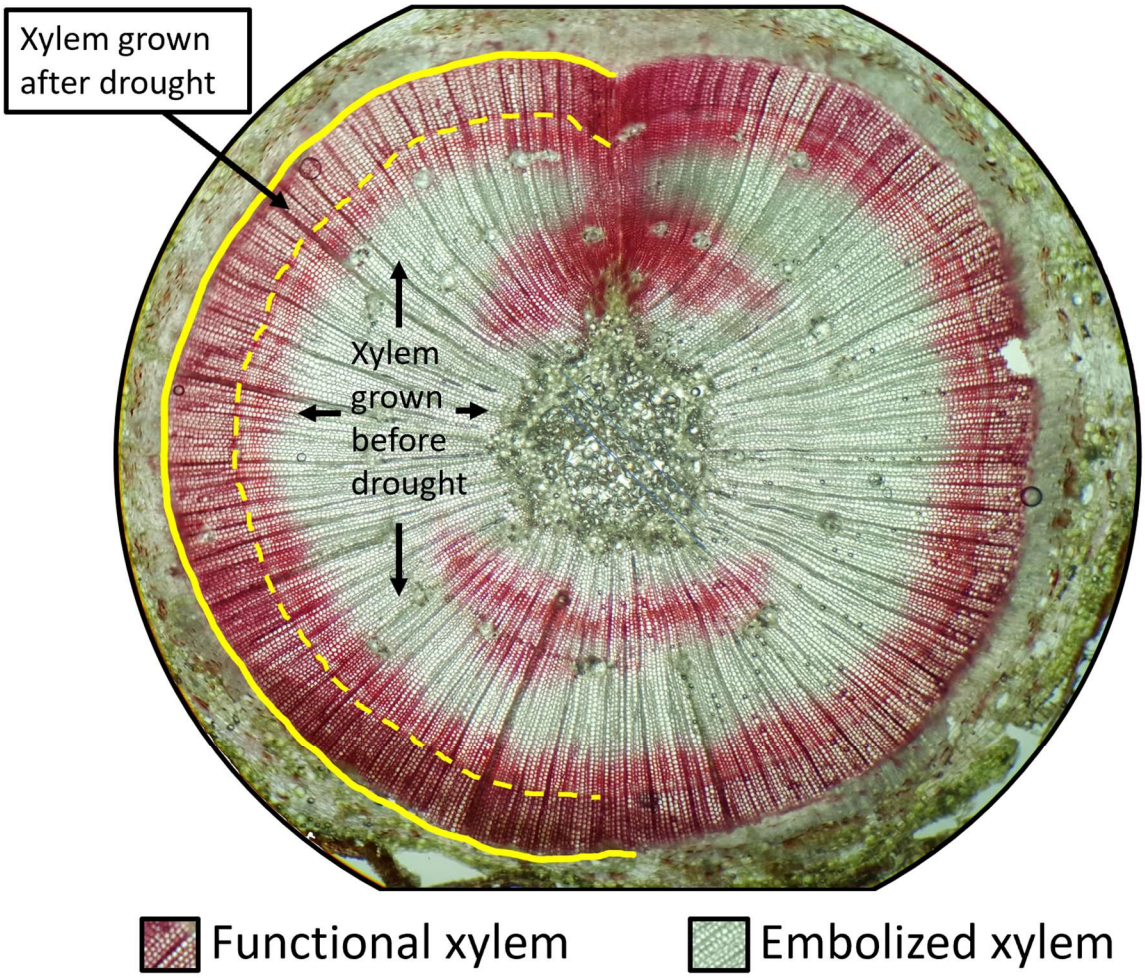

Figure 4. Cross-section of a stem segment taken from an active xylem stain of a tree which experienced extreme (96 PLC) hydraulic failure, yet recovered after re-watering. This cross section was taken from a stem segment excised 85 days after re-watering, after radial growth had occurred following relief of the drought. Active xylem is indicated by red (stained by 0.1% safranin solution), while embolized xylem is unstained. During the drought, the vascular cambium's location is indicated by a yellow dashed line, while the position of the vascular cambium at the time of cross-sectioning is indicated by a solid yellow line. As can be seen, xylem remained functional close to the location of the vascular cambium at re-watering (indicated by a yellow dashed line) of this tree surviving extreme stress, and hydraulic function after 85 days of recovery has been restored via new radial growth. All markers appear only on the left half of the cross-section, so that the right side may be inspected visually.

Discussion

We found that the point of no return (the LD50 at a population level) for directly measured PLC at re-watering was 80.2, indicating that some loblolly pine saplings were able to survive with less than 20% (or even 10%) of their xylem functional at re-watering. Interpolating from our results, we would predict only 9% (95% CI: 1–39%) mortality at 60 PLC, much lower than the 50% mortality (LD50) we expected based on previous indirect estimates (Brodribb & Cochard, 2009; Choat *et al.*, 2018). Observations of *Pinus halpensis* (Miller) under drought in the field noted that trees can survive >80 PLC (Klein *et al.*, 2012), but we believe our result is the first direct determination of LD50 for PLC to quantify the point of no return with measured individuals monitored for survival or mortality. Our experiment provides a hydraulic failure function for risk of mortality that can be directly input to vegetation models (e.g. TREES, CLM(ED(X)), SurEau; Johnson *et al.*, 2018; Mackay *et al.*, 2015; Martin-StPaul *et al.*, 2017; McDowell *et al.*, 2016), although more work is needed to generalize these functions across life-stages and species (see below). Our results enable predictions of mortality risk that can be based on either 1) a threshold that represents the point of no return from hydraulic failure (LD50), rather than complete desiccation of the xylem (i.e. 100 PLC), or 2) a continuous prediction of mortality risk across all possible PLC values.

It is remarkable that some pine trees were able to survive extreme levels (> 90 PLC) of hydraulic failure. In our study, trees were re-watered completely (to field capacity) on the day we measured the target PLC, and weekly thereafter. This rapid cessation of drought and switch to abundant soil moisture in our experiment could have enabled increased survival probability at very high PLC. Drought in the field is not typically relieved so immediately, completely, and persistently, which could result in fewer trees surviving very high PLC under natural conditions.

Our data suggest that as long as there was supply of water to the vascular cambium, and xylem tension was able to relax before complete (P100) hydraulic failure, there is a chance for survival. Our measurements of both hydraulic conductivity and active xylem staining after re-watering showed that surviving trees restored conductivity via radial growth (Fig. 4). Therefore, an ability to grow new xylem tissue following drought may be key to a tree's long-term survival. Past studies estimated 50 PLC to be a likely threshold for life or death for gymnosperms (Brodribb & Cochard, 2009; Choat *et al.*, 2018), yet no trees re-watered below 72 PLC died in our experiment. Additional species should be investigated to determine if the ability to survive such extreme hydraulic failure (e.g., > 90 PLC) is widespread for gymnosperm trees.

Characterizing mortality risk along a drought-stress gradient provides a critical parameter for global vegetation modelling (Hartmann *et al.*, 2018a). While our finding provides a point of no return (LD50), beyond which it is more likely trees will die than survive, we also characterize risk across the entire range of possible values for hydraulic failure. Indeed, our model predicts less than 5% mortality until PLC > 55. At the other extreme, our model predicts 75% probability of mortality at 90 PLC (Fig. 2). Utilizing our continuous probability predictor of mortality risk, even at high levels of PLC some trees are predicted to survive—as is often observed in forests affected by drought-induced tree mortality. Thus, we recommend utilization of continuous predictors of mortality risk over threshold-like approaches only including binary outcomes of 100% life or death on opposing sides of the threshold (Hartmann *et al.*, 2018a).

When investigating what kills trees under drought, the definition and quantification of death matter if we wish to truly determine mechanism. In the present study, we have quantified the point of no return from drought stress—such that if the lethal stressor is relieved, there is still a failure to recover and death results. It is especially important to distinguish between physiological causes of death, assessed at the point of no return when trees begin dying, and non-causative symptoms or correlates that occur after this point and are evident at tree death (Adams *et al.*,

2017; Hartmann *et al.*, 2018a). Symptoms that have often been used to infer tree death include foliar browning and other visual indications of dieback (Adams *et al.*, 2009; Anderegg *et al.*, 2012), and cessation of respiration, assessed directly, or through tissue staining (Sevanto et al. 2014). It is possible that physiological variables measured when such criteria are met are those for a tree already long past the point of no return, which has been committed to die for some time. Physiological responses measured after the point of no return (e.g. at foliar color change or cessation of respiration) cannot have caused death, and may differ from responses measured at or prior to the point of no return. Future studies seeking to understand the physiology of tree death from drought should measure additional responses to drought stress (e.g., NSC, spectral reflectance, water content) at the point of return (if known, or if not, along a gradient of drought stress) to determine if responses precede, follow, or are concurrent with the point of no return from hydraulic failure.

Though we observed that foliar color in trees was significantly different at the time of re-watering, there was much overlap in canopy color between trees that survived and those that died (Fig. 3B, 3D). Foliar color was not wholly separated between these groups until our measurement at 60 days after re-watering (Fig. 3C), and thus was a better indicator of trees that are already dead, rather than those which are in the process of dying. Studies relying on foliar color to determine the timing of tree death have likely overshot the moment when trees passed the point of no return, and therefore measurements of physiological function at this point can confuse non-causative symptoms of having died for actual causes of mortality (Leuzinger *et al.*, 2009). However, measurement of foliar color after tree death, rather than at the point of no return, has remote sensing applications for detecting recent tree mortality in evergreen forests, before changes become obscured by a green understory, provided a baseline color is available prior to drought (Hartmann *et al.*, 2018a). Improved characterization of foliar color changes at additional spectra as hydraulic failure occurs during drought may improve the predictive power of foliar

color in remote sensing of drought-induced tree mortality, an approach which will require additional experimentation to measure across an array of wavelengths.

By directly measuring PLC across a water-stress gradient ranging from mild to lethal in loblolly pine saplings, we observed that the lethal threshold was higher than our expectation of 60%. Our observation raises the question—do other species exhibit similarly high lethal thresholds for hydraulic failure? We hypothesize that this threshold may be relevant for conifer species, and that species differences in hydraulic vulnerability affect timing to reach the lethal threshold in PLC, rather than alter the threshold directly. Here it is important to distinguish between the lethal threshold in PLC, a normalized response for the loss of hydraulic function which may correlate consistently with mortality risk across species, and the degree of tension in the xylem required to reach this threshold in a given tree, which is not normalized (Cochard *et al.*, 2013). Vulnerability to embolism, quantified as the relationship between water potential and PLC, has been observed to vary by nearly an order of magnitude in gymnosperms, with water potential corresponding to 50 PLC spanning -1.5MPa (*Podocarpus latifolius*) to -14.1 MPa (*Actinostrobus acuminatus;* Maherali *et al.*, 2004). We also expect wide variation in traits which mediate the progression of water potential —and xylem embolism accumulation—during drought. Such traits include stomatal control, minimum conductance rates following stomatal closure, allocation and leaf area to root or sapwood area ratios, root water uptake and hydraulic isolation from the soil (Blackman *et al.*, 2019; Choat *et al.*, 2018; Hammond and Adams, 2019). If, as multiple lines of recent research have suggested, a major evolutionary pressure exists to keep woody tissues from experiencing damaging levels of hydraulic impairment (PLC; e.g. Anderegg *et al.*, 2018; Martin-StPaul *et al.*, 2017; Sperry *et al.*, 2016; Wolf *et al.*, 2016), and if embolism repair is relatively rare (Brodersen & McElrone, 2013; Choat *et al.*, 2015), then lethal thresholds in PLC may be fairly consistent across species. However, plant traits and species differences will influence how and when species reach this threshold. Experiments are needed to

test whether lethal thresholds in PLC vary with species, phylogeny, anatomical factors such as lumen area and xylem cell wall thickness, environmental factors, including temperature and vapor pressure deficit, and non-structural carbohydrate status (Martínez-Vilalta *et al.*, 2018; Trifilò *et al.*, 2017).

Given that experimental data similar in nature is lacking for mature trees, one important consideration is how these results apply to larger trees under field conditions. While it is true that earlier developmental stages (e.g., seedlings, saplings) frequently experience higher rates of background mortality in the field (Van Mantgem *et al.*, 2009), there are at least two contributing factors that should be considered. First, it is important to recognize that earlier developmental stages utilize considerably less environmental space (above and below-ground) and store less water and carbon than their mature counterparts and are thus more strongly affected by atmospheric demand and soil moisture during drought (Hartmann *et al.*, 2018b). Second, anatomical changes across the ontogeny of a tree could affect vulnerability to drought. Such changes may lead to a difference in the level of tension in the xylem (water potential) required to reach a lethal level of hydraulic failure (such as our observed 80 PLC). Both of these factors could contribute to an earlier death of seedlings and saplings during drought relative to larger and more mature trees, even if the LD50 for PLC was unchanged with ontogeny. Notably, P50 in mature *Pinus taeda* trees (quantified as water potential inducing 50 PLC) was found to be -3.13 MPa (Maherali *et al.*, 2006), which is within the 95% confidence interval of P50 for the vulnerability curve we measured in our sapling population of the same species (-3.22 MPa, Fig. S1). Acknowledging that our experimental approach would be challenging for mature trees in a forest, we propose that the best way to validate extrapolations of mortality risk from sapling experiments is to use this type of experimental data to explain past mortality in the field before attempting to predict mortality under future climate scenarios (Anderegg *et al.*, 2015).

Conclusion

Our direct measurement of a lethal PLC threshold of loblolly pine near 80% demonstrates that the point of no return was higher than expected for a gymnosperm species, and that some trees can survive near complete hydraulic failure. In experimental determinations of lethal hydraulic thresholds in angiosperms, prior studies indicate that trees can survive 88 PLC, but these studies inferred PLC from measurements of water potential using vulnerability curves, rather than direct measurement (Li *et al.*, 2015; Urli *et al.*, 2013), although direct measurements of PLC in two angiosperm species support a high threshold (Barigah *et al.*, 2013). In combination, these results and our finding of a relatively high LD50 for PLC in loblolly pine raise questions of how lethal thresholds vary among tree species, populations, and ontogeny. Continued experimentation will be necessary to assess this, but we hypothesize that differences among trees (both within and between species) in vulnerability to drought-induced mortality may be primarily caused by variable embolism resistance, and variable rates of declines in water potential, more than differences in the degree of hydraulic failure (PLC) that is lethal. Overall, our results quantify tree mortality risk from hydraulic failure, a parameter critical for process-based models of forest response to climate change.

Acknowledgements: This research was supported by the NSF Graduate Research Fellowship Program, the Oklahoma NSF EPSCoR Research Infrastructure Improvement Award (OIA-1301789), and the Oklahoma State University College of Arts & Sciences. Greenhouse space was supported by the Department of Natural Resources Ecology and Management at Oklahoma State University, and by McIntire-Stennis project OKL0 2929. W.R.L.A. acknowledges funding from the David and Lucille Packard Foundation, the University of Utah Global Change and Sustainability Center, NSF Grants 1714972 and 1802880, and the USDA National Institute of

Food and Agriculture, Agricultural and Food Research Initiative Competitive Program, Ecosystem Services and Agro-ecosystem Management, grant no. 2018-67019-27850. We thank Daniel Johnson, Gerald Schoenknecht, and Mona Papeş for helpful discussions of results and comments on the manuscript, and Adam Maggard for discussion of study methods and physiological measurement of loblolly pine. We also wish to thank three anonymous reviewers for their insight and feedback on this manuscript.

References:

Adams HD, Guardiola-Claramonte M, Barron-Gafford GA, Villegas JC, Breshears DD, Zou CB, Troch PA, Huxman TE. 2009. Temperature sensitivity of drought-induced tree mortality portends increased regional die-off under global-change-type drought. *Proceedings of the National Academy of Sciences* **106**(17): 7063-7066.

Adams HD, Zeppel MJ, Anderegg WR, Hartmann H, Landhäusser SM, Tissue DT, Huxman TE, Hudson PJ, Franz TE, Allen CD *et al*. 2017. A multi-species synthesis of physiological mechanisms in drought-induced tree mortality. *Nature Ecology and Evolution* **1**(9): 1285.

Allen CD, Macalady AK, Chenchouni H, Bachelet D, McDowell N, Vennetier M, Kitzberger T, Rigling A, Breshears DD, Hogg ET. 2010. A global overview of drought and heat-induced tree mortality reveals emerging climate change risks for forests. *Forest Ecology and Management* **259**(4): 660-684.

Anderegg WR, Berry JA, Smith DD, Sperry JS, Anderegg LD, Field CB. 2012. The roles of hydraulic and carbon stress in a widespread climate-induced forest die-off. *Proceedings of the National Academy of Sciences* **109**(1): 233-237.

Anderegg WR, Flint A, Huang C-y, Flint L, Berry JA, Davis FW, Sperry JS, Field CB. 2015. Tree mortality predicted from drought-induced vascular damage. *Nature Geoscience* **8**(5): 367-371.

Anderegg WR, Kane JM, Anderegg LD. 2013. Consequences of widespread tree mortality triggered by drought and temperature stress. *Nature Climate Change* **3**(1): 30.

Anderegg WR, Klein T, Bartlett M, Sack L, Pellegrini AF, Choat B, Jansen S. 2016. Meta-analysis reveals that hydraulic traits explain cross-species patterns of drought-induced tree mortality across the globe. *Proceedings of the National Academy of Sciences* **113**(18): 5024-5029.

Anderegg WRL, Wolf A, Arango-Velez A, Choat B, Chmura DJ, Jansen S, Kolb T, Li S, Meinzer FC, Pita P, Resco de Dios, V. 2018. Woody plants optimise stomatal behaviour relative to hydraulic risk. *Ecology letters* **21**(7): 968-977.

Barigah TS, Charrier O, Douris M, Bonhomme M, Herbette S, Améglio T, Fichot R, Brignolas F, Cochard H. 2013. Water stress-induced xylem hydraulic failure is a causal factor of tree mortality in beech and poplar. *Annals of botany* **112**(7): 1431-1437.

Beaudette, D.E., Roudier P., and A.T. O'Geen. 2013. Algorithms for Quantitative Pedology: A Toolkit for Soil Scientists. *Computers & Geosciences* **52**:258 - 268.**Blackman CJ, Creek D, Maier C, Aspinwall MJ, Drake JE, Pfautsch S, O'Grady A, Delzon S, Medlyn BE, Tissue DT, Choat, B.** Drought response strategies and hydraulic traits contribute to mechanistic understanding of plant dry-down to hydraulic failure. *Tree physiology*.

Bolte A, Czajkowski T, Cocozza C, Tognetti R, De Miguel M, Pšidová E, Ditmarová Ľ, Dinca L, Delzon S, Cochard H. 2016. Desiccation and mortality dynamics in seedlings of different European beech (Fagus sylvatica L.) populations under extreme drought conditions. *Frontiers in Plant Science* **7**: 751.

Bonan GB. 2008. Forests and climate change: forcings, feedbacks, and the climate benefits of forests. *Science* **320**(5882): 1444-1449.

Brodersen CR, McElrone AJ. 2013. Maintenance of xylem Network Transport Capacity: A Review of Embolism Repair in Vascular Plants. *Frontiers in Plant Science* **4**:108.

Brodribb TJ, Bowman DJ, Nichols S, Delzon S, Burlett RJNP. 2010. Xylem function and growth rate interact to determine recovery rates after exposure to extreme water deficit. *New Phytologist* **188**(2): 533-542.

Brodribb TJ, Cochard H. 2009. Hydraulic failure defines the recovery and point of death in water-stressed conifers. *Plant Physiology* **149**(1): 575-584.

Cailleret M, Bigler C, Bugmann H, Camarero JJ, Cufar K, Davi H, Mészáros I, Minunno F, Peltoniemi M, Robert E, Suarez, ML. 2016. Towards a common methodology for developing logistic tree mortality models based on ring-width data. *Ecological Applications* **26**(6): 1827-1841.

Choat B, Brodersen CR, McElrone AJ. 2015. Synchrotron X-ray microtomography of xylem embolism in Sequoia sempervirens saplings during cycles of drought and recovery. *New Phytologist* **205**(3): 1095-1105.

Choat B, Brodribb TJ, Brodersen CR, Duursma RA, López R, Medlyn BE. 2018. Triggers of tree mortality under drought. *Nature* **558**(7711): 531.

Cochard H, Badel E, Herbette S, Delzon S, Choat B, Jansen S. 2013. Methods for measuring plant vulnerability to cavitation: a critical review. *Journal of Experimental Botany* **64**(15): 4779-4791.

Cochard H, Cruiziat P, Tyree MT. 1992. Use of Positive Pressures to Establish Vulnerability Curves : Further Support for the Air-Seeding Hypothesis and Implications for Pressure-Volume Analysis. *Plant Physiology* **100**(1): 205-209.

Friedlingstein P, Cox P, Betts R, Bopp L, Von Bloh W, Brovkin V, Cadule P, Doney S, Eby M, Fung I, et al. 2006. Climate–Carbon Cycle Feedback Analysis: Results from the C4MIP Model Intercomparison. *Journal of Climate* **19**(14): 3337-3353.

Friedlingstein P, Meinshausen M, Arora VK, Jones CD, Anav A, Liddicoat SK, Knutti R. 2014. Uncertainties in CMIP5 climate projections due to carbon cycle feedbacks. *Journal of Climate* **27**(2): 511-526.

Friend AD, Lucht W, Rademacher TT, Keribin R, Betts R, Cadule P, Ciais P, Clark DB, Dankers R, Falloon PD. 2014. Carbon residence time dominates uncertainty in terrestrial vegetation responses to future climate and atmospheric CO2. *Proceedings of the National Academy of Sciences* **111**(9): 3280-3285.

Hartmann H, Moura CF, Anderegg WR, Ruehr NK, Salmon Y, Allen CD, Arndt SK, Breshears DD, Davi H, Galbraith D. 2018a. Research frontiers for improving our understanding of drought-induced tree and forest mortality. *New Phytologist* **218**(1): 15-28.

Hartmann H, Adams HD, Hammond WM, Hoch G, Landhäusser SM, Wiley E, Zaehle S. 2018b. Identifying differences in carbohydrate dynamics of seedlings and mature trees to improve carbon allocation in models for trees and forests. *Environmental and Experimental Botany* **152**: 7-18.

Hammond, WM and Adams, HD. 2019. Dying on time: Traits influencing the dynamics of tree mortality risk from drought. *Tree Physiology*. **39**(6)**:** 906-909.

IPCC. 2014. *Climate Change 2014: Impacts, Adaptation, and Vulnerability. Part A: Global and Sectoral Aspects. Contribution of Working Group II to the Fifth Assessment Report of the*

Intergovernmental Panel on Climate Change [Field, C.B., V.R. Barros, D.J. Dokken, K.J. Mach, M.D. Mastrandrea, T.E. Bilir, M. Chatterjee, K.L. Ebi, Y.O. Estrada, R.C. Genova, B. Girma, E.S. Kissel, A.N. Levy, S. MacCracken, P.R. Mastrandrea, and L.L. White (eds.)]. Cambridge, United Kingdom and New York, NY, USA: Cambridge University Press.

Johnson DM, Domec JC, Berry ZC, Schwantes AM, Woodruff DR, McCulloh KA, Polley HW, Wortemann R, Swenson JJ, Mackay DS. 2018. Co-occurring woody species have diverse hydraulic strategies and mortality rates during an extreme drought. *Plant, Cell & Environment* **41**(3): 576-588.

Klein T, Di Matteo G, Rotenberg E, Cohen S, Yakir D. 2012. Differential ecophysiological response of a major Mediterranean pine species across a climatic gradient. *Tree physiology* **33**(1): 26-36.

Kulbaba SP. 2014. Evaluating trembling aspen (Populus tremuloides Michx.) seedling stock characteristics in response to drought and out-planting on a reclamation site. *Doctoral Diss.*

Kursar TA, Engelbrecht BM, Burke A, Tyree MT, EI Omari B, Giraldo JP. 2009. Tolerance to low leaf water status of tropical tree seedlings is related to drought performance and distribution. *Functional Ecology* **23**(1): 93-102.

Leuzinger S, Bigler C, Wolf A, Körner C. 2009. Poor methodology for predicting large-scale tree die-off. *Proceedings of the National Academy of Sciences* **106**(38): E106-E106.

Li S, Feifel M, Karimi Z, Schuldt B, Choat B, Jansen S. 2015. Leaf gas exchange performance and the lethal water potential of five European species during drought. *Tree physiology* **36**(2): 179-192.

Mackay DS, Roberts DE, Ewers BE, Sperry JS, McDowell NG, Pockman WT. 2015. Interdependence of chronic hydraulic dysfunction and canopy processes can improve integrated models of tree response to drought. *Water Resources Research* **51**(8): 6156-6176.

Maherali H, Moura CF, Caldeira MC, Willson CJ, Jackson RB. 2006. Functional coordination between leaf gas exchange and vulnerability to xylem cavitation in temperate forest trees. *Plant, Cell, & Environment* **29**(4): 571-583.

Maherali H, Pockman WT, Jackson RB. 2004. Adaptive variation in the vulnerability of woody plants to xylem cavitation. *Ecology* **85**(8): 2184-2199.

Martin-StPaul N, Delzon S, Cochard H. 2017. Plant resistance to drought depends on timely stomatal closure. *Ecology Letters* **20**(11): 1437-1447.

Martínez-Vilalta J, Anderegg WR, Sapes G, Sala. 2018. Greater focus on water pools may improve our ability to understand and anticipate drought-induced mortality in plants. *New Phytologist*

McDowell N, Pockman WT, Allen CD, Breshears DD, Cobb N, Kolb T, Plaut J, Sperry J, West A, Williams DG. 2008. Mechanisms of plant survival and mortality during drought: why do some plants survive while others succumb to drought? *New Phytologist* **178**(4): 719-739.

McDowell NG, Beerling DJ, Breshears DD, Fisher RA, Raffa KF, Stitt M. 2011. The interdependence of mechanisms underlying climate-driven vegetation mortality. *Trends in Ecology & Evolution* **26**(10): 523-532.

McDowell NG, Williams A, Xu C, Pockman W, Dickman L, Sevanto S, Pangle R, Limousin J, Plaut J, Mackay D. 2016. Multi-scale predictions of massive conifer mortality due to chronic temperature rise. *Nature Climate Change* **6**(3): 295.

Menard S. 2002. *Applied logistic regression analysis*: Vol. 106 Sage.

Morillas L, Pangle RE, Maurer GE, Pockman WT, McDowell N, Huang CW, Krofcheck DJ, Fox AM, Sinsabaugh RL, Rahn TA. 2017. Tree mortality decreases water availability and ecosystem resilience to drought in piñon-juniper woodlands in the southwestern USA. *Journal of Geophysical Research: Biogeosciences*.

O'Brien MJ, Leuzinger S, Philipson CD, Tay J, Hector A. 2014. Drought survival of tropical tree seedlings enhanced by non-structural carbohydrate levels. *Nature Climate Change* **4**(8): 710.

R Core Team. 2013. R: A language and environment for statistical computing.

Sala A, Piper F, Hoch G. 2010. Physiological mechanisms of drought-induced tree mortality are far from being resolved. *New Phytologist* **186**(2): 274-281.

Sevanto S, McDowell NG, Dickman LT, Pangle R, Pockman WT. 2014. How do trees die? A test of the hydraulic failure and carbon starvation hypotheses. *Plant, Cell & Environment* **37**(1): 153-161.

Sperry J, Donnelly J, Tyree M. 1988. A method for measuring hydraulic conductivity and embolism in xylem. *Plant, Cell & Environment* **11**(1): 35-40.

Sperry JS, Christman MA, TORRES-RUIZ JM, Taneda H, Smith DD. 2012. Vulnerability curves by centrifugation: is there an open vessel artefact, and are 'r'shaped curves necessarily invalid? *Plant, Cell & Environment* **35**(3): 601-610.

Sperry JS, Love DM. 2015. What plant hydraulics can tell us about responses to climate-change droughts. *New Phytologist* **207**(1): 14-27.

Sperry JS, Tyree MT. 1988. Mechanism of Water Stress-Induced Xylem Embolism. *Plant Physiology* **88**(3): 581-587.

Sperry JS, Venturas MD, Anderegg WRL, Mencuccini M, Mackay DS, Wang Y, Love DM. 2016. Predicting stomatal responses to the environment from the optimization of photosynthetic gain and hydraulic cost. *Plant, Cell & Environment* 40(6), 816-830.

Torres-Ruiz JM, Jansen S, Choat B, McElrone AJ, Cochard H, Brodribb TJ, Badel E, Burlett R, Bouche PS, Brodersen CR. 2015. Direct X-ray microtomography observation confirms the induction of embolism upon xylem cutting under tension. *Plant physiology* **167**(1): 40-43.

Trifilò P, Casolo V, Raimondo F, Petrussa E, Boscutti F, Gullo MAL, Nardini A. 2017. Effects of prolonged drought on stem non-structural carbohydrates content and post-drought hydraulic recovery in Laurus nobilis L.: The possible link between carbon starvation and hydraulic failure. *Plant Physiology and Biochemistry* **120**: 232-241.

Tucker AO, Maciarello MJ, Tucker SS. 1991. A survey of color charts for biological descriptions. *Taxon*: 201-214.

Urli M, Porté AJ, Cochard H, Guengant Y, Burlett R, Delzon S. 2013. Xylem embolism threshold for catastrophic hydraulic failure in angiosperm trees. *Tree physiology* **33**(7): 672-683.

Van Mantgem PJ, Stephenson NL, Byrne JC, Daniels LD, Franklin JF, Fulé PZ, Harmon ME, Larson AJ, Smith JM, Taylor AH. 2009. Widespread increase of tree mortality rates in the western United States. *Science* **323**(5913): 521-524.

Venturas MD, MacKinnon ED, Jacobsen AL, Pratt RB. 2015. Excising stem samples underwater at native tension does not induce xylem cavitation. *Plant, Cell & Environment* **38**(6): 1060-1068.

Venturas MD, Sperry JS, Love DM, Frehner EH, Allred MG, Wang Y, Anderegg. 2018. A stomatal control model based on optimization of carbon gain versus hydraulic risk predicts aspen sapling responses to drought. *New Phytologist* **220**(3): 836-850.

Wheeler JK, Huggett BA, Tofte AN, Rockwell FE, Holbrook NM. 2013. Cutting xylem under tension or supersaturated with gas can generate PLC and the appearance of rapid recovery from embolism. *Plant, Cell & Environment* **36**(11): 1938-1949.

Wiley E, Hoch G, Landhäusser SM. 2017. Dying piece by piece: carbohydrate dynamics in aspen (Populus tremuloides) seedlings under severe carbon stress. *Journal of Experimental Botany* **68**(18): 5221-5232.

Wolf S, Keenan TF, Fisher JB, Baldocchi DD, Desai AR, Richardson AD, Scott RL, Law BE, Litvak ME, Brunsell NA. 2016. Warm spring reduced carbon cycle impact of the 2012 US summer drought. *Proceedings of the National Academy of Sciences*. **113**(21): 5880-5885.

CHAPTER V

A MATTER OF LIFE AND DEATH: ALTERNATIVE STABLE STATES IN TREES, FROM XYLEM TO ECOSYSTEMS

WILLIAM M. HAMMOND

Author's note: This chapter was published in *Frontiers in Forests and Global Change* November, 2020, doi: 10.3389/ffgc.2020.560409

Abstract

Global forests are experiencing widespread climate-induced mortality. Predicting this phenomenon has proven difficult, despite recent advances in understanding physiological mechanisms of mortality in individual trees along with environmental drivers of mortality at broad scales. With heat and drought as primary climatic drivers, and convergence on hydraulic failure as a primary physiological mechanism, new models are needed to improve our predictions of Earth's forests under future climate conditions. While much of ecology focuses on equilibrium states, transitions from one stable state to another are often described with alternative stable state theory (ASST), where systems can settle to more than one stable condition. Recent studies have identified threshold responses of hydraulic failure during tree mortality, indicating that alternative stable states may be present. Here, I demonstrate that the xylem of trees has characteristics indicative of alternative stable states. Through empirical evidence, I identify a catastrophic shift during hydraulic failure which prevents tree from returning to pre-droughted

physiological states after environmental stressors (e.g., drought, heat) are relieved. Thus, the legacy of climate-induced hydraulic failure likely contributes to reduced resilience of forests under future climate. I discuss the implications and future directions for including ASST in models of tree mortality.

Introduction

"All that lives must die", wrote Shakespeare in *Hamlet*, "passing through nature to eternity". Indeed, most all individuals eventually cease living—with only one of Earth's estimated > 8 million species found to be biologically immortal (Mora *et al.*, 2011; Lisenkova *et al.*, 2017). Organisms exist then in a chaotic state—persisting against the eventuality of death. Of life on Earth, individuals escaping death the longest are trees. Methuselah (a bristlecone pine, *Pinus longaeva*), is the oldest living individual—estimated to be 4,850 years old (Salzer *et al.*, 2019). Despite the ability of individual trees to escape death for millennia, widespread climate-induced mortality of trees in recent decades has become a global concern (Allen *et al.*, 2010). Every forest-bearing continent experienced climate-induced (associated with drought, heat, or both) tree mortality events—with effects ranging from canopy thinning to the transition of entire ecosystems to a non-forested state (Allen & Breshears, 1998; Scheffer *et al.*, 2001; Allen *et al.*, 2010; Gonzalez *et al.*, 2010; Choat *et al.*, 2012). As loss of forest cover corresponds to a loss of important ecosystem services such as carbon storage, biodiversity richness, and climate regulation (Foley, 2005), understanding conditions and mechanisms of tree mortality has been a focus of research at scales from individual trees to the entire planet (Brodribb & Cochard, 2009; Barigah *et al.*, 2013; Allen *et al.*, 2015; Hammond *et al.*, 2019).

Across global forests, observations have converged on the physiological process of hydraulic failure as ubiquitous in climate-induced tree mortality (Adams *et al.*, 2017). Hydraulic failure occurs when water under tension in the xylem becomes occluded by air emboli, interrupting transport of water and potentially resulting in whole-tree desiccation from which it is impossible to recover, e.g., death (Cochard & Delzon, 2013). Recent work has identified a threshold-like response between hydraulic failure and mortality, including direct quantification of a lethal dose of hydraulic failure in tree species for the first time (Urli *et al.*, 2013; Hammond *et al.*, 2019). While hydraulic failure has been ubiquitously associated with drought-induced mortality, other important agents of mortality include windthrow, lightning, and associated crown damage from storms (Negrón-Juárez *et al.*, 2010; Fontes *et al.*, 2018; Arellano *et al.*, 2019; Yanoviak *et al.*, 2020). Hotter droughts can induce leaf senescence via oxidative stress, leading to rapid canopy collapse (Matusick *et al.*, 2013; Jardine *et al.*, 2015). Finally, biotic agents (e.g., bark beetles, fungal pathogens) may drive drought- and heat-stressed trees to the breaking point (Cobb *et al.*, 2012; Anderegg *et al.*, 2015). While the complex and interactive effects of these multiple agents are not considered here, their amplification of tree mortality is likely to accelerate under further anthropogenic warming and drought (Allen *et al.*, 2015).

Existing tree mortality frameworks include that of McDowell (2008) which considers the physiological trade-off between hydraulic failure and so-called “carbon starvation”, when a tree exhausts available carbon to meet maintenance respiration during sufficiently long, source-limiting droughts (McDowell *et al.*, 2008). Others have quantified environmental signals to predict mortality (Hogg *et al.*, 2008; Phillips *et al.*, 2009), without explicitly considering the role of physiological responses to environment, while more recent attempts have combined environmental signals with physiological responses (Breshears *et al.*, 2005; Anderegg *et al.*, 2012; Schwantes *et al.*, 2016; Johnson *et al.*, 2018). With an aim toward anticipating ecosystem shifts and management actions which might promote or inhibit these changes, state-and-transition

models have been developed for managing forests following die-off events (Cobb *et al.*, 2017). Whatever the framework, all have included the concept of thresholds—that there exist conditions beyond which it becomes more likely trees will die, than survive. Despite these advances, the ability to predict mortality at any scale (and especially, across scales) remains a grand challenge for Ecology. It is natural then to ask—what improvements can be made in our ability to predict when a tree, stand, or entire forest is likely to die?

Transitions in ecosystems have long been investigated through alternative stable states theory (ASST) (Holling, 1973; May, 1977; Scheffer *et al.*, 2001). While threshold responses such as those observed during climate induced tree mortality are an indicator that a system may have more than one stable state—other criteria must also be met. Alternative stable states for a system exist only if that system can settle to alternative states under the same external conditions (Scheffer, 2009a). What are the applications, limitations, and extensions of our understanding that can be brought to bear by considering climate-induced tree mortality through the lens of ASST? First, I must acknowledge that ASST has already been used to investigate vegetation shifts at the ecosystem level for some time. Observations in the west African Sahel have shown that communities of woody vegetation show clear signs of having alternative stable states—oscillating at multi-decadal periods between savannah and forested states that track with changes in regional climate (Scheffer *et al.*, 2001; Gonzalez *et al.*, 2010). Here, I propose the application of ASST to the xylem tissue of trees, and implications of such an ASST approach to individuals and higher levels of ecological organization.

Brief review of Alternative Stable States (ASST) concepts

First, a few definitions should be established with which we can discuss ASST in the context of a single tree. Attractors can be defined as a single state toward which a system can converge and may include cycles or stable points; in ball and hill models the valleys/basins are stable attractors, or states, and the depth of these basins indicates how resilient they are to shifts. Catastrophic shifts occur when some minor change at a critical point (the so-called tipping point, or catastrophic bifurcation) shifts a system from one attractor to an alternative attractor. These catastrophic shifts are unidirectional, such that hysteresis exists and transitions between two stable states require an unequal change in external conditions. These concepts are visually communicated via stability landscapes¸ using a ball to represent the ecosystem's present state, basins as attractors, and hills as tipping points (as later in this paper, in Fig 1, 2). While these brief definitions suffice for the present paper, I refer readers interested in a deep review of these concepts to Scheffer et al. 2009b.

Xylem as a study system

From embryogenesis through reproductive maturity, trees have a remarkable diversity of forms and functions, all of which depend upon the availability of water (Givnish, 1979; Givnish, 2002). Within a single tree, connected cell types, tissues, and organs carry out many processes necessary for survival, growth, and reproduction of the whole organism (Holbrook & Zwieniecki, 2011). Of Earth's diverse plant forms, trees are best distinguished by their xylem. This extensive secondary woody tissue functions in mechanical support—responsible for trees being the tallest, and also the

largest (by volume) organisms on the planet (Hacke & Sperry, 2015), leading to their dominance in global estimates of biomass (Bar-On *et al.*, 2018). More than just a scaffold, xylem conducting large volumes of water across long distances efficiently (Tyree & Zimmermann, 2013), at minimal energy costs operating under cohesion-tension, was critical to the development of trees as a life form on Earth (Dixon & Joly, 1894). For an individual tree, xylem function is central to growth, survival, and reproduction (Hacke & Sperry, 2015). As hydraulic failure of xylem has been identified as one of the most important agents in climate-driven tree mortality (Adams *et al.*, 2017; Brodribb *et al.*, 2020), I will demonstrate the characteristics of xylem physiology which make it suitable for the application of ASST.

Whole-plant Xylem as a system with alternative stable states: case study in *Juniperus*

Xylem is composed of vascular elements (in Angiosperms) and tracheids (in gymnosperms, and in combination with vessels in some angiosperms) which are dead at functional maturity (Holbrook & Zwieniecki, 2011). During drought, the combination of increased atmospheric demand for moisture and decreased soil water availability creates tension in the xylem's water column, a force quantified as water potential (Scholander *et al.*, 1965; Breshears *et al.*, 2013). Considering water potential (hereafter, Ψ) as an external condition to the system of xylem, we can acknowledge that as Ψ declines (becomes more negative), tension ($|\Psi|$) builds to the point that eventually, embolism is seeded into the xylem and begins to spread, occluding water transport (Sperry & Tyree, 1988; Cochard *et al.*, 1992). While debates are ongoing regarding the capacity of xylem to refill (Klein *et al.*, 2018; Lamarque *et al.*, 2018), in this paper I provide observations from a manipulative experiment showing that trees which survived extreme

hydraulic failure, eventually restored function via radial growth—a lengthy process—and did not refill appreciable amounts of embolized xylem.

What evidence qualifies xylem as a system which possesses alternative stable states? The first evidence that xylem has more than one alternative stable state, is that hydraulic failure occurs over a relatively narrow range of water potentials, resulting in typical "s-shaped" vulnerability curves with sharp transitions between near zero and near complete embolism of xylem (Cochard *et al.*, 2005). Threshold-like responses are an indicator of alternative stable states within a system (Scheffer, 2009a), but alone are insufficient to indicate the existence of alternative stable states (Scheffer, 2009b). In addition to a threshold-like response, it must be possible for the system (here, xylem hydraulic function) to stabilize in alternate states under similar external conditions (here, Ψ). Using observations from a recent empirical study, I demonstrate that hydraulic failure not only shows a threshold response, but also catastrophic shifts to alternative stable states in the xylem of trees.

In a greenhouse experiment, I imposed drought on reproductively mature *Juniperus virginiana* L. (family *Cupressaceae*) in pots. Withholding water until pre-assigned targets of water potential, I monitored trees for death or survival after relieving drought. Prior to the onset of drought, I conducted active xylem staining to identify which xylem in the tree was functioning and found across the population (42 trees) that nearly all the xylem was functional (stained red, as in Figure 1A, left side). By comparison, I present a similar active xylem stain taken at the end of a full growing season's recovery (Figure 1A, right side) from the same tree, which survived a minimum water potential of < -9 MPa, resulting in > 84 percent loss of conductivity (hereafter, PLC). Substantial radial growth (tissue produced past the position of the vascular cambium at drought's maximum, Fig 1A, dashed yellow line) was required to restore conductivity of the woody tissue and embolism remained even five months after water potentials returned to pre-drought conditions (Fig 1A, right side).

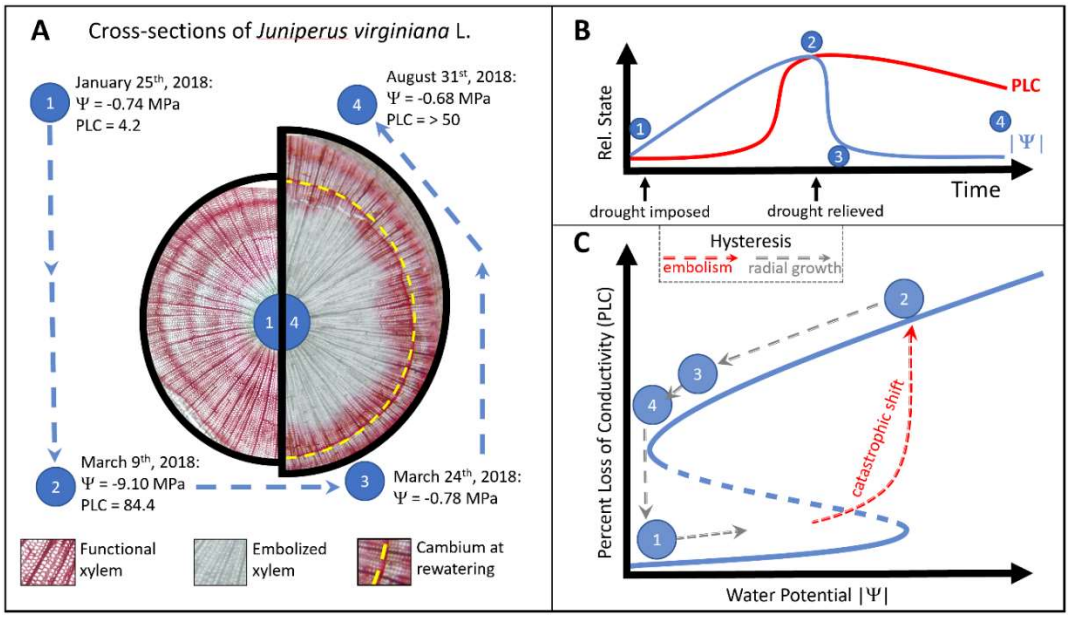

Figure 1. In panel (A), cross-sections taken from a single *Juniperus virginiana* L. tree at time point (1) and (4) are shown on the left and right, respectively. Physiological measures of drought stress (Ψ, percent loss of conductivity—PLC) are shown for four time points during the drought-rewatering experiment from the same tree (points 1-4, data from Hammond *et al*., in prep). Panel (B) shows the relationship between the relative state of PLC (red line) or the absolute value of water potential (|Ψ|, blue line) during the duration of the experiment. While |Ψ| rapidly resumes the pre-drought condition after drought is relieved, PLC remains high as the xylem is in an alternative stable state. The transition between (1) and (2) is shown in panel (C) as a catastrophic shift, where once a large portion of the xylem is embolized, function cannot be restored by the simple relaxation of xylem tension. Arrows indicate the direction of hysteresis, with counterclockwise arrows indicating hysteresis. Red arrows represent a catastrophic shift to an alternative, embolized stable state, which requires radial growth (grey arrows) to return to the previous state.

Despite returning to the pre-drought state in xylem tension, the system state of hydraulic failure lingered—demonstrating that a hysteresis exists between the alternative states of fully functional xylem, and xylem having experienced extreme hydraulic failure (Fig 1B). Consequently, when changes in Ψ during drought led to a state shift (from functional, to embolized xylem), a return to the Ψ associated with function (a water potential near zero) was not accompanied by restoration of xylem function. This meets the qualifications of a catastrophic shift, as there is hysteresis—conductivity of water through the xylem cannot resume its prior state, even though the external condition (xylem tension, |Ψ|) has returned to initial conditions (Fig 1C).

Resilience: from xylem to individual trees to communities

While xylem possesses alternative stable states, the same concept cannot be applied to the "life or death" of an individual tree. As illustrated in Fig. 2A, death of an organism does not represent an alternative state, but rather a terminal one. Once an organism is committed to death (e.g., past the tipping point in Fig. 2A), it leaves the stability landscape—and cannot return. Thus, once whole-organism death occurs, it is best described as an irreversible threshold transition, without an alternative stable state (Scheffer, 2009b). On the other hand, trees may die-back at extremities—fusing off fine roots and terminal branches due to excessive embolism limiting available water to canopy function (Johnson *et al.*, 2016; Jump *et al.*, 2017). In the context of stability landscapes, mortality can be represented as a cliff—once the organism passes the tipping point, it is committed to death (Fig. 2A). It is important to mention, that the concept of resilience can and should be invoked regarding hydraulic function and failure in the xylem of trees. Increasing diversity of the xylem network (e.g., broad vessel, tracheid, or pit size distributions, or inclusion of hyper-embolism-resistant vasicentric tracheids, as in many Mediterranean plants) will increase the strength of the attractor of hydraulic function (Carlquist, 1985). Species of trees

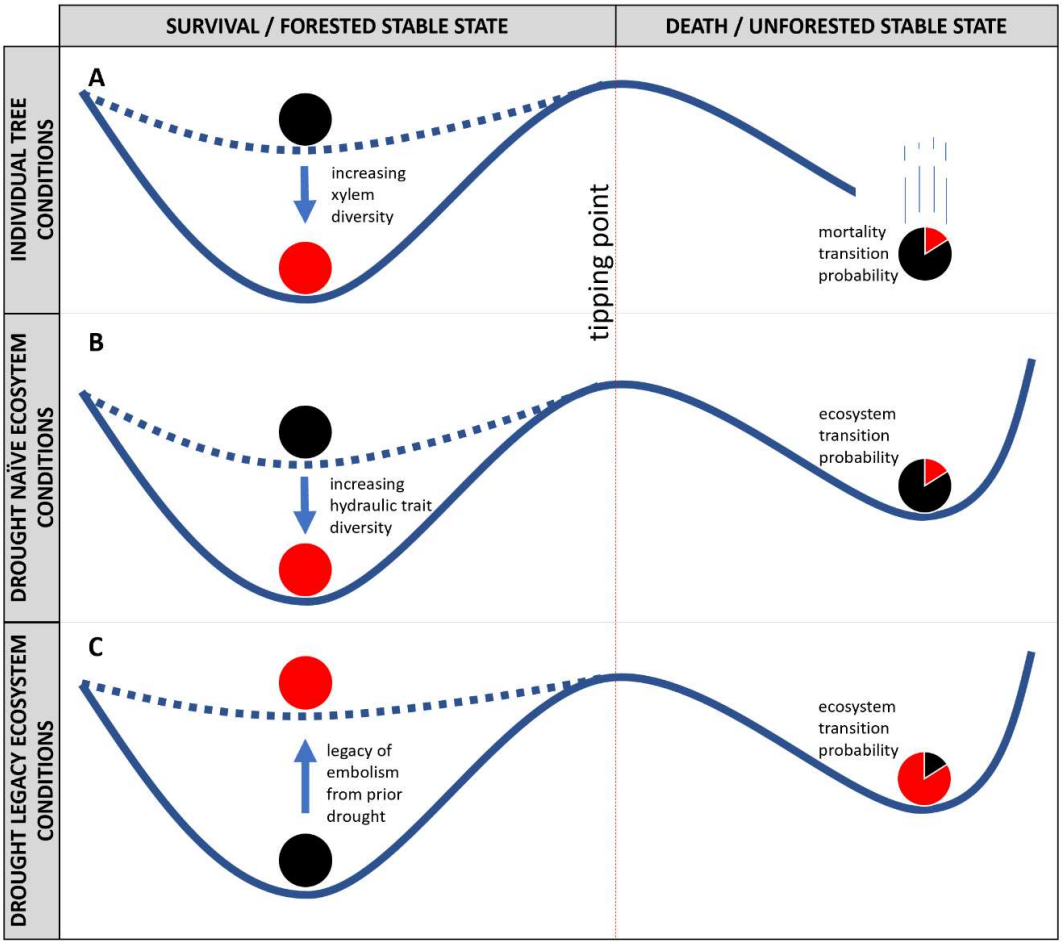

Figure 2: Stability landscape models for an individual tree (A), drought naïve ecosystems (B), and drought legacy ecosystems (C), with tree or ecosystem state on x-axis, and conditions on the y-axis. The tipping point between survival and permanent death of an individual tree (A), and for forest die-off of an ecosystem (B,C) is represented by a dashed red line. The depth of basins of attraction to the left of the tipping point can increase from shallow (low resilience, black ball) as diversity in hydraulic traits within an ecosystem (as in panel B), (or within a tree, xylem anatomical heterogeneity, as in panel A) increases (high resilience, red ball). To the right of the tipping point, the proportional shading of the ball illustrates that it is less likely a resilient system would transition from forest to non-forest, relative to a less hydraulically diverse system (or tree). In panel (C), the legacy of hydraulic failure decreases ecosystem resilience (red ball), and ecosystem transition probability to a non-forested state is thus increased.

surviving in some of Earth's driest habitats have accomplished such a feat by including both efficient (yet vulnerable to embolism) vessel elements and less efficient (yet safer from embolism) vasicentric tracheids in their xylem anatomy (Carlquist, 1985), such that a much broader range of water potentials must be experienced in order to induce a system-wide

catastrophic shift (Fig. 2A). Increasing xylem anatomical diversity within an individual tree is thus expected to increase resilience (Fig. 2A, red ball), reducing the probability of a transition to mortality.

In contrast to the outcomes of individual trees, potential outcomes at population and community levels include alternative stable states (Fig 2B, 2C). Communities of trees display remarkable diversity in hydraulic traits, such as the water potential corresponding to 50% loss of conductivity in the xylem (P50). For example, global observations have shown that P50 can vary within a biome by up to an order of magnitude, while across biomes the median value of P50 is relatively stable (McCulloh et al., 2019). Furthermore, traits like P50 seem to be conserved within lineages of plants (Maherali *et al.*, 2004; Sanchez-Martinez *et al.*, 2020) indicating that biodiversity of species and higher taxonomic orders within a forest correspond to increased diversity in hydraulic traits. Increased hydraulic trait diversity within an ecosystem would thus increase ecosystem resilience (Fig 2B, red ball), as not all species within a system would experience catastrophic shifts within their xylem under the same amount of environmental stress; thus reducing the whole-ecosystem transition probability for a given set of environmental drivers. An example of diversity's benefit was apparent during recent widespread mortality of pinyon pine (*Pinus edulis*) in pinyon-juniper woodlands of the southwestern United States (McDowell et al., 2008). Pinyon trees died during hot droughts, but junipers survived. In subsequent years, junipers facilitated (by providing a shaded, cooler, and wetter microclimate) recruitment of pinyon back into the system, a phenomenon known to prevent mortality in recruiting trees (Breshears et al., 2018). In contrast, if junipers were not present, the system may lack sufficient resilience to remain forested as recruitment in the open would be more difficult than recruiting beneath the shady canopy of a mature nurse tree. Similarly phenomena have been documented during globally distributed climate-induced tree mortality events, for example relatively

embolism-prone *Eucalyptus* species saw significant mortality during recent droughts in eastern Australia, while more embolism-resistant *Callitris* species survived (Brodribb *et al.*, 2020).

Finally, trees surviving extreme drought retain the legacy of hydraulic failure (as in Fig. 1A, Fig. 3), which could reduce resilience across an ecosystem (Fig. 2C). The extent to which the increasing resilience from within tree hydraulic diversity (Fig. 2A) and within community hydraulic diversity (Fig. 2B) can buffer ecosystem resilience decreases due to the legacy of hydraulic failure (as in Fig. 2C) is unknown, and of critical importance for future investigations. Common gardens, including urban forests, may provide some insight as study systems, to investigate responses to intensified local microclimates in anticipation of eventually drier and warmer regional climates on natural forests. Presently diverse forests (e.g., warm tropical forests) may experience reductions in diversity as climate continues to warm and dry, while cooler temperate and boreal forests may increase their species and hydraulic diversities as warming makes recruitment of newer species possible.

Conclusions and future directions

When it comes to life and death of trees, alternative stable state theory is a useful tool to highlight the catastrophic shifts occurring in xylem tissues of individual trees, and the additive ecosystem-wide effect for potential transitions to alternative states. Transitions from a forested to non-forested state may appear abrupt (Allen & Breshears, 1998; Breshears et al., 2009), yet the underlying conditions of hydraulic function could be changing gradually. As demonstrated in Fig.

1A, monitoring physiological drivers like water potential (the most commonly reported indicator of drought stress) is insufficient to detect the hydraulic state of trees which have survived

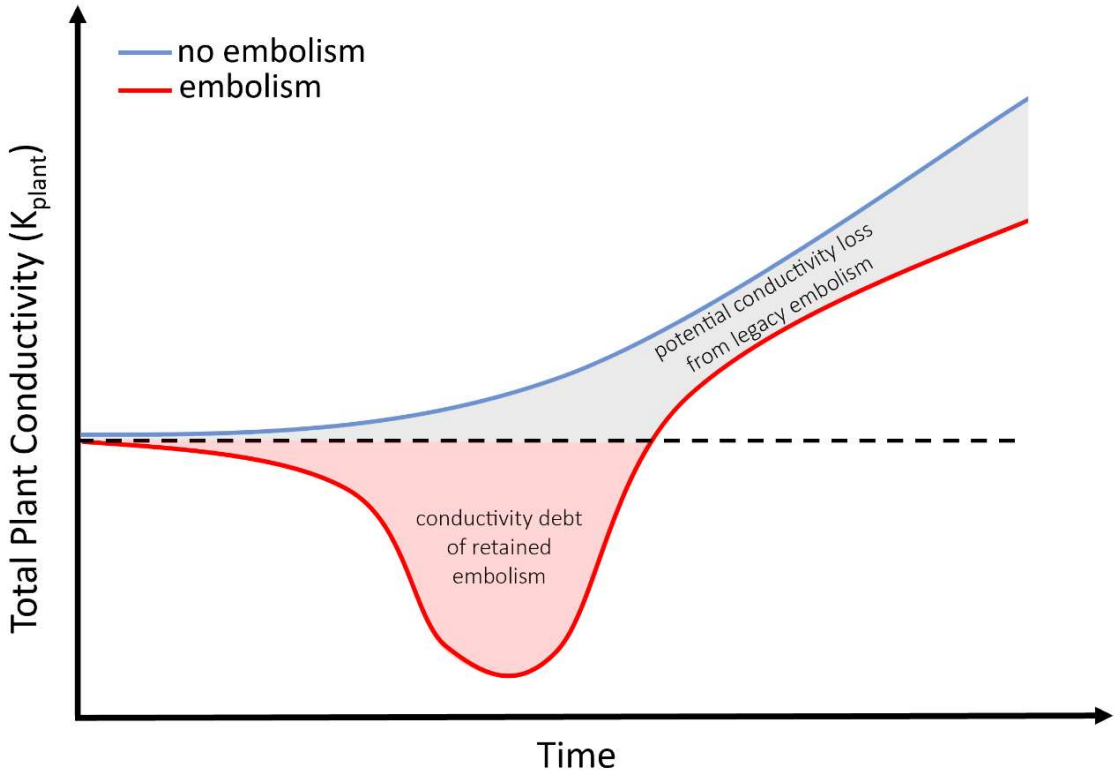

Figure 3. Conceptual diagram comparing the increasing total plant conductivity of a tree that has not experienced embolism-inducing drought stress (blue line) with a tree which has survived drought (red line) and retained significant embolism. Red shading indicates hydraulic debt, or loss of function from pre-drought levels (indicated by the dashed black line). Grey shading indicates the potential conductivity loss from legacy embolism once pre-drought conductivity has been restored via radial growth

prolonged drought stress resulting in the accrual of embolism in woody tissues. Measuring water potentials even a few weeks after drought's relief would imply healthy, functional water relations when in fact a tree's xylem may have experienced and retained significant levels of embolism. Thus, while there exists some maximum level of perturbation in (temperature, soil moisture deficit) beyond which it becomes more likely that populations of trees composing the forest will die, rather than survive during a single climatic event, we must also consider the legacy of drought (Fig. 2C). Using an ASST approach to understand state of xylem within trees provides a

framework to include drought's legacy in future models of forest mortality. Models should include both an accounting for the immediate hydraulic debt (actual loss of hydraulic function due to embolism) and the legacy of lost potential hydraulic function had trees not experienced and retained embolism (as in Fig. 3). For example, as growth rates and growing seasons of many important forest trees are well described, along with growing databases of species-specific embolism resistance (Choat et al. 2012.), future models will be able to account for both the accumulation of embolism under stress, and the long period of growth required to erase the functional debt incurred by this legacy of embolism via regrowth. Emerging evidence suggests the legacy of embolism has severe downstream consequences, as it was found to nearly halve gas exchange rates after drought relief in seedlings of *Pinus Sylvestris* (Rehschuh et al., 2020). Future work could include an analysis of die-back dependent upon repeated non-lethal drought events, preceding a lethal drought event. Secondary effects of retaining xylem embolism (canopy and fine root die-back) may slow growth, produce less vulnerable xylem in subsequent years of growth, and buffer or offset the perceived cost of retained hydraulic dysfunction. From meta-analysis of empirical data, to hindcasting of known mortality on local to regional scales, including a measure of retained hydraulic dysfunction (as demonstrated through ASST methods here) will enhance our ability to predict the fates of future forests.

Acknowledgements

I wish to thank Henry Adams for asking me to consider the intersection of xylem embolism and critical transitions. W.M.H. was supported by the NSF GRFP (1-746055) and by the Oklahoma Center for the Advancement of Science and Technology Plant Basic Research Program (PS17-006).

References

Adams HD, Zeppel MJB, Anderegg WRL, Hartmann H, Landhäusser SM, Tissue DT, Huxman TE, Hudson PJ, Franz TE, Allen CD, et al. 2017. A multi-species synthesis of physiological mechanisms in drought-induced tree mortality. *Nature Ecology & Evolution* **1**(9): 1285-1291.

Allen CD, Breshears DD. 1998. Drought-induced shift of a forest–woodland ecotone: rapid landscape response to climate variation. *Proceedings of the National Academy of Sciences* **95**(25): 14839-14842.

Allen CD, Breshears DD, McDowell NG. 2015. On underestimation of global vulnerability to tree mortality and forest die-off from hotter drought in the Anthropocene. *Ecosphere* **6**(8): art129.

Allen CD, Macalady AK, Chenchouni H, Bachelet D, McDowell N, Vennetier M, Kitzberger T, Rigling A, Breshears DD, Hogg ET. 2010. A global overview of drought and heat-induced tree mortality reveals emerging climate change risks for forests. *Forest ecology and management* **259**(4): 660-684.

Anderegg WR, Berry JA, Smith DD, Sperry JS, Anderegg LD, Field CB. 2012. The roles of hydraulic and carbon stress in a widespread climate-induced forest die-off. *Proceedings of the National Academy of Sciences* **109**(1): 233-237.

Anderegg WR, Hicke JA, Fisher RA, Allen CD, Aukema J, Bentz B, Hood S, Lichstein JW, Macalady AK, McDowell N. 2015. Tree mortality from drought, insects, and their interactions in a changing climate. *New Phytologist* **208**(3): 674-683.

Arellano G, Medina NG, Tan S, Mohamad M, Davies SJ. 2019. Crown damage and the mortality of tropical trees. *New Phytologist* **221**(1): 169-179.

Bar-On YM, Phillips R, Milo R. 2018. The biomass distribution on Earth. *Proceedings of the National Academy of Sciences* **115**(25): 6506-6511.

Barigah TS, Charrier O, Douris M, Bonhomme M, Herbette S, Améglio T, Fichot R, Brignolas F, Cochard H. 2013. Water stress-induced xylem hydraulic failure is a causal factor of tree mortality in beech and poplar. *Annals of botany* **112**(7): 1431-1437.

Breshears DD, Adams HD, Eamus D, McDowell NG, Law DJ, Will RE, Williams AP, Zou CB. 2013. The critical amplifying role of increasing atmospheric moisture demand on tree mortality and associated regional die-off. **4**.

Breshears DD, Carroll CJW, Redmond MD, Wion AP, Allen CD, Cobb NS, Meneses N, Field JP, Wilson LA, Law DJ, et al. 2018. A Dirty Dozen Ways to Die: Metrics and Modifiers of Mortality Driven by Drought and Warming for a Tree Species. *Frontiers in Forests and Global Change* **1**.

Breshears DD, Cobb NS, Rich PM, Price KP, Allen CD, Balice RG, Romme WH, Kastens JH, Floyd ML, Belnap J, et al. 2005. Regional vegetation die-off in response to global-change-type drought. *Proceedings of the National Academy of Sciences* **102**(42): 15144-15148.

Breshears DD, Myers OB, Meyer CW, Barnes FJ, Zou CB, Allen CD, McDowell NG, Pockman WT. 2009. Tree die-off in response to global change-type drought: Mortality insights from a decade of plant water potential measurements. *Frontiers in Ecology and the Environment* **7**(4): 185-189.

Brodribb TJ, Cochard H. 2009. Hydraulic failure defines the recovery and point of death in water-stressed conifers. *Plant Physiology* **149**(1): 575-584.

Brodribb TJ, Powers J, Cochard H, Choat B. 2020. Hanging by a thread? Forests and drought. *Science* **368**(6488): 261-266.

Carlquist S. 1985. Vasicentric tracheids as a drought survival mechanism in the woody flora of southern California and similar regions; review of vasicentric tracheids. *Aliso: A Journal of Systematic and Evolutionary Botany* **11**(1): 37-68.

Choat B, Jansen S, Brodribb TJ, Cochard H, Delzon S, Bhaskar R, Bucci SJ, Feild TS, Gleason SM, Hacke UG, et al. 2012. Global convergence in the vulnerability of forests to drought. *Nature* **491**(7426): 752-755.

Cobb RC, Filipe JA, Meentemeyer RK, Gilligan CA, Rizzo DM. 2012. Ecosystem transformation by emerging infectious disease: loss of large tanoak from California forests. *Journal of Ecology* **100**(3): 712-722.

Cobb RC, Ruthrof KX, Breshears DD, Lloret F, Aakala T, Adams HD, Anderegg WR, Ewers BE, Galiano L, Grünzweig JM. 2017. Ecosystem dynamics and management after forest die-off: a global synthesis with conceptual state-and-transition models. *Ecosphere* **8**(12).

Cochard H, Cruiziat P, Tyree MT. 1992. Use of positive pressures to establish vulnerability curves: further support for the air-seeding hypothesis and implications for pressure-volume analysis. *Plant Physiology* **100**(1): 205-209.

Cochard H, Damour G, Bodet C, Tharwat I, Poirier M, Améglio T. 2005. Evaluation of a new centrifuge technique for rapid generation of xylem vulnerability curves. *Physiologia Plantarum* **124**(4): 410-418.

Cochard H, Delzon S. 2013. Hydraulic failure and repair are not routine in trees. *Annals of Forest Science* **70**(7): 659-661.

Dixon HH, Joly J. 1894. On the ascent of sap. *Proceedings of the Royal Society of London* **57**: 3-5.

Foley JA. 2005. Global Consequences of Land Use. *Science* **309**(5734): 570-574.

Fontes CG, Chambers JQ, Higuchi N. 2018. Revealing the causes and temporal distribution of tree mortality in Central Amazonia. *Forest ecology and management* **424**: 177-183.

Givnish T 1979. On the adaptive significance of leaf form. *Topics in plant population biology*: Springer, 375-407.

Givnish TJ. 2002. Adaptive significance of evergreen vs. deciduous leaves: solving the triple paradox. *Silva fennica* **36**(3): 703-743.

Gonzalez P, Neilson RP, Lenihan JM, Drapek RJ. 2010. Global patterns in the vulnerability of ecosystems to vegetation shifts due to climate change. *Global Ecology and Biogeography* **19**(6): 755-768.

Hacke U, Sperry JS. 2015. *Functional and ecological xylem anatomy*: Springer.

Hammond WM, Yu K, Wilson LA, Will RE, Anderegg WRL, Adams HD. 2019. Dead or dying? Quantifying the point of no return from hydraulic failure in drought-induced tree mortality. *New Phytologist*.

Hogg EH, Brandt JP, Michaelian M. 2008. Impacts of a regional drought on the productivity, dieback, and biomass of western Canadian aspen forests. *Canadian journal of forest research* **38**(6): 1373-1384.

Holbrook NM, Zwieniecki MA. 2011. *Vascular transport in plants*: Elsevier.

Holling CS. 1973. Resilience and Stability of Ecological Systems. *Annual Review of Ecology and Systematics* **4**(1): 1-23.

Jardine KJ, Chambers JQ, Holm J, Jardine AB, Fontes CG, Zorzanelli RF, Meyers KT, De Souza VF, Garcia S, Gimenez BO. 2015. Green leaf volatile emissions during high temperature and drought stress in a central amazon rainforest. *Plants* **4**(3): 678-690.

Johnson DM, Domec JC, Berry ZC, Schwantes AM, Woodruff DR, McCulloh KA, Polley HW, Wortemann R, Swenson JJ, Mackay DS. 2018. Co-occurring woody species have diverse hydraulic strategies and mortality rates during an extreme drought. *Plant, Cell & Environment*.

Johnson DM, Wortemann R, McCulloh KA, Jordan-Meille L, Ward E, Warren JM, Palmroth S, Domec J-C. 2016. A test of the hydraulic vulnerability segmentation hypothesis in angiosperm and conifer tree species. *Tree Physiology* **36**(8): 983-993.

Jump AS, Ruiz-Benito P, Greenwood S, Allen CD, Kitzberger T, Fensham R, Martínez-Vilalta J, Lloret F. 2017. Structural overshoot of tree growth with climate variability and the global spectrum of drought-induced forest dieback. *Global Change Biology* **23**(9): 3742-3757.

Klein T, Zeppel MJ, Anderegg WR, Bloemen J, De Kauwe MG, Hudson P, Ruehr NK, Powell TL, von Arx G, Nardini A. 2018. Xylem embolism refilling and resilience against drought-induced mortality in woody plants: processes and trade-offs. *Ecological research* **33**(5): 839-855.

Lamarque LJ, Corso D, Torres-Ruiz JM, Badel E, Brodribb TJ, Burlett R, Charrier G, Choat B, Cochard H, Gambetta GA. 2018. An inconvenient truth about xylem resistance to embolism in the model species for refilling Laurus nobilis L. *Annals of Forest Science* **75**(3): 88.

Lisenkova A, Grigorenko A, Tyazhelova T, Andreeva T, Gusev F, Manakhov A, Goltsov AY, Piraino S, Miglietta M, Rogaev E. 2017. Complete mitochondrial genome and evolutionary analysis of Turritopsis dohrnii, the "immortal" jellyfish with a reversible life-cycle. *Molecular Phylogenetics and Evolution* **107**: 232-238.

Maherali H, Pockman WT, Jackson RB. 2004. ADAPTIVE VARIATION IN THE VULNERABILITY OF WOODY PLANTS TO XYLEM CAVITATION. **85**(8): 2184-2199.

Matusick G, Ruthrof KX, Brouwers NC, Dell B, Hardy GSJ. 2013. Sudden forest canopy collapse corresponding with extreme drought and heat in a mediterranean-type eucalypt forest in southwestern Australia. *European Journal of Forest Research* **132**(3): 497-510.

May RM. 1977. Thresholds and breakpoints in ecosystems with a multiplicity of stable states. *Nature* **269**(5628): 471-477.

McCulloh KA, Domec JC, Johnson DM, Smith DD, Meinzer FC. 2019. A dynamic yet vulnerable pipeline: Integration and coordination of hydraulic traits across whole plants. *Plant, Cell & Environment* **42**(10): 2789-2807.

McDowell N, Pockman WT, Allen CD, Breshears DD, Cobb N, Kolb T, Plaut J, Sperry J, West A, Williams DG. 2008. Mechanisms of plant survival and mortality during drought: why do some plants survive while others succumb to drought? *New Phytologist* **178**(4): 719-739.

Mora C, Tittensor DP, Adl S, Simpson AG, Worm B. 2011. How many species are there on Earth and in the ocean? *PLoS Biol* **9**(8): e1001127.

Negrón-Juárez RI, Chambers JQ, Guimaraes G, Zeng H, Raupp CF, Marra DM, Ribeiro GH, Saatchi SS, Nelson BW, Higuchi N. 2010. Widespread Amazon forest tree mortality from a single cross-basin squall line event. *Geophysical Research Letters* **37**(16).

Phillips OL, Aragao LEOC, Lewis SL, Fisher JB, Lloyd J, Lopez-Gonzalez G, Malhi Y, Monteagudo A, Peacock J, Quesada CA, et al. 2009. Drought Sensitivity of the Amazon Rainforest. *Science* **323**(5919): 1344-1347.

Rehschuh R, Cecilia A, Zuber M, Faragó T, Baumbach T, Hartmann H, Jansen S, Mayr S, Ruehr N. 2020. Drought-induced xylem embolism limits the recovery of leaf gas exchange in Scots pine. *Plant Physiology* **184**(2): 852-864.

Salzer MW, Pearson CL, Baisan CH. 2019. Dating the methuselah walk bristlecone pine floating chronologies. *Tree-Ring Research* **75**(1): 61-66.

Sanchez-Martinez P, Martínez-Vilalta J, Dexter KG, Segovia RA, Mencuccini M. 2020. Adaptation and coordinated evolution of plant hydraulic traits. *Ecology Letters*.

Scheffer M. 2009a. Alternative stable states and regime shifts in ecosystems. *The Princeton guide to ecology, Princeton, Princeton university press* **809**: 395-406.

Scheffer M. 2009b. *Critical transitions in nature and society*: Princeton University Press.

Scheffer M, Carpenter S, Foley JA, Folke C, Walker B. 2001. Catastrophic shifts in ecosystems. *Nature* **413**(6856): 591-596.

Scholander PF, Bradstreet ED, Hemmingsen E, Hammel H. 1965. Sap pressure in vascular plants: negative hydrostatic pressure can be measured in plants. *Science* **148**(3668): 339-346.

Schwantes AM, Swenson JJ, Jackson RB. 2016. Quantifying drought-induced tree mortality in the open canopy woodlands of central Texas. *Remote sensing of environment* **181**: 54-64.

Sperry JS, Tyree MT. 1988. Mechanism of water stress-induced xylem embolism. *Plant Physiology* **88**(3): 581-587.

Tyree MT, Zimmermann MH. 2013. *Xylem structure and the ascent of sap*: Springer Science & Business Media.

Urli M, Porté AJ, Cochard H, Guengant Y, Burlett R, Delzon S. 2013. Xylem embolism threshold for catastrophic hydraulic failure in angiosperm trees. *Tree Physiology* **33**(7): 672-683.

Yanoviak SP, Gora EM, Bitzer PM, Burchfield JC, Muller-Landau HC, Detto M, Paton S, Hubbell SP. 2020. Lightning is a major cause of large tree mortality in a lowland neotropical forest. *New Phytologist* **225**(5): 1936-1944.

CHAPTER VI

DYING ON TIME: TRAITS INFLUENCING THE DYNAMICS OF TREE MORTALITY RISK FROM DROUGHT

William M. Hammond[1] and Henry D. Adams[1]

[1]Oklahoma State University, Department of Plant Biology, Ecology, and Evolution. Stillwater, OK, USA.

Author's note: This chapter was published in *Tree Physiology* June, 2019, doi: 10.1093/treephys/tpz050

Understanding physiological responses that occur during drought-induced stress and mortality are important for advancing our capability to predict tree death. In recent decades, widespread elevated tree mortality has inspired a large volume of research attempting to understand why and when trees will die under drought stress (Hartmann et al. 2018a). Much of this research has described the physiological responses as trees die from drought, yet reliably predicting when trees will die remains elusive. Improving tree mortality predictions requires a pivot from describing the process of tree mortality to identifying which risk factors influence the timing of tree death (Hartmann et al. 2018a). Many experiments have studied tree mortality mechanisms through the lens of McDowell *et al*. (2008), investigating hydraulic failure, carbon starvation, and (rarely) biotic attack; later, a synthesis of global observations shows that hydraulic failure was ubiquitously associated with drought-induced tree mortality (Adams et al. 2017). In contrast, identifying common responses in non-structural carbohydrate (NSC) dynamics

during tree mortality has proven difficult, and while responses have varied considerably, NSCs can play an important role in mitigating drought stress (Hartmann et al. 2018b; O'Brien et al. 2014). For example, manipulating the amount of NSCs available to a plant at the onset of drought stress was found to influence survival (O'Brien et al. 2014), and observations of delayed mortality in the field following drought can be explained by carbon dynamics over years (Trugman et al. 2018). Due to the extensive cost and challenge of causing drought-induced death in a forest, experiments determining which physiological responses and traits have the most influence during lethal drought stress are often investigated with juvenile trees growing in pots. It should be noted that there is a middle ground, where larger, and/or older trees could be droughted over longer time-scales (multiple years) to understand lethal physiological responses to a slower progression of water stress, as is often observed during drought in natural systems (Dickman et al. 2015, McDowell et al. 2019).

In their recent article, Blackman *et al.* (2019) investigate the time to critical plant water potentials (Ψ_{crit}) for four tree species representative of broad water-use strategies, and consider the influence of physiological and growth responses. These Ψ_{crit} values, water potentials corresponding to 88% loss of hydraulic conductivity for angiosperms and 50% for gymnosperms, are thought to represent a physiological point of no return from drought-induced hydraulic failure (Barigah et al. 2013; Brodribb and Cochard 2009; Urli et al. 2013). In their paper, Blackman *et al.* conducted a lethal dry-down of four tree species representing drought response strategies. They studied three angiosperms native to Australia (*Casuarina cunninghamia, Eucalyptus sideroxylon,* and *Eucalyptus tereticornis*) and one introduced gymnosperm (*Pinus radiata*) that occupy a wide range of ecohydrological niches. The three angiosperm trees reached Ψ_{crit} much more rapidly (39 – 57 days) than the gymnosperm (156 days). Of note, many traits measured also showed large differences: angiosperm species generally had narrower hydraulic safety margins (0.75 to 1.67 MPa), lower turgor loss points (TLP, -2.04 to -2.57 MPa), lower leaf capacitance (0.41 to 0.81

mol m^{-2} MPa^{-1}), lower leaf saturated water content (1.23 to 1.64 g g^{-1}) and much higher minimum leaf conductance (12.6 to 19.7 mmol m^{-2} s^{-1}). In contrast, the gymnosperm *P. radiata* showed a wide safety margin (2.36 MPa), higher TLP (-1.07 MPa), higher leaf capacitance (2.76 mol m^{-2} MPa^{-1}), higher leaf saturated water content (2.37 g g^{-1}), and a minimum leaf conductance an order of magnitude lower (1.9 mmol m^{-2} s^{-1}) than the angiosperms. Despite much lower Ψ_{crit} values in the angiosperms (-5.52 to -6.64 MPa) than the gymnosperm (Ψ_{crit} = -4.09 MPa), angiosperm trees reached Ψ_{crit} in a third of the time it took the gymnosperm *P. radiata*. This underscores an important finding—that time to mortality depends on more than resistance to embolism alone. Regardless of species, the NSC observations of Blackman *et al.* add to growing uncertainty in interpretation of NSC responses during critical water stress—as their findings of lower soluble sugar in foliage of droughted trees compared with controls, but no difference in starch, were atypical of NSC responses associated with mortality (Adams et al. 2017; Li et al. 2018). To expound the findings of Blackman *et al.* with an aim toward understanding how different traits influence probability of mortality, here we provide a conceptual framework describing the progression of mortality risk during drought stress (Figure 1).

Our framework advances the idea that functional traits influencing the progression of mortality risk can broadly be divided into two groups which influence critical points in this progression. These include the point of incipient mortality risk, at which the risk of mortality is no longer zero (Sapes 2018), and the point of no return, at which it is more likely a tree will die than survive if drought stress is relieved (Hammond *et al*., 2019). Control of water loss during drought is initially dominated by stomatal conductance, which can vary by orders of magnitude through stomatal regulation. We propose that traits associated with stomatal regulation, such as

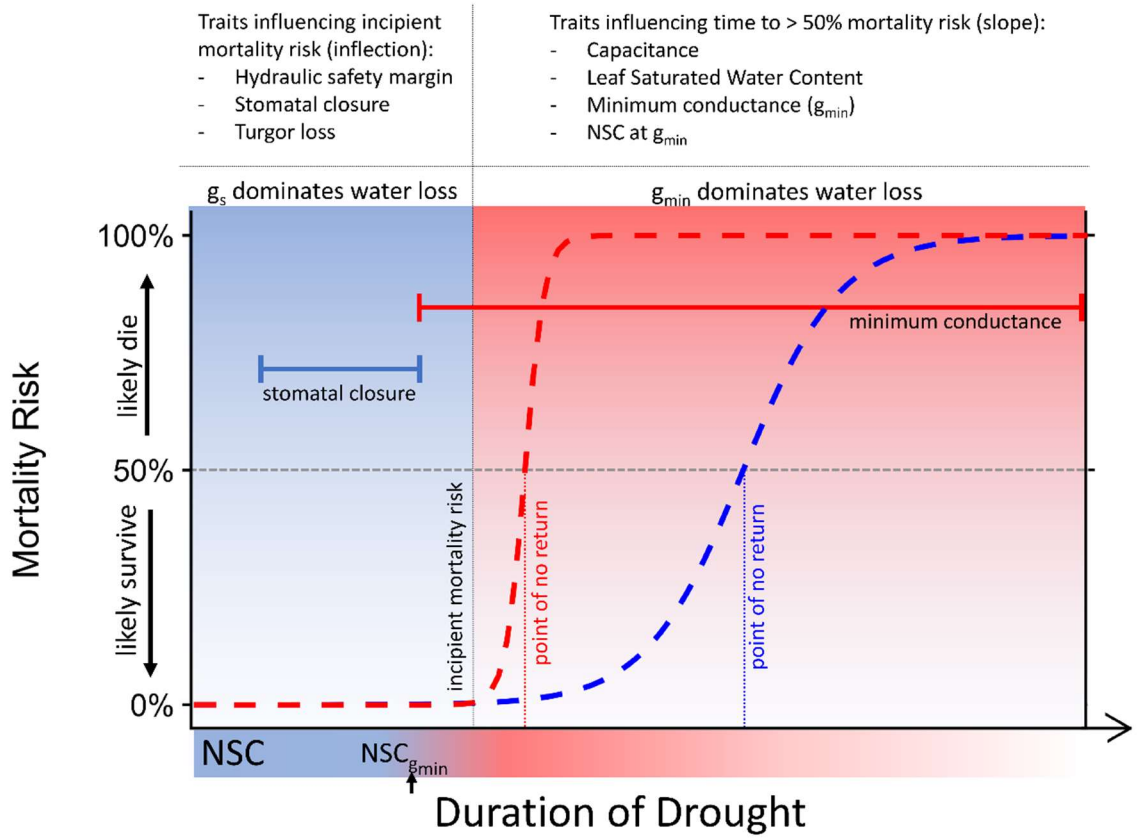

Figure 1. A conceptual diagram of the progression of mortality risk during drought. Two lines illustrate how species may differ in the progression of mortality risk. During drought, two phases of mortality risk are likely governed by separate groups of traits. The first group of traits, which primarily influences incipient mortality risk (the point of non-zero mortality probability), includes hydraulic safety margin (the difference between water potential points for 90% reduction in stomatal conductance and 50% loss of xylem hydraulic conductivity, as per *Blackman* et al.), the duration of stomatal closure (from onset to completion), and foliar turgor loss point. During this phase, non-structural carbohydrates (NSC) are dynamic as photosynthesis and mobilization continue. Beyond incipient mortality risk (shaded in red), traits governing the progression of mortality risk switch as minimum conductance (g_{min}) dominates water loss, and traits indicative of water storage (e.g., capacitance, leaf saturated water content) and retention (g_{min}) will either delay or accelerate the progression of mortality risk. During this phase photosynthesis is zero, and metabolism and mobilization are inhibited, thus the NSC at the onset of g_{min} sets the stage for available carbon during prolonged drought. Beyond the point of no return it is more likely trees will die from drought than survive. Dashed lines illustrate the difference in mortality risk trajectory for species with a less (red) and more-resistant (blue) point of no return, which corresponds with the angiosperm and gymnosperm observations of Blackman *et al*., respectively. Although not explicitly shown here, we hypothesize that point of incipient mortality risk may also vary among species that differ in functional traits.

hydraulic safety margin, the range of water potential across which stomatal closure occurs (from initial decline to < 10% of maximum), and the interval across which mesophyll cells lose turgor, will dominate how long it takes trees to reach incipient mortality risk. While water loss is under stomatal control, sufficient turgor exists for some amount of carbon assimilation and mobilization during this first phase, which is characterized by dynamic fluctuations in NSC content and components resulting from fixation and assimilation. Since the stomata are closed prior to incipient mortality (Delzon and Cochard 2014, Choat *et al*. 2018), we propose that traits relating to stomatal conductance bear little influence on the progression of mortality risk beyond this point. Instead we expect that mortality risk through the point of no return is dominated by a separate group of traits that relate to water storage and loss after stomatal closure. Minimum conductance (g_{min}) should be the major contributor to water loss at this phase (Duursma et al. 2018; Martin-StPaul et al. 2017), and we expect its rate—which may be highly sensitive to temperature (Cochard 2019)—coupled with specific leaf area and water storage through capacitance, will dominate the progression of mortality risk. The slope of the probability function for mortality in this phase ultimately determines when trees will pass the point of no return (Figure 1). Notably, once stomata are closed, NSC content must be less dynamic during this phase—with carbon assimilation arrested and phloem transport potentially impaired, we hypothesize that the "die is cast" for NSC once g_{min} becomes the dominant mode of water loss. Therefore NSC content at stomatal closure may also influence the progression of mortality risk beyond the incipient point (Sapes 2018).

Within this framework, we can consider Blackman *et al.*'s observations that angiosperm trees had high rates of water use initially—as evidenced by the quick recovery and growth after cyclical drought. The conifer *P. radiata*, in contrast, showed a more conservative strategy, minimizing water loss via earlier stomatal closure, which we expect would delay incipient

mortality risk. Specifically, we hypothesize that species with low hydraulic safety margins, prolonged stomatal closure, and that have relatively later turgor loss during drought progression will approach incipient mortality risk more quickly than species with opposite trends for these traits. Beyond this point, we hypothesize that species with lower g_{min} and higher NSC at g_{min}, and higher capacitance and saturated leaf water content will take longer to reach the point of no return. Our framework is consistent with the rapid approach to the point of no return for angiosperms relative to the slower approach of the gymnosperm reported in Blackman *et al*. All three angiosperm species were more resistant to embolism compared to the gymnosperm *P. radiata*, yet they all reached Ψ_{crit} before the conifer. This is an effective demonstration that that Ψ_{crit} does not predict how fast a tree will die during drought. Importantly, Blackman *et al*. observed that *P. radiata* had a g_{min} that was tenfold smaller than the angiosperm trees—a difference that should strongly promote a longer survival after stomatal closure, a delay in reaching the point of no return (Cochard 2019).

If the aim in understanding tree mortality is predicting vegetation change, the greatest impacts to landscapes from tree die-off occur after the point of incipient mortality risk, when rates of tree mortality climb higher. Studying traits leading to incipient mortality risk alone will not allow us to quantify the magnitude of tree mortality across a full progression of drought stress. Therefore we advocate increased study of traits that influence a species progress through the point of no return in order to fully characterize the shape of the mortality probability curve in response to drought stress. The study of Blackman *et al.* sheds a light on the relative importance of traits regarding the progression of mortality risk under drought stress. By measuring many physiological and growth response traits throughout drought-induced water stress during a dry-down to Ψ_{crit}, they were able to discern which traits were associated with the short time to Ψ_{crit} observed in angiosperms, and the long time to Ψ_{crit} observed in the gymnosperm. Their study provided the basis for our conceptual framework, which offers a hypothesis for the ways in which

specific traits which will impact the progression of tree mortality risk under drought. By contrasting the responses of the angiosperm and gymnosperm species in Blackman *et al*., we can observe that there is more than one way to die—and that likely much remains to be uncovered regarding the dynamics of drought-induced tree mortality risk. Future work on tree mortality should continue to describe risk factors as they relate to the probability of death, and specifically seek to understand the traits that predict incipient mortality risk, and those that predict the point of no return, at which death becomes more likely than survival.

Acknowledgements:

The authors would like to thank numerous individuals for conversations leading to the development of the conceptual framework, including Hervé Cochard, José M. Torres-Ruiz, Daniel Johnson, and Frederick Meinzer.

Funding:

W.M.H. was supported by the NSF Graduate Research Fellowship program (#1-653428). W.M.H and H.D.A were supported by the Oklahoma Center for the Advancement of Science and Technology's Basic Plant Science Research program.

Contributions:

W.M.H. developed the conceptual framework with input from H.D.A. W.M.H. wrote the manuscript with substantial assistance from H.D.A.

References:

Adams, H.D., M.J. Zeppel, W.R. Anderegg, *et al*., 2017. A multi-species synthesis of physiological mechanisms in drought-induced tree mortality. Nature Ecology and Evolution.

Barigah, T.S., O. Charrier, M. Douris, M. Bonhomme, S. Herbette, T. Améglio, R. Fichot, F. Brignolas and H. Cochard. 2013. Water stress-induced xylem hydraulic failure is a causal factor of tree mortality in beech and poplar. Annals of botany. 112:1431-1437.

Brodribb, T.J. and H. Cochard. 2009. Hydraulic failure defines the recovery and point of death in water-stressed conifers. Plant physiology. 149:575-584.

Choat, B., T.J. Brodribb, C.R. Brodersen, R.A. Duursma, R. López and B.E. Medlyn. 2018. Triggers of tree mortality under drought. Nature. 558(7711):531.

Cochard, H. 2019. "A new mechanism for tree mortality due to drought and heatwaves." bioRxiv doi: https://doi.org/10.1101/531632

Delzon, S. and H. Cochard. 2014. Recent advances in tree hydraulics highlight the ecological significance of the hydraulic safety margin. New Phytologist. 203:355-358.

Dickman, L.T., N.G. McDowell, S. Sevanto, R.E. Pangle and W.T. Pockman. 2015. Carbohydrate dynamics and mortality in a piñon-juniper woodland under three future precipitation scenarios. Plant, Cell & Environment. 38:729-739.

Duursma, R.A., C.J. Blackman, R. Lopéz, N.K. Martin-Stpaul, H. Cochard and B.E. Medlyn. 2018. On the minimum leaf conductance: its role in models of plant water use, and ecological and environmental controls. New Phytologist 221.2: 693-705.

Hammond, W.M., Yu, K.L., Wilson, L.A., Will, R.E., Anderegg, W.R.L., and Adams, H.D. 2019 "Dead or dying? Quantifying the point of no return from hydraulic failure in drought-induced tree mortality." New Phytologist. 223(4): 1834-1843.

Hartmann, H., C.F. Moura, W.R. Anderegg, N.K. Ruehr, Y. Salmon, C.D. Allen, S.K. Arndt, D.D. Breshears, H. Davi and D. Galbraith. 2018b. Research frontiers for improving our understanding of drought-induced tree and forest mortality. New Phytologist. 218:15-28.

Hartmann, H., Adams, H. D., Hammond, W. M., Hoch, G., Landhäusser, S. M., Wiley, E., & Zaehle, S. (2018). Identifying differences in carbohydrate dynamics of seedlings and mature trees to improve carbon allocation in models for trees and forests. Environmental and Experimental Botany, 152, 7-18.

Li, W., H. Hartmann, H.D. Adams, H. Zhang, C. Jin, C. Zhao, D. Guan, A. Wang, F. Yuan and J. Wu. 2018. The sweet side of global change–dynamic responses of non-structural carbohydrates to drought, elevated CO2 and nitrogen fertilization in tree species. Tree Physiology 38:1706-1723.

Martin-StPaul, N., S. Delzon and H. Cochard. 2017. Plant resistance to drought depends on timely stomatal closure. Ecology Letters 20:1437-1447.

McDowell, N.G., W.T. Pockman, C.D. Allen, D.D. Breshears, N. Cobb, T. Kolb, J. Plaut, J. Sperry, A. West and D.G. Williams. 2008. Mechanisms of plant survival and mortality during drought: why do some plants survive while others succumb to drought? New Phytologist. 178:719-739.

McDowell, N., C. Grossiord, H. Adams, S. Pinzon Navarro, S. Mackay, D.D. Breshears, C. Allen, I. Borrego, T. Dickman, A. Collins, M. Gaylord, N. McBranch, W. Pockman, A.

Vilagrosa, B. Aukema, D. Goodsman and C. Xu. 2019. Mechanisms of a coniferous woodland persistence under drought and heat. Environmental Research LettersO'Brien, M.J., S. Leuzinger, C.D. Philipson, J. Tay and A. Hector. 2014. Drought survival of tropical tree seedlings enhanced by non-structural carbohydrate levels. Nature Climate Change. 4:710.

Sapes, G. 2018. Why does drought kill trees? Interactions between water, carbon, and fungal symbionts. PhD Dissertation. University of Montana. #11283.

Trugman, A.T., M. Detto, M.K. Bartlett, D. Medvigy, W.R.L. Anderegg, C. Schwalm, B. Schaffer and S.W. Pacala. 2018. Tree carbon allocation explains forest drought-kill and recovery patterns. Ecology Letters. 21:1552-1560.

Urli, M., A.J. Porté, H. Cochard, Y. Guengant, R. Burlett and S. Delzon. 2013. Xylem embolism threshold for catastrophic hydraulic failure in angiosperm trees. Tree Physiology. 33:672-683.

APPENDICES

Supplemetal Materials for Chapters III and IV.

Author's note: *Supplemental data, in the form of comma-separated values files too large to be textually included in these apendices can be found published alongside chapter IV, and is available directly from the New Phytologist website. Similarly, data files for chapter III, also too large to list textually here, will be available at both tree-mortality.net and as supplemental data files upon its eventual publication. Supplemental data legends are included below, with a reminder of their online (or intended) availability.*

Supplemental materials for Chapter III: *A HOTTER-DROUGHT FINGERPRINT ON EARTH'S FOREST MORTALITY SITES—WARMING ACCELERATES RISKS*

Supplemental Data: Supplemental data file of comma-separated values (supplemental_data.csv) containing the reference ID matching Table S1, below (Ref_ID), longitude (long) and latitude (lat) in decimal degrees, and the year of onset of mortality (mortality_year). ***Author's note:*** *This supplemental data will be published alongside the paper at both the journal's website, and at tree-mortality.net*.

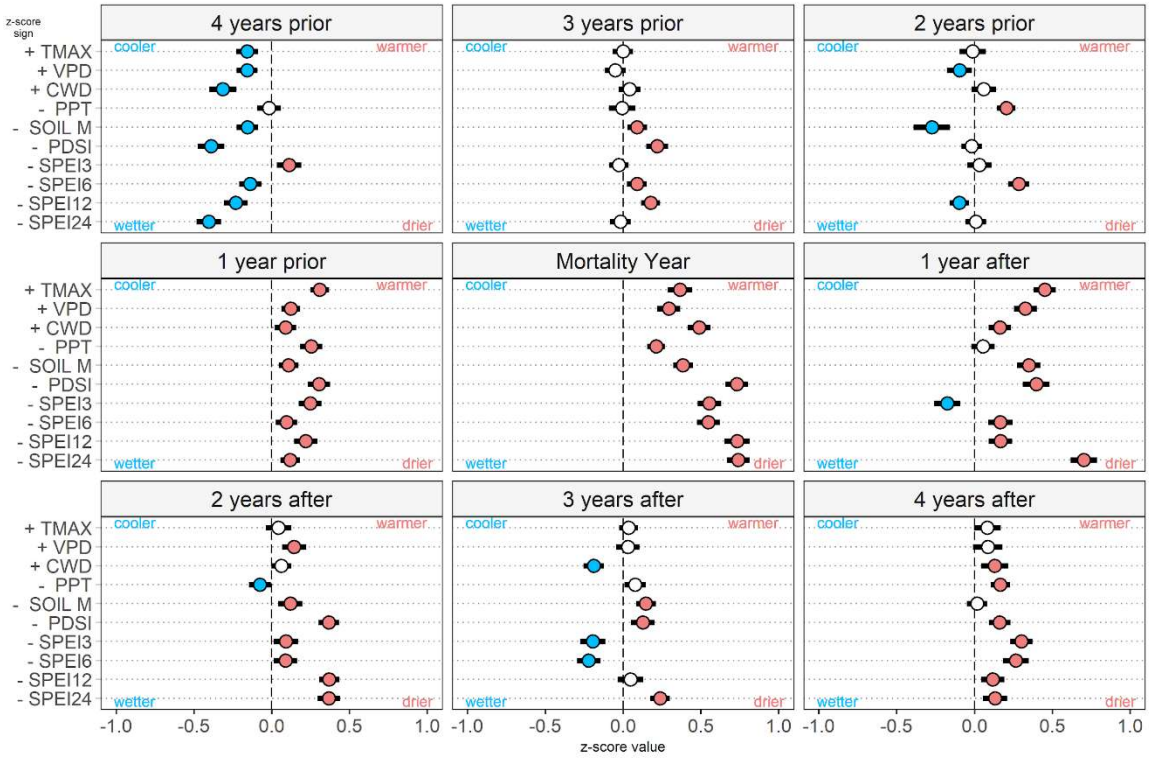

Figure S1. Hotter-drought fingerprint including SPEI3, 6, 12, and 24. Figure showing same data as Fig. 3 of the main text, with Standardized Precipitation-Evapotranspiration Index (SPEI) added at 3, 6, 9, 12, and 24 month calculations (SPEI3, SPEI6, SPEI12, SPEI24 respectively). For the mortality year, this expanded figure shows all SPEI metrics are significantly drier than the long-term mean, with SPEI12 and SPEI24 not being significantly different from the Palmer Drought Severity Index (PDSI) included in Figure 3, which consequently provides a more parsimonious hotter-drought fingerprint. As in Figure 3 of the main text, dots represent mean values across all sites, with color indicating z-score difference (blue = cooler/wetter, red = hotter/drier, white = not significant) from long-term climate. Whiskers represent 95% confidence intervals.

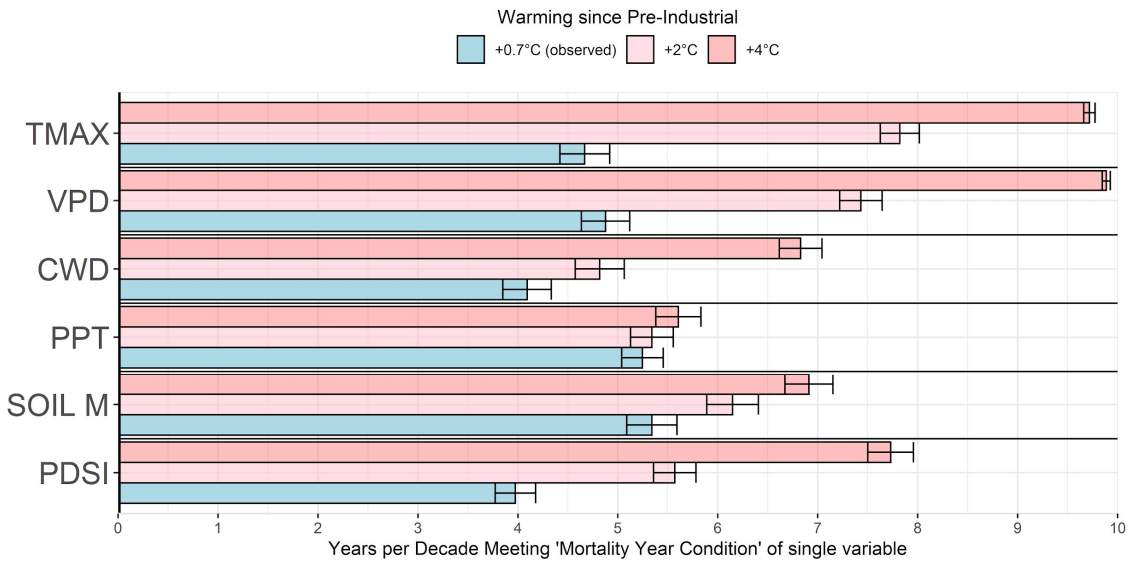

Figure S2. Per-variable mortality year condition frequency. Years per decade exceeding mortality year conditions for each variable (on y-axis) independently in the fingerprint of hotter-drought shown in Figure 5D. Bar height represents mean frequency across all sites, while whiskers indicate 95% confidence interval of the mean. Bar fill color indicates a warming scenario, where the observed baseline (+0.7ºC) is blue, and warmed scenarios are in pink and red for +2ºC and +4ºC respectively. In contrast to the combined-filtering approach in Fig. 5D, here each variable is independently plotted in response to warming (from baseline, +0.7ºC, to a maximum of +4ºC.

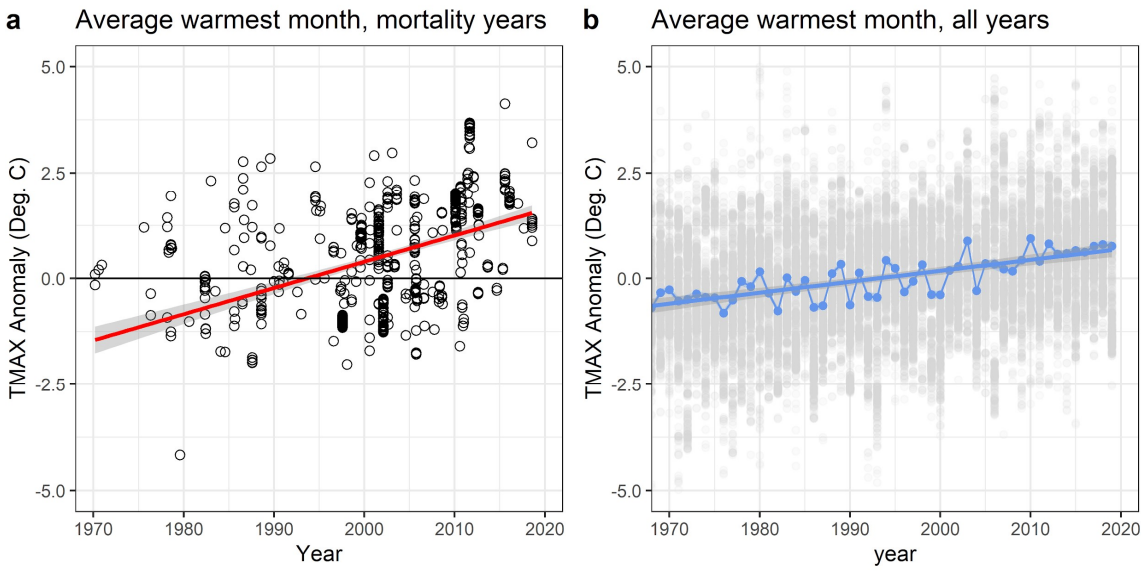

Figure S3. Mortality year TMAX warming faster than all years.

Trend of TMAX Anomaly during mortality years across sites in the analysis, and the TMAX anomaly trend for all years at all sites. Panel (**a**) is a repeat of Figure 4a from the main text, but panel (**b**) shows instead the mean values (blue dots) for TMAX anomaly during the typically warmest month, for all years at all sites, and the faded grey dots the raw data. Linear regression is fit to the raw data, and the slope of this regression is lower than that of the mortality year line (red, left panel). For both regressions, grey shading represents standard error of model fit.

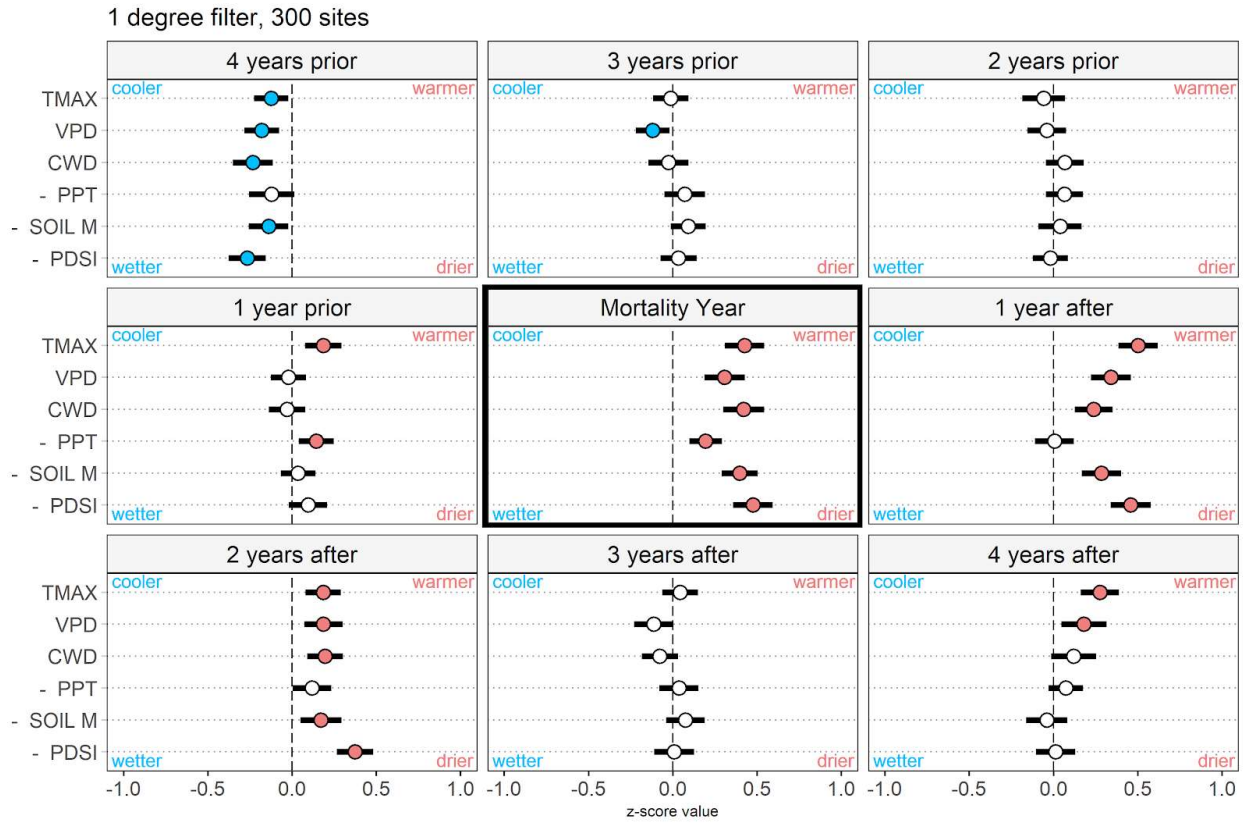

Figure S4. Hotter-drought fingerprint detected at 1 degree (coarse) resolution.

Additionally, we randomly sampled our 675 sites to include only one site per 1 degree of latitude/longitude for a given mortality year (compared to 1/24 degree resolution of our main analysis, as in Fig. 3). This reduced the number of sites to 300, aiming to dissipate any doubt about possible bias due aggregation of sites with heavy mortality in relatively small geographic areas. Even at this very coarse spatial scale (no more than 1 site per 111 km^2) there is still a clear hotter-drought fingerprint during the mortality year (and the two subsequent years), suggesting that spatial aggregation (sites being close to one another) did not play a significant role in our main finding. Notably, at this coarse resolution our hotter-drought fingerprint's z-score means are not significantly different (95% CI's overlap) for 5 of the 6 climate metrics (PDSI was significantly 'drier' in main text Fig. 3) during the mortality year. Furthermore, this additional analysis highlights the potential application of our hotter-drought fingerprint across spatial scales.

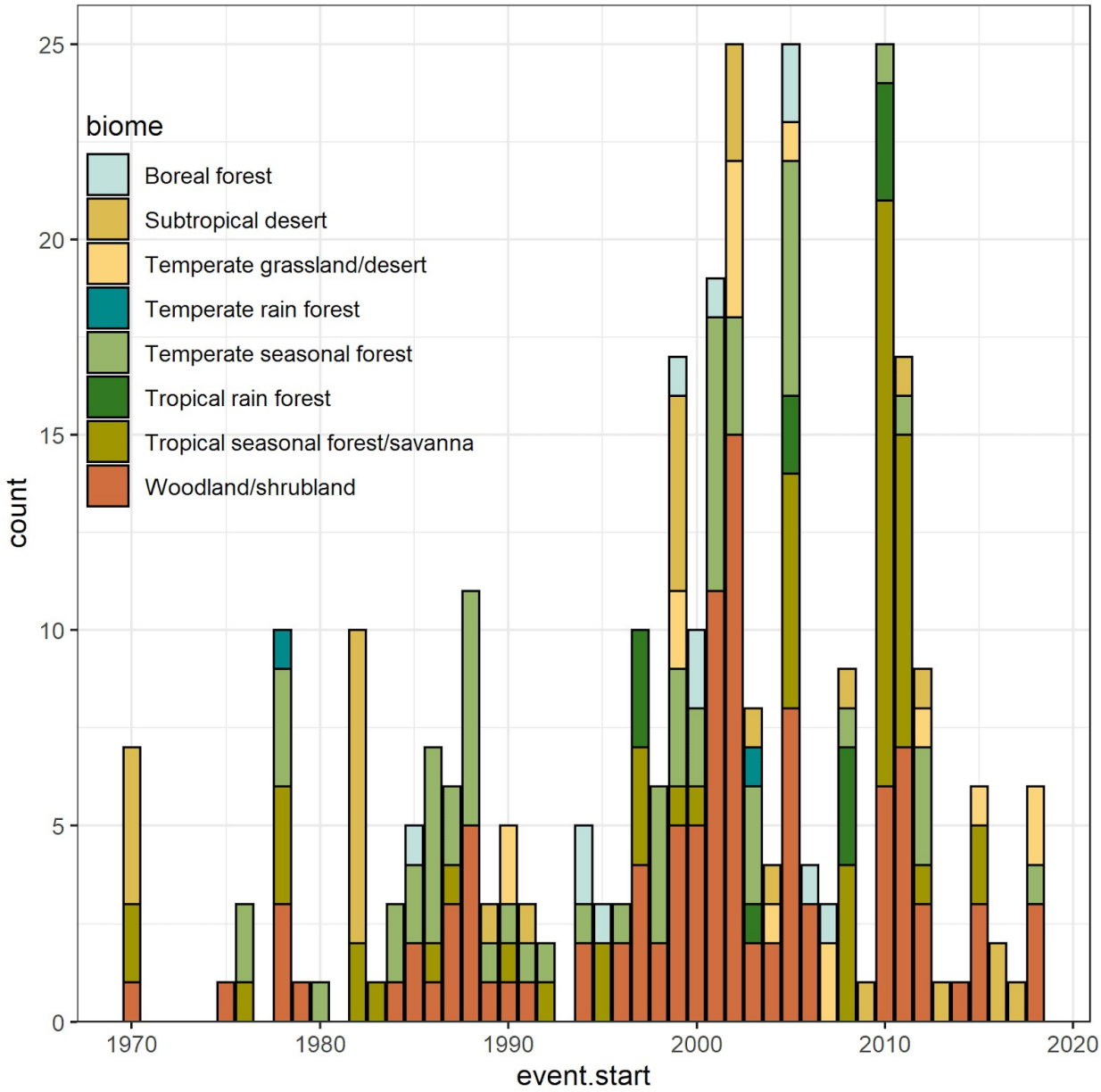

Figure S5. Proportion of mortality events from 1970-2018 by biome.

Through time, most years included multiple biomes of mortality. Below, a bar plot of the 300 sites (filtered to 1 degree, as in Fig. S4 above). While some years of high mortality representation align with global atmospheric events (e.g., ENSO in 1997-1998, 16 total sites), other years with high representation do not seemingly align with such phenomena. Our database and analyses are limited by the present combined peer-reviewed knowledge of where forests have died during hotter droughts, yet still cover many biomes in most years.

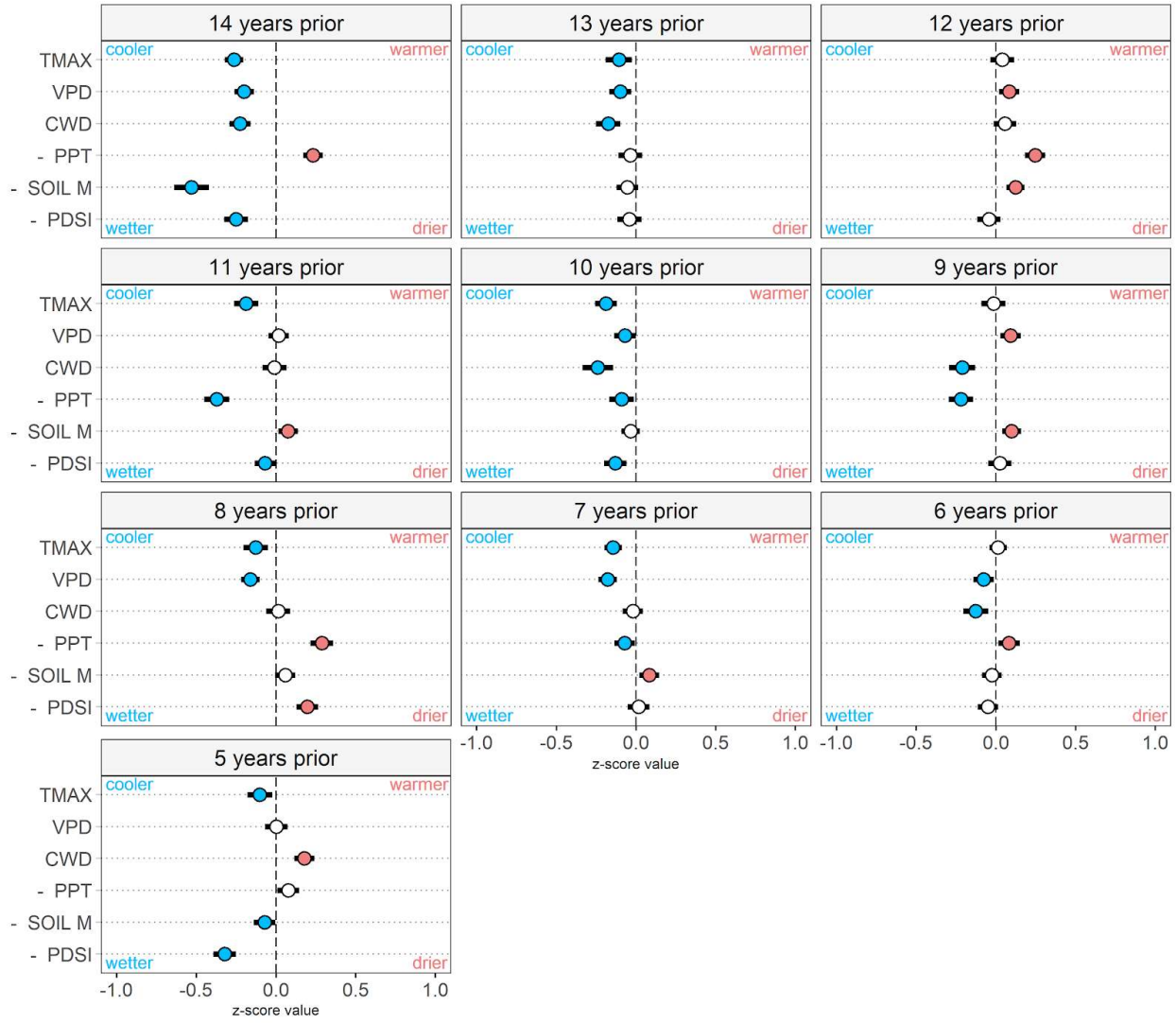

Figure S6. Fourteen years prior to mortality start show no 'hotter-drought' signal as in the mortality year.

We re-centered our 'hotter-drought fingerprint' analysis, as described in the paper (and displayed in its Fig. 3), 10 years prior to the mortality start year (note, we also appended 5 years prior to mortality, so that together with Fig. 3 of the main text, 14 years prior to mortality may be continuously inspected), exploring possible long-term or very delayed legacy effects. No consistent signal for hotter-drought appears as it does when the same analysis is centered on the observed mortality start year.

Figure S7. Hotter-drought fingerprints on a per-biome basis.

The three-year window, centered on the mortality start year, displayed for each biome. Above each biome triptych the number of sites included is listed. Hotter-drought signal certainty is tied to sample size, yet significant hotter-drought signals occur across nearly all biomes. Strong signals appear in temperate and tropical seasonal forests, and even boreal forests (with a small sample) show significant indicators of hotter drought. Tropical rain forests do not show hotter-drought signal in our present analyses, yet a combination of data scarcity, uncertainty in climate projections, and diverse responses of various forest types in the tropics will need further investigation.

(Figure on next page)

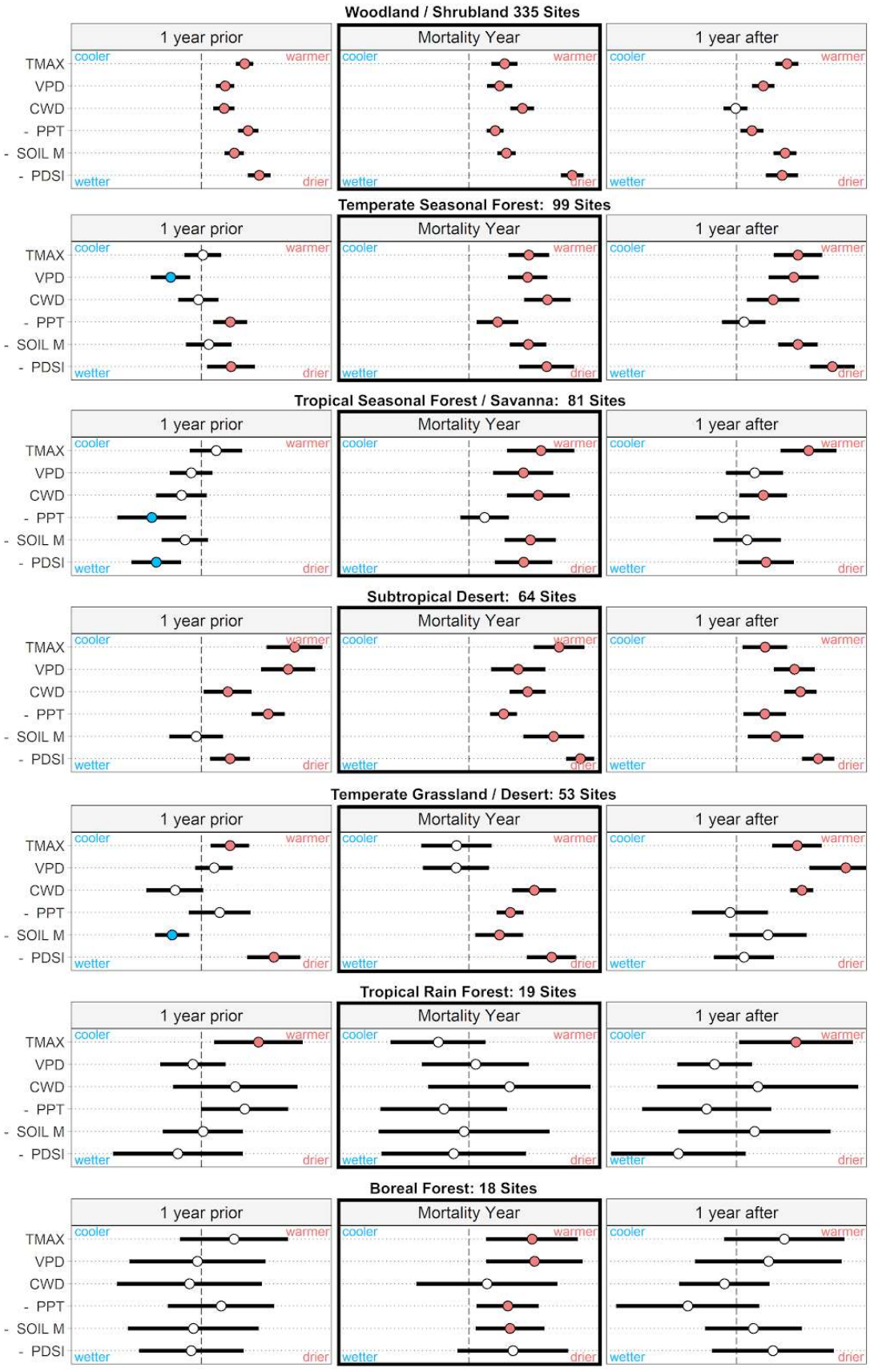
Woodland / Shrubland 335 Sites
1 year prior
Mortality Year
1 year after
TMAX
VPD
CWD
- PPT
- SOIL M
- PDSI
cooler
warmer
wetter
drier
Temperate Seasonal Forest: 99 Sites
Tropical Seasonal Forest / Savanna: 81 Sites
Subtropical Desert: 64 Sites
Temperate Grassland / Desert: 53 Sites
Tropical Rain Forest: 19 Sites
Boreal Forest: 18 Sites

Supplemental Table 1. Data sources with climate and biome summary.
Data references supporting database observations of drought and/or heat-induced tree mortality. Each reference includes the number of discrete locations (sites) considered in our analysis, along with the total number of plots. Climatic data and biome are also listed, with mean annual temperature (MAT, °C), mean annual precipitation (MAP, cm), and elevation (ELEV, m) all averages across plots for each reference. Whittaker biomes are listed, following the same isolines shown in figure 2 of the main text. Biomes are abbreviated as: SDT = subtropical desert, TSF = tropical seasonal forest/savanna, TGD = temperate grassland/desert, WS = woodland/shrubland, TRF = tropical rain forest, BOR = boreal forest, TERF = temperate rain forest.

ID	*Short Reference*	*Continent*	*Sites*	*Plots*	*MAT*	*MAP*	*ELEV*	*Biome(s)*
1	(MacGregor and O'Connor, 2002)[1]	Africa	1	1	21.48	34.75	640	STD
2	(Tafangenyasha, 2001; 1998; 1997)[2–4]	Africa	1	1	23.72	58.13	179	STD
3	(Viljoen, 1995)[5]	Africa	1	1	21.74	57.95	379	STD
4	(O'Connor, 1999)[6]	Africa	1	1	21.26	35.32	685	STD
5	(Lwanga, 2003)[7]	Africa	1	1	20.30	130.18	1358	TSF
6	(Foden *et al.*, 2007)[8]	Africa	1	1	14.94	14.88	1440	TGD
7	(Bentouati, 2008)[9]	Africa	1	1	11.28	44.44	1540	WS
8	(Werner, 1988)[10]	Asia	1	1	15.18	219.86	2018	TSF
9	(Woods, 1989)[11]	Asia	1	1	26.35	211.66	206	TSF
10	(Khan *et al.*, 1994)[12]	Asia	1	1	25.77	75.40	209	TSF
11	(Gardner and Fisher, 1996)[13]	Asia	1	1	15.41	40.91	2328	TGD
12	(Fisher, 1997)[14]	Asia	1	1	16.38	30.08	2611	TGD
13	(Kinnaird and O'Brein, 1998)[15]	Asia	1	1	22.33	285.07	570	TRF
14	(van Nieuwstadt and Shiel, 2005)[16]	Asia	1	1	27.81	257.62	8	TSF
15	(Nishimua *et al.*, 2007)[17]	Asia	1	1	27.40	247.09	23	TSF
16	(Nakagawa *et al.*, 2000)[18]	Asia	1	1	26.99	317.34	24	TRF
17	(Semerci *et al.*, 2008)[19]	Eurasia	1	1	9.01	51.47	1330	WS

18	(Hosking and Kershaw, 1985)[20]	Australia	1	1	9.57	227.85	436	TERF
19	(Hosking and Hutcheson, 1988)[21]	Australia	1	1	8.83	174.36	965	TSF
20	(Fensham, 1998)[22]	Australia	1	1	22.26	82.47	492	TRSF
21	(Fensham *et al.,* 2003)[23]	Australia	1	1	21.78	65.71	525	TRSF
22	(Fensham and Fairfax, 2007)[24]	Australia	1	1	21.61	51.13	366	STD
23	(Ogaya and Peñuelas, 2007)[25]	Europe	1	1	12.07	62.49	671	WS
24	(Siwkcki and Ufnaski, 1998)[26]	Europe	1	1	8.35	54.48	133	WS
25	(Markalas, 1992)[27]	Europe	1	1	11.34	84.95	895	WS
26	(Vertui and Tagliaferro, 1996)[28]	Europe	1	1	1.75	125.80	1495	BF
27	(Peñuelas *et al*., 2001)[29]	Europe	1	1	8.15	58.65	1511	WS
28	(Solberg, 2004)[30]	Europe	1	1	4.70	75.56	73	TSF
29	(Sarris *et al.*, 2007)[31]	Europe	1	1	16.96	75.33	150	WS
30	(Oberhuber, 2001)[32]	Europe	1	1	3.16	125.85	1654	TSF
31	(Tsopelas *et al*., 2004)[33]	Europe	1	1	13.20	64.53	741	WS
32	(Raftoyannis *et al*., 2008)[34]	Europe	1	1	10.75	93.92	1120	WS
33	(Bigler et al., 2006)[35]	Europe	1	1	6.08	92.63	1180	TSF
34	(Wermelinger *et al*., 2008)[36]	Europe	1	1	4.82	82.05	1466	TSF
35	(Dobbertin *et al.*, 2007)[37]	Europe	1	1	7.03	89.61	1051	TSF
36	(Petercord, 2008)[38]	Europe	1	1	8.96	75.99	340	WS
37	(Vennetier, 2008)[39]	Europe	1	1	14.28	84.02	179	WS
38	(Stringer *et al*., 1989)[40]	N. America	1	1	12.05	116.94	386	TSF
39	(Starkey et al., 2004)[41]	N. America	2	2	13.71	107.83	267	TSF/WS
40	(Clinton *et al*., 1993)[42]	N. America	1	1	11.87	179.79	848	TSF
41	(Law and Gott, 1987)[43]	N. America	1	1	13.33	115.84	228	TSF

42	(Jenkins and Pallardy, 1995)[44]	N. America	3	3	13.28	114.16	234	TSF
43	(Olano and Palmer, 2003)[45]	N. America	1	1	9.28	151.88	1335	TSF
44	(Faber-Langendoen and Tester, 1993)[46]	N. America	1	1	6.01	72.29	278	TSF
45	(Jones and Hendershot, 1989)[47]	N. America	1	1	3.41	112.16	336	TSF
46	(Savage, 1997)[48]	N. America	2	2	8.97	77.14	2171	WS
47	(Guarín and Taylor, 2005)[49]	N. America	1	1	9.47	92.90	1686	TSF
48	(Macomber and Woodcock, 1994)[50]	N. America	1	1	4.31	101.75	2139	TSF
49	(Millar *et al.*, 2007)[51]	N. America	1	1	3.60	47.03	2590	WS
50	(Mueller *et al.*, 2005)[52]	N. America	1	1	8.61	45.51	2154	WS
51	(Ogle *et al.*, 2000)[53]	N. America	1	1	8.12	45.54	2142	WS
52	(Hogg *et al.*, 2002)[54]	N. America	1	1	2.25	46.39	807	WS
53	(Voelker *et al.*, 2008)[55]	N. America	1	1	13.41	113.91	192	TSF
54	(Berg *et al.*, 2006)[56]	N. America	2	2	0.42	56.80	467	TSF/WS
55	(Breshears *et al.*, 2005)[57]	N. America	1	1	9.56	40.36	2120	WS
56	(Swaty *et al.*, 2004)[58]	N. America	2	3	7.44	48.29	2237	WS
57	(Greenwood and Weisberg, 2008)[59]	N. America	1	1	8.10	25.82	1875	TGD
58	(Floyd *et al.*, 2009)[60]	N. America	3	3	7.68	46.23	2270	TGD/ WS
59	(Hogg *et al.*, 2008)[61]	N. America	8	13	1.66	42.09	605	TSF/ WS/BF
60	(Kurz *et al.*, 2008)[62]	N. America	1	1	2.39	49.65	898	TSF
61	(Worall *et al.*, 2008)[63]	N. America	1	1	3.03	72.41	3054	TSF
62	(Condit *et al.*, 1995)[64]	S. America	1	1	26.36	238.85	57	TRSF
63	(Rolim *et al.*, 2005)[65]	S. America	1	1	23.46	116.75	39	TRSF
64	(Williamson *et al.*, 2000)[66]	S. America	1	1	26.37	238.26	111	TRSF

65	(Chazdon *et al*., 2005)[67]	S. America	1	1	25.50	388.41	142	TRF
66	(Suarez *et al.,* 2004)[68]	N. America	1	1	7.68	108.59	916	TSF
67	(Phillips *et al*., 2009)[69]	S. America	14	17	25.81	225.86	135	TRF/ TRSF
68	(Mehl *et al*., 2010)[70]	Africa	1	1	17.82	78.66	1060	WS
69	(Van der Line *et al*., 2012)[71]	Africa	3	3	18.88	56.48	1183	TRSF
70	(Fauset *et al*., 2012)[72]	Africa	2	2	26.01	171.24	174	TRSF
71	(Gonzalez *et al*., 2012)[73]	Africa	11	11	28.58	42.50	337	STD
72	(Kherchouche *et al*., 2012)[74]	Africa	1	1	9.16	56.24	1903	WS
73	(Dulamsuren *et al*., 2009)[75]	Asia	2	2	-1.64	32.31	1131	WS
74	(Kharuk, 2013)[76]	Asia	1	1	-2.34	34.53	577	BF
75	(Zhou *et al*., 2013)[77]	Asia	1	1	22.13	173.35	30	TRSF
76	(Brouwers *et al*., 2013)[78]	Australia	62	236	15.85	103.13	292	WS/ TSF
77	(Fensham et al., 2012)[79]	Australia	1	1	21.72	36.30	266	STD
78	(Kharuk, 2013)[80]	Asia	1	1	-1.85	66.65	974	BF
79	(Keith *et al*., 2012)[81]	Australia	1	1	9.01	141.57	1227	TSF
80	(Matusick *et al*., 2012)[82]	Australia	1	1	18.28	83.12	6	WS
81	(Brouwers *et al*., 2013)[83]	Australia	51	66	15.65	47.59	288	TGD/WS/STD
82	(Peterken and Mountford)[84]	Europe	1	1	9.15	85.55	170	WS
83	(Linares *et al*., 2009)[85]	Europe	1	2	12.63	88.50	1144	WS
84	(Galiano *et al*., 2010)[86]	Europe	1	1	9.39	89.55	1056	TSF
85	(Aakala *et al*., 2011)[87]	Europe	2	5	0.16	60.24	180	BF
86	(Linares *et al.*, 2011)[88]	Africa, Europe	3	3	12.17	62.28	1271	WS
87	(Sarris *et al*., 2011)[89]	Europe	4	4	16.70	73.81	278	WS/TGD
88	(Marini *et al*., 2012)[90]	Europe	1	1	7.72	144.83	907	TSF
89	(Cailleret *et al*., 2014)[91]	Europe	3	14	8.98	106.79	1019	TSF
90	(Vilà-Cabrera *et al*., 2013)[92]	Europe	5	28	9.93	79.17	985	TSF/ WS
91	(Fahey, 1998)[93]	N. America	1	1	7.27	91.51	495	TSF

92	(Ganey and Vojta, 2011)[94]	N. America	83	113	7.67	57.72	2208	WS
93	(Michaelian *et al*., 2011)[95]	N. America	55	58	1.47	41.02	627	WS/ BF/TSF
94	(DeRose and Long, 2012)[96]	N. America	12	14	2.50	53.03	2979	WS/ BF/TSF
95	(Fellows and Goulden, 2012)[97]	N. America	1	1	10.08	75.73	2085	WS
96	(Kaiser *et al*., 2013)[98]	N. America	1	1	1.81	53.10	2178	TSF
97	(Millar *et al*., 2012)[99]	N. America	1	1	8.24	29.73	1947	TGD
98	(Garrity *et al*., 2013)[100]	N. America	1	1	10.21	37.53	2007	TGD
99	(Enquist and Enquist, 2011)[101]	N. America	1	1	25.67	173.19	272	TRSF
100	(Mokria *et al*., 2015)[102]	Africa	1	1	19.91	65.95	1809	TRSF
101	(Baguskas *et al*., 2014)[103]	N. America	2	80	14.52	41.77	349	TGD
102	(Hart *et al*., 2014)[104]	N. America	4	4	-0.06	59.80	3327	BF/TSF
103	(Kane *et al*., 2014)[105]	N. America	2	3	6.25	60.17	2510	WS/TSF
104	(Gu *et al*., 2015)[106]	N. America	1	1	12.40	97.47	216	WS
105	(Smith *et al*., 2015)[107]	N. America	4	7	1.48	55.90	3129	BF/ WS/TSF
106	(Zhou *et al*., 2014)[108]	Asia	6	8	19.92	154.35	752	WS/ TSF/TRSF
107	(Čater, 2015)[109]	Europe	3	4	9.69	104.68	201	WS/TSF
108	(Aynekulu *et al*., 2011)[110]	Africa	2	3	19.28	70.60	1875	TRSF/WS
109	(Liang *et al*., 2016)[111]	Asia	1	1	-1.09	38.65	2834	BOR
110	(Challis *et al*., 2016)[112]	Australia	2	2	18.41	76.96	19	WS
111	(Matusick *et al*., 2016)[113]	Australia	5	12	15.84	107.61	307	WS/TSF
112	(Drobyshev *et al*., 2007)[114]	Europe	13	13	6.75	73.70	82	WS/TSF
113	(Andersson, *et al*., 2011)[115]	Europe	3	3	6.32	54.76	57	WS
114	(Martin *et al*., 2015)[116]	Europe	1	1	9.90	76.58	36	WS
115	(García de la Serrana *et al*., 2015)[117]	Europe	3	3	17.50	32.55	87	STD
116	(Herguido *et al*., 2016)[118]	Europe	2	2	9.90	61.37	1238	STD

117	(Bendixsen *et al*., 2015)[119]	N. America	1	1	15.61	98.51	205	WS
118	(Billings *et al*., 2016)[120]	N. America	3	3	13.89	118.48	509	TSF
119	(Berdanier and Clark, 2016)[121]	N. America	1	1	15.49	117.01	86	TSF
120	(Feeley *et al*., 2013)[122]	N. America	6	9	21.08	347.03	969	TRF/ TERF
121	(Duque *et al*., 2015)[123]	S. America	10	10	25.69	262.87	420	TRF/ TRSF
122	(Amoroso *et al*., 2015)[124]	S. America	2	4	9.66	104.62	474	TSF
123	(Schwantes *et al*., 2016)[125]	N. America	6	10	18.73	74.73	331	WS/ TRSF
124	(Assal *et al*., 2016)[126]	N. America	12	21	3.10	31.31	2572	WS
125	(Feldpausch *et al*., 2016)[127]	S. America	25	34	25.54	214.68	229	TRF/ TRSF
126	(Freeman *et al*., 2017)[128]	N. America	8	39	15.28	78.74	25	WS
127	(Harrison, 2001)[129]	Asia	1	1	26.62	311.58	128	TRF
128	(Wood *et al*., 2018)[130]	N. America	1	1	12.40	97.47	216	WS
129	(Paz *et al*., 2017)[131]	N. America	1	1	6.95	65.97	2003	WS
130	(Xu *et al*., 2018)[132]	Asia	5	5	1.08	38.95	1291	BF/ WS/TSF
131	(Crouchet *et al*., 2019)[133]	N. America	17	30	18.87	76.50	417	TRSF/ WS
132	(Preisler, *et al*., 2019)[134]	Asia	1	1	17.37	29.46	689	STD
133	(Kunert, 2020)[135]	Europe	1	1	8.45	71.48	356	WS
134	(Powers *et al*., 2020)[136]	N. America	2	3	26.56	179.90	112	TRSF
135	(Johnson *et al*., 2018)[137]	N. America	1	2	18.08	64.27	520	WS
136	(Jaime *et al*., 2019)[138]	Europe	15	22	8.83	91.75	1168	TSF/ WS
137	(Navarro-Cerrillo *et al*., 2007)[139]	Europe	4	4	10.34	60.18	1561	WS/ TGD
138	(Prieto-Recio *et al*., 2015)[140]	Europe	12	12	11.03	59.90	818	WS/ TGD
139	(Pernek *et al*., 2019)[141]	Europe	4	4	15.47	78.09	53	WS
140	(Savi *et al*., 2019)[142]	Europe	1	1	11.87	154.32	372	TSF
141	(Klein *et al*., 2019)[143]	Asia	18	20	19.15	33.93	227	STD

142	(Dorman *et al*., 2015a)[144]	Asia	2	2	17.59	58.97	525	WS/STD
143	(Dorman *et al*., 2015b)[145]	Asia	2	2	18.71	29.49	372	STD
144	(Swemmer, 2020)[146]	Africa	18	125	22.01	55.24	247	STD
145	(Saenz-Romero *et al*., 2020)[147]	N. America	6	6	15.57	92.54	2001	WS/ TSF/TRSF
146	(Allen, 2007)[148]	N. America	1	3	10.57	34.46	1939	TGD
147	(Rodríguez-Catón *et al*., 2019)[149]	S. America	3	3	5.42	88.95	1428	TSF
148	(Das *et al*., 2020)[150]	N. America	5	15	11.94	31.99	1643	TGD
149	(Stephenson *et al*., 2019)[151]	N. America	3	64	12.49	30.10	1563	TGD
150	(Csank *et al*., 2016)[152]	N. America	4	4	1.62	66.71	134	BF
151	(Kannenberg *et al*., 2020)[153]	N. America	6	8	10.08	30.61	1898	TGD
152	(Schuldt *et al*., 2020)[154]	Europe	1	1	8.58	118.42	514	TSF

Supplemental Data Table 1 References:

1. Macgregor, S. D. & O'Connor, T. G. Patch dieback of Colophospermum mopane in a dysfunctional semi-arid African savanna: MOPANE PATCH DIEBACK. *Austral Ecol.* **27**, 385–395 (2002).
2. Tafangenyasha, C. Decline of the mountain acacia, Brachystegia glaucescens in Gonarezhou National Park, southeast Zimbabwe. *J. Environ. Manage.* **63**, 37–50 (2001).
3. Tafangenyasha, C. Phenology and mortality of common woody plants during and after severe drought in south-eastern Zimbabwe. *Trans. Zimb. Sci. Assoc.* **72**, 1–6 (1998).
4. Tafangenyasha, C. Tree loss in the Gonarezhou National Park (Zimbabwe) between 1970 and 1983. *J. Environ. Manage.* **49**, 355–366 (1997).
5. Viljoen, A. J. The influence of the 1991/92 drought on the woody vegetation of the Kruger National Park. *Koedoe* **38**, 85–97 (1995).
6. O'Connor, T. G. Impact of sustained drought on a semi-arid *Colophospermum mopane* savanna. *Afr. J. Range Forage Sci.* **15**, 83–91 (1998).
7. Lwanga, J. S. Localized tree mortality following the drought of 1999 at Ngogo, Kibale National Park, Uganda. *Afr. J. Ecol.* **41**, 194–196 (2003).
8. Foden, W. *et al.* A changing climate is eroding the geographical range of the Namib Desert tree Aloe through population declines and dispersal lags: Namib Desert trees feel the heat of climate change. *Divers. Distrib.* **13**, 645–653 (2007).
9. Bentouati, A. La situation du cèdre de l'Atlas en Algérie. *For. Méditerranéenne* (2008).
10. Werner, W. L. Canopy dieback in the upper montane rain forests of Sri Lanka. *GeoJournal* **17**, 245–248 (1988).
11. Woods, P. Effects of Logging, Drought, and Fire on Structure and Composition of Tropical Forests in Sabah, Malaysia. *Biotropica* **21**, 290 (1989).
12. Khan, J. A., Rodgers, W. A., Johnsingh, A. J. T. & Mathur, P. K. Tree and shrub mortality and debarking by sambar Cervus unicolor (kerr) in Gir after a drought in Gujarat, India. *Biol. Conserv.* **68**, 149–154 (1994).
13. Gardner, A. S. & Fisher, M. The distribution and status of the montane juniper woodlands of Oman. *J. Biogeogr.* **23**, 791–803 (1996).
14. Fisher, M. Decline in the Juniper Woodlands of Raydah Reserve in Southwestern Saudi Arabia: A Response to Climate Changes? *Glob. Ecol. Biogeogr. Lett.* **6**, 379 (1997).
15. Kinnaird, M. F. & O'Brien, T. G. Ecological Effects of Wildfire on Lowland Rainforest in Sumatra. *Conserv. Biol.* **12**, 954–956 (1998).
16. Van Nieuwstadt, M. G. L. & Sheil, D. Drought, fire and tree survival in a Borneo rain forest, East Kalimantan, Indonesia. *J. Ecol.* **93**, 191–201 (2005).
17. Nishimua, T. B., Suzuki, E., Kohyama, T. & Tsuyuzaki, S. Mortality and Growth of Trees in Peat-swamp and Heath Forests in Central Kalimantan After Severe Drought. *Plant Ecol.* **188**, 165–177 (2007).
18. Nakagawa, M. *et al.* Impact of severe drought associated with the 1997–1998 El Niño in a tropical forest in Sarawak. *J. Trop. Ecol.* **16**, 355–367 (2000).

19. Semerci, A. *et al.* Examination of tree mortalities in semi-arid central Anatolian region of Turkey during last six-year period (2002–2007). in *Book of Abstracts of the International Conference '"Adaptation of Forests and Forest Management to Changing Climate with Emphasis on Forest Health: A Review of Science, Policies, and Practices"', Umea, Sweden, FAO/IUFRO* 262 (2008).

20. Hosking, G. P. & Kershaw, D. J. Red beech death in the Maruia Valley South Island, New Zealand. *N. Z. J. Bot.* **23**, 201–211 (1985).

21. Hosking, G. P. & Hutcheson, J. A. Mountain beech (*Nothofagus solandri* var. *cliffortioides*) decline in the Kaweka Range, North Island, New Zealand. *N. Z. J. Bot.* **26**, 393–400 (1988).

22. Fensham, R. J. The influence of cattle grazing on tree mortality after drought in savanna woodland in north Queensland. *Austral Ecol.* **23**, 405–407 (1998).

23. Fensham, R. J., Fairfax, R. J., Butler, D. W. & Bowman, D. M. J. S. Effects of fire and drought in a tropical eucalypt savanna colonized by rain forest: Effects of fire and drought in eucalypt savanna. *J. Biogeogr.* **30**, 1405–1414 (2003).

24. Fensham, R. J. & Fairfax, R. J. Drought-related tree death of savanna eucalypts: Species susceptibility, soil conditions and root architecture. *J. Veg. Sci.* **18**, 71–80 (2007).

25. Ogaya, R. & Peñuelas, J. Tree growth, mortality, and above-ground biomass accumulation in a holm oak forest under a five-year experimental field drought. *Plant Ecol.* **189**, 291–299 (2007).

26. Siwkcki, R. & Ufnalski, K. Review of oak stand decline with special reference to the role of drought in Poland. *For. Pathol.* **28**, 99–112 (1998).

27. Markalas, S. Site and stand factors related to mortality rate in a fir forest after a combined incidence of drought and insect attack. *For. Ecol. Manag.* **47**, 367–374 (1992).

28. Vertui, F. & Tagliaferro, F. Scots pine (Pinus sylvestris L.) die-back by unknown causes in the Aosta Valley, Italy. *Chemosphere* **36**, 1061–1065 (1998).

29. Peñuelas, J., Lloret, F. & Montoya, R. Severe Drought Effects on Mediterranean Woody Flora in Spain. *For. Sci.* **47**, 214–218 (2001).

30. Solberg, S. Summer drought: a driver for crown condition and mortality of Norway spruce in Norway. *For. Pathol.* **34**, 93–104 (2004).

31. Sarris, D., Christodoulakis, D. & Körner, C. Recent decline in precipitation and tree growth in the eastern Mediterranean. *Glob. Change Biol.* **13**, 1187–1200 (2007).

32. Oberhuber, W. The role of climate in the mortality of Scots pine (Pinus sylvestris L.) exposed to soil dryness. *Dendrochronologia* **19**, 45–55 (2001).

33. Tsopelas, P., Angelopoulos, A., Economou, A. & Soulioti, N. Mistletoe (Viscum album) in the fir forest of Mount Parnis, Greece. *For. Ecol. Manag.* **202**, 59–65 (2004).

34. Raftoyannis, Y., Spanos, I. & Radoglou, K. The decline of Greek fir (*Abies cephalonica* Loudon): Relationships with root condition. *Plant Biosyst. - Int. J. Deal. Asp. Plant Biol.* **142**, 386–390 (2008).

35. Bigler, C., Bräker, O. U., Bugmann, H., Dobbertin, M. & Rigling, A. Drought as an Inciting Mortality Factor in Scots Pine Stands of the Valais, Switzerland. *Ecosystems* **9**, 330–343 (2006).

36. Wermelinger, B., Rigling, A., Schneider Mathis, D. & Dobbertin, M. Assessing the role of bark- and wood-boring insects in the decline of Scots pine (Pinus sylvestris) in the Swiss Rhone valley. *Ecol. Entomol.* **33**, 239–249 (2008).

37. Dobbertin, M. *et al.* Linking Increasing Drought Stress to Scots Pine Mortality and Bark Beetle Infestations. 10 (2007).

38. Petercord, R. Zukünftige Gefährdung der Rotbuche durch rinden- und holzbrütende Käfer in Baden-Württemberg. 5 (2008).

39. Vennetier, M. *et al.* Etude de l'impact d'incendies de forêt répétés sur la biodiversité et sur les sols. Recherche d'indicateurs. Rapport final. (2008) doi:10.13140/RG.2.1.1450.3923.

40. Stringer, J. W., Kimmerer, T. W., Overstreet, J. C. & Dunn, J. P. Oak Mortality in Eastern Kentucky. *South. J. Appl. For.* **13**, 86–91 (1989).

41. Starkey, D. A., Oliveria, F., Mangini, A. & Mielke, M. Oak Decline and Red Oak Borer in the interior highlands of Arkansas and Missouri: natural phenomena, severe occurrences. in *Upland Oak Ecology Symposium: History, Current Conditions, and Sustainability: Fayetteville, Arkansas, October 7-10, 2002* vol. 73 217–222 (Southern Research Station, 2004).

42. Clinton, B. D., Boring, L. R. & Swank, W. T. Canopy Gap Characteristics and Drought Influences in Oak Forests of the Coweeta Basin. *Ecology* **74**, 1551–1558 (1993).

43. Law, J. R. & Gott, J. D. Oak mortality in the Missouri Ozarks. in *Proceedings of the Central Hardwood Forest Conference* vol. 6 427–436 (University of Tennessee: Knoxville, TN, USA, 1987).

44. Jenkins, M. A. & Pallardy, S. G. The influence of drought on red oak group species growth and mortality in the Missouri Ozarks. *Can. J. For. Res.* **25**, 1119–1127 (1995).

45. Olano, J. M. & Palmer, M. W. Stand dynamics of an Appalachian old-growth forest during a severe drought episode. *For. Ecol. Manag.* **174**, 139–148 (2003).

46. Faber-Langendoen, D. & Tester, J. R. Oak Mortality in Sand Savannas Following Drought in East-Central Minnesota. *Bull. Torrey Bot. Club* **120**, 248 (1993).

47. Jones, A. R. C. & Hendershot, W. H. Maple Decline in Quebec: A Discussion of Possible Causes and the Use of Fertilizers to Limit Damage. *For. Chron.* **65**, 280–287 (1989).

48. Savage, M. The role of anthropogenic influences in a mixed-conifer forest mortality episode. *J. Veg. Sci.* **8**, 95–104 (1997).

49. Guarín, A. & Taylor, A. H. Drought triggered tree mortality in mixed conifer forests in Yosemite National Park, California, USA. *For. Ecol. Manag.* **218**, 229–244 (2005).

50. Macomber, S. A. & Woodcock, C. E. Mapping and monitoring conifer mortality using remote sensing in the Lake Tahoe Basin. *Remote Sens. Environ.* **50**, 255–266 (1994).

51. Millar, C. I., Westfall, R. D. & Delany, D. L. Response of high-elevation limber pine (*Pinus flexilis*) to multiyear droughts and 20th-century warming, Sierra Nevada, California, USA. *Can. J. For. Res.* **37**, 2508–2520 (2007).

52. Mueller, R. C. *et al.* Differential tree mortality in response to severe drought: evidence for long-term vegetation shifts. *J. Ecol.* **93**, 1085–1093 (2005).

53. Ogle, K., Whitham, T. G. & Cobb, N. S. TREE-RING VARIATION IN PINYON PREDICTS LIKELIHOOD OF DEATH FOLLOWING SEVERE DROUGHT. *Ecology* **81**, 3237–3243 (2000).

54. Hogg, E. H., Brandt, J. P. & Kochtubajda, B. Growth and dieback of aspen forests in northwestern Alberta, Canada, in relation to climate and insects. **32**, 11 (2002).

55. Voelker, S. L., Muzika, R.-M. & Guyette, R. P. Individual Tree and Stand Level Influences on the Growth, Vigor, and Decline of Red Oaks in the Ozarks. *For. Sci.* **54**, 13 (2008).

56. Berg, E. E., David Henry, J., Fastie, C. L., De Volder, A. D. & Matsuoka, S. M. Spruce beetle outbreaks on the Kenai Peninsula, Alaska, and Kluane National Park and Reserve, Yukon Territory: Relationship to summer temperatures and regional differences in disturbance regimes. *For. Ecol. Manag.* **227**, 219–232 (2006).

57. Breshears, D. D. *et al.* Regional vegetation die-off in response to global-change-type drought. *Proc. Natl. Acad. Sci.* **102**, 15144–15148 (2005).

58. Swaty, R. L., Deckert, R. J., Whitham, T. G. & Gehring, C. A. ECTOMYCORRHIZAL ABUNDANCE AND COMMUNITY COMPOSITION SHIFTS WITH DROUGHT: PREDICTIONS FROM TREE RINGS. *Ecology* **85**, 1072–1084 (2004).

59. Greenwood, D. L. & Weisberg, P. J. Density-dependent tree mortality in pinyon-juniper woodlands. *For. Ecol. Manag.* **255**, 2129–2137 (2008).

60. Floyd, M. L. *et al.* Relationship of stand characteristics to drought-induced mortality in three Southwestern piñon–juniper woodlands. *Ecol. Appl.* **19**, 1223–1230 (2009).

61. Hogg, E. H. (Ted), Brandt, J. P. & Michaelian, M. Impacts of a regional drought on the productivity, dieback, and biomass of western Canadian aspen forests. *Can. J. For. Res.* **38**, 1373–1384 (2008).

62. Kurz, W. A. *et al.* Mountain pine beetle and forest carbon feedback to climate change. *Nature* **452**, 987–990 (2008).

63. Worrall, J. J. *et al.* Rapid mortality of Populus tremuloides in southwestern Colorado, USA. *For. Ecol. Manag.* **255**, 686–696 (2008).

64. Condit, R., Hubbell, S. P. & Foster, R. B. Mortality Rates of 205 Neotropical Tree and Shrub Species and the Impact of a Severe Drought. *Ecol. Monogr.* **65**, 419–439 (1995).

65. Rolim, S. G., Jesus, R. M., Nascimento, H. E. M., do Couto, H. T. Z. & Chambers, J. Q. Biomass change in an Atlantic tropical moist forest: the ENSO effect in permanent sample plots over a 22-year period. *Oecologia* **142**, 238–246 (2005).

66. Williamson, G. B. *et al.* Amazonian Tree Mortality during the 1997 El Nino Drought. *Conserv. Biol.* **14**, 1538–1542 (2000).

67. Chazdon, R. L., Redondo Brenes, A. & Vilchez Alvarado, B. EFFECTS OF CLIMATE AND STAND AGE ON ANNUAL TREE DYNAMICS IN TROPICAL SECOND-GROWTH RAIN FORESTS. *Ecology* **86**, 1808–1815 (2005).

68. Suarez, M. L., Ghermandi, L. & Kitzberger, T. Factors predisposing episodic drought-induced tree mortality in Nothofagus- site, climatic sensitivity and growth trends. *J. Ecol.* **92**, 954–966 (2004).

69. Phillips, O. L. *et al.* Drought Sensitivity of the Amazon Rainforest. *Science* **323**, 1344–1347 (2009).

70. Mehl, J. W., Geldenhuys, C. J., Roux, J. & Wingfield, M. J. Die-back of kiaat (*Pterocarpus angolensis*) in southern Africa: a cause for concern? *South. For. J. For. Sci.* **72**, 121–132 (2010).

71. Van Der Linde, J. A., Roux, J., Wingfield, M. J. & Six, D. L. Die-off of giant Euphorbia trees in South Africa: Symptoms and relationships to climate. *South Afr. J. Bot.* **83**, 172–185 (2012).

72. Fauset, S. *et al.* Drought-induced shifts in the floristic and functional composition of tropical forests in Ghana. *Ecol. Lett.* **15**, 1120–1129 (2012).

73. Gonzalez, P., Tucker, C. J. & Sy, H. Tree density and species decline in the African Sahel attributable to climate. *J. Arid Environ.* **78**, 55–64 (2012).

74. Kherchouche, D., Kalla, M., Gutiérrez, E. M., Attalah, S. & Bouzghaia, M. Impact of droughts on Cedrus atlantica forests dieback in the Aurès (Algeria). *J. Life Sci.* **6**, 1262 (2012).

75. Dulamsuren, C. *et al.* Performance of Siberian elm (Ulmus pumila) on steppe slopes of the northern Mongolian mountain taiga: Drought stress and herbivory in mature trees. *Environ. Exp. Bot.* **66**, 18–24 (2009).

76. Kharuk, V. I., Ranson, K. J., Oskorbin, P. A., Im, S. T. & Dvinskaya, M. L. Climate induced birch mortality in Trans-Baikal lake region, Siberia. *For. Ecol. Manag.* **289**, 385–392 (2013).

77. Zhou, G. *et al.* A climate change-induced threat to the ecological resilience of a subtropical monsoon evergreen broad-leaved forest in Southern China. *Glob. Change Biol.* **19**, 1197–1210 (2013).

78. Brouwers, N., Matusick, G., Ruthrof, K., Lyons, T. & Hardy, G. Landscape-scale assessment of tree crown dieback following extreme drought and heat in a Mediterranean eucalypt forest ecosystem. *Landsc. Ecol.* **28**, 69–80 (2013).

79. Fensham, R. J., Fairfax, R. J. & Dwyer, J. M. Potential aboveground biomass in drought-prone forest used for rangeland pastoralism. *Ecol. Appl.* **22**, 894–908 (2012).

80. Kharuk, V. I., Im, S. T., Oskorbin, P. A., Petrov, I. A. & Ranson, K. J. Siberian pine decline and mortality in southern siberian mountains. *For. Ecol. Manag.* **310**, 312–320 (2013).

81. Keith, H., van Gorsel, E., Jacobsen, K. L. & Cleugh, H. A. Dynamics of carbon exchange in a Eucalyptus forest in response to interacting disturbance factors. *Agric. For. Meteorol.* **153**, 67–81 (2012).

82. Matusick, G., Ruthrof, K. X. & Hardy, G. St. J. Drought and Heat Triggers Sudden and Severe Dieback in a Dominant Mediterranean-Type Woodland Species. *Open J. For.* **02**, 183–186 (2012).

83. Brouwers, N. C. *et al.* Climate and landscape drivers of tree decline in a Mediterranean ecoregion. *Ecol. Evol.* **3**, 67–79 (2013).

84. Peterken, G. & Mountford, E. Effects of drought on beech in Lady Park Wood, an unmanaged mixed deciduous woodland. *Forestry* **69**, 125–136 (1996).

85. Linares, J. C., Camarero, J. J. & Carreira, J. A. Interacting effects of changes in climate and forest cover on mortality and growth of the southernmost European fir forests. *Glob. Ecol. Biogeogr.* **18**, 485–497 (2009).

86. Galiano, L., Martínez-Vilalta, J. & Lloret, F. Drought-Induced Multifactor Decline of Scots Pine in the Pyrenees and Potential Vegetation Change by the Expansion of Co-occurring Oak Species. *Ecosystems* **13**, 978–991 (2010).

87. Aakala, T., Kuuluvainen, T., Wallenius, T. & Kauhanen, H. Tree mortality episodes in the intact Picea abies-dominated taiga in the Arkhangelsk region of northern European Russia: Episodic tree mortality in intact spruce taiga. *J. Veg. Sci.* **22**, 322–333 (2011).

88. Linares, J. C. *et al. Tree growth decline on relict Western-Mediterranean mountain forests: Causes and impacts*. *Forest Decline: Causes and Impacts* 1–20 (Nova Science Publishers Inc.: Hauppauge, NY, USA, 2011).

89. Sarris, D., Christodoulakis, D. & Körner, C. Impact of recent climatic change on growth of low elevation eastern Mediterranean forest trees. *Clim. Change* **106**, 203–223 (2011).

90. Marini, L., Ayres, M. P., Battisti, A. & Faccoli, M. Climate affects severity and altitudinal distribution of outbreaks in an eruptive bark beetle. *Clim. Change* **115**, 327–341 (2012).

91. Cailleret, M., Nourtier, M., Amm, A., Durand-Gillmann, M. & Davi, H. Drought-induced decline and mortality of silver fir differ among three sites in Southern France. *Ann. For. Sci.* **71**, 643–657 (2014).

92. Vilà-Cabrera, A., Martínez-Vilalta, J., Galiano, L. & Retana, J. Patterns of Forest Decline and Regeneration Across Scots Pine Populations. *Ecosystems* **16**, 323–335 (2013).

93. Fahey, T. J. Recent Changes in an Upland Forest in South-Central New York. *J. Torrey Bot. Soc.* **125**, 51 (1998).

94. Ganey, J. L. & Vojta, S. C. Tree mortality in drought-stressed mixed-conifer and ponderosa pine forests, Arizona, USA. *For. Ecol. Manag.* **261**, 162–168 (2011).

95. Michaelian, M., Hogg, E. H., Hall, R. J. & Arsenault, E. Massive mortality of aspen following severe drought along the southern edge of the Canadian boreal forest: ASPEN MORTALITY FOLLOWING SEVERE DROUGHT. *Glob. Change Biol.* **17**, 2084–2094 (2011).

96. DeRose, R. J. & Long, J. N. Drought-driven disturbance history characterizes a southern Rocky Mountain subalpine forest. *Can. J. For. Res.* **42**, 1649–1660 (2012).

97. Fellows, A. W. & Goulden, M. L. Rapid vegetation redistribution in Southern California during the early 2000s drought: DROUGHT DRIVEN VEGETATION REDISTRIBUTION. *J. Geophys. Res. Biogeosciences* **117**, n/a-n/a (2012).

98. Kaiser, K. E., McGlynn, B. L. & Emanuel, R. E. Ecohydrology of an outbreak: mountain pine beetle impacts trees in drier landscape positions first: ECOHYDROLOGY OF A MOUNTAIN PINE BEETLE OUTBREAK. *Ecohydrology* **6**, 444–454 (2013).

99. Millar, C. I. *et al.* Forest mortality in high-elevation whitebark pine (*Pinus albicaulis*) forests of eastern California, USA; influence of environmental context, bark beetles, climatic water deficit, and warming. *Can. J. For. Res.* **42**, 749–765 (2012).

100. Garrity, S. R. *et al.* Quantifying tree mortality in a mixed species woodland using multitemporal high spatial resolution satellite imagery. *Remote Sens. Environ.* **129**, 54–65 (2013).

101. Enquist, B. J. & Enquist, C. A. F. Long-term change within a Neotropical forest: assessing differential functional and floristic responses to disturbance and drought:

DIFFERENTIAL FUNCTIONAL RESPONSES TO CLIMATE CHANGE IN A TROPICAL FOREST. *Glob. Change Biol.* **17**, 1408–1424 (2011).

102. Mokria, M., Gebrekirstos, A., Aynekulu, E. & Bräuning, A. Tree dieback affects climate change mitigation potential of a dry afromontane forest in northern Ethiopia. *For. Ecol. Manag.* **344**, 73–83 (2015).

103. Baguskas, S. A., Peterson, S. H., Bookhagen, B. & Still, C. J. Evaluating spatial patterns of drought-induced tree mortality in a coastal California pine forest. *For. Ecol. Manag.* **315**, 43–53 (2014).

104. Hart, S. J., Veblen, T. T., Eisenhart, K. S., Jarvis, D. & Kulakowski, D. Drought induces spruce beetle (*Dendroctonus rufipennis*) outbreaks across northwestern Colorado. *Ecology* **95**, 930–939 (2014).

105. Kane, J. M., Kolb, T. E. & McMillin, J. D. Stand-scale tree mortality factors differ by site and species following drought in southwestern mixed conifer forests. *For. Ecol. Manag.* **330**, 171–182 (2014).

106. Gu, L., Pallardy, S. G., Hosman, K. P. & Sun, Y. Predictors and mechanisms of the drought-influenced mortality of tree species along the isohydric to anisohydic continuum in a decade-long study of a central US temperate forest. *Biogeosciences Discuss.* **12**, 1285–1325 (2015).

107. Smith, J. M., Paritsis, J., Veblen, T. T. & Chapman, T. B. Permanent forest plots show accelerating tree mortality in subalpine forests of the Colorado Front Range from 1982 to 2013. *For. Ecol. Manag.* **341**, 8–17 (2015).

108. Zhou, G. *et al.* Substantial reorganization of China's tropical and subtropical forests: based on the permanent plots. *Glob. Change Biol.* **20**, 240–250 (2014).

109. Čater, M. A 20-Year Overview of Quercus robur L. Mortality and Crown Conditions in Slovenia. *Forests* **6**, 581–593 (2015).

110. Aynekulu, E. *et al.* Dieback affects forest structure in a dry Afromontane forest in northern Ethiopia. *J. Arid Environ.* **75**, 499–503 (2011).

111. Liang, E., Leuschner, C., Dulamsuren, C., Wagner, B. & Hauck, M. Global warming-related tree growth decline and mortality on the north-eastern Tibetan plateau. *Clim. Change* **134**, 163–176 (2016).

112. Challis, A., Stevens, J. C., McGrath, G. & Miller, B. P. Plant and environmental factors associated with drought-induced mortality in two facultative phreatophytic trees. *Plant Soil* **404**, 157–172 (2016).

113. Matusick, G., Ruthrof, K. X., Fontaine, J. B. & Hardy, G. E. St. J. *Eucalyptus* forest shows low structural resistance and resilience to climate change-type drought. *J. Veg. Sci.* **27**, 493–503 (2016).

114. Drobyshev, I., Linderson, H. & Sonesson, K. Temporal mortality pattern of pedunculate oaks in southern Sweden. *Dendrochronologia* **24**, 97–108 (2007).

115. Andersson, M., Milberg, P. & Bergman, K.-O. Low pre-death growth rates of oak (Quercus robur L.)—Is oak death a long-term process induced by dry years? *Ann. For. Sci.* **68**, 159–168 (2011).

116. Martin, P. A., Newton, A. C., Cantarello, E. & Evans, P. Stand dieback and collapse in a temperate forest and its impact on forest structure and biodiversity. *For. Ecol. Manag.* **358**, 130–138 (2015).

117. García de la Serrana, R., Vilagrosa, A. & Alloza, J. A. Pine mortality in southeast Spain after an extreme dry and warm year: interactions among drought stress, carbohydrates and bark beetle attack. *Trees* **29**, 1791–1804 (2015).

118. Herguido, E. *et al.* Contrasting growth and mortality responses to climate warming of two pine species in a continental Mediterranean ecosystem. *For. Ecol. Manag.* **363**, 149–158 (2016).

119. Bendixsen, D. P., Hallgren, S. W. & Frazier, A. E. Stress factors associated with forest decline in xeric oak forests of south-central United States. *For. Ecol. Manag.* **347**, 40–48 (2015).

120. Billings, S. A., Boone, A. S. & Stephen, F. M. Tree-ring δ^{13}C and δ^{18}O, leaf δ^{13}C and wood and leaf N status demonstrate tree growth strategies and predict susceptibility to disturbance. *Tree Physiol.* **36**, 576–588 (2016).

121. Berdanier, A. B. & Clark, J. S. Multiyear drought-induced morbidity preceding tree death in southeastern U.S. forests. *Ecol. Appl.* **26**, 17–23 (2016).

122. Feeley, K. J., Hurtado, J., Saatchi, S., Silman, M. R. & Clark, D. B. Compositional shifts in Costa Rican forests due to climate-driven species migrations. *Glob. Change Biol.* n/a-n/a (2013) doi:10.1111/gcb.12300.

123. Duque, A., Stevenson, P. R. & Feeley, K. J. Thermophilization of adult and juvenile tree communities in the northern tropical Andes. *Proc. Natl. Acad. Sci.* **112**, 10744–10749 (2015).

124. Amoroso, M. M., Daniels, L. D., Villalba, R. & Cherubini, P. Does drought incite tree decline and death in *Austrocedrus chilensis* forests? *J. Veg. Sci.* **26**, 1171–1183 (2015).

125. Schwantes, A. M., Swenson, J. J. & Jackson, R. B. Quantifying drought-induced tree mortality in the open canopy woodlands of central Texas. *Remote Sens. Environ.* **181**, 54–64 (2016).

126. Assal, T. J., Anderson, P. J. & Sibold, J. Spatial and temporal trends of drought effects in a heterogeneous semi-arid forest ecosystem. *For. Ecol. Manag.* **365**, 137–151 (2016).

127. Feldpausch, T. R. *et al.* Amazon forest response to repeated droughts: AMAZON FOREST RESPONSE TO DROUGHTS. *Glob. Biogeochem. Cycles* **30**, 964–982 (2016).

128. Freeman, M. P., Stow, D. A. & An, L. Patterns of mortality in a montane mixed-conifer forest in San Diego County, California. *Ecol. Appl.* **27**, 2194–2208 (2017).

129. Harrison, R. D. Drought and the consequences of El Niño in Borneo: a case study of figs. *Popul. Ecol.* **43**, 63–75 (2001).

130. Wood, J. D., Knapp, B. O., Muzika, R.-M., Stambaugh, M. C. & Gu, L. The importance of drought–pathogen interactions in driving oak mortality events in the Ozark Border Region. *Environ. Res. Lett.* **13**, 015004 (2018).

131. Paz-Kagan, T. *et al.* What mediates tree mortality during drought in the southern Sierra Nevada? 2549248 Bytes (2017) doi:10.6084/M9.FIGSHARE.5281273.V1.

132. Xu, C. *et al.* Enhanced sprout-regeneration offsets warming-induced forest mortality through shortening the generation time in semiarid birch forest. *For. Ecol. Manag.* **409**, 298–306 (2018).

133. Crouchet, S. E., Jensen, J., Schwartz, B. F. & Schwinning, S. Tree Mortality After a Hot Drought: Distinguishing Density-Dependent and -Independent Drivers and Why It Matters. *Front. For. Glob. Change* **2**, 21 (2019).

134. Preisler, Y. *et al.* Mortality versus survival in drought-affected Aleppo pine forest depends on the extent of rock cover and soil stoniness. *Funct. Ecol.* **33**, 901–912 (2019).

135. Kunert, N. Preliminary indications for diverging heat and drought sensitivities in Norway spruce and Scots pine in Central Europe. *IForest - Biogeosciences For.* **13**, 89–91 (2020).

136. Powers, J. S. *et al.* A catastrophic tropical drought kills hydraulically vulnerable tree species. *Glob. Change Biol.* **26**, 3122–3133 (2020).

137. Johnson, D. M. *et al.* Co-occurring woody species have diverse hydraulic strategies and mortality rates during an extreme drought. *Plant Cell Environ.* (2018).

138. Jaime, L., Batllori, E., Margalef-Marrase, J., Pérez Navarro, M. Á. & Lloret, F. Scots pine (Pinus sylvestris L.) mortality is explained by the climatic suitability of both host tree and bark beetle populations. *For. Ecol. Manag.* **448**, 119–129 (2019).

139. Navarro Cerrillo, R. M., Varo, M. A., Lanjeri, S. & Clemente, R. H. Cartografía de defoliación en los pinares de pino silvestre (Pinus sylvestris L.) y pino salgareño (Pinus nigra Arnold.) en la Sierra de los Filabres. *Ecosistemas* **16**, 9 (2007).

140. Prieto-Recio, C., Martín-García, J., Bravo, F. & Diez, J. J. Unravelling the associations between climate, soil properties and forest management in Pinus pinaster decline in the Iberian Peninsula. *For. Ecol. Manag.* **356**, 74–83 (2015).

141. Pernek, M., Lacković, N., Lukić, I., Zorić, N. & Matošević, D. Outbreak of *Orthotomicus erosus* (Coleoptera, Curculionidae) on Aleppo Pine in the Mediterranean Region in Croatia. *South-East Eur. For.* **10**, 19–27 (2019).

142. Savi, T. *et al.* Drought-induced dieback of Pinus nigra: a tale of hydraulic failure and carbon starvation. *Conserv. Physiol.* **7**, coz012 (2019).

143. Klein, T., Cahanovitc, R., Sprintsin, M., Herr, N. & Schiller, G. A nation-wide analysis of tree mortality under climate change: Forest loss and its causes in Israel 1948–2017. *For. Ecol. Manag.* **432**, 840–849 (2019).

144. Dorman, M., Perevolotsky, A., Sarris, D. & Svoray, T. The effect of rainfall and competition intensity on forest response to drought: lessons learned from a dry extreme. *Oecologia* **177**, 1025–1038 (2015).

145. Dorman, M., Svoray, T., Perevolotsky, A., Moshe, Y. & Sarris, D. What determines tree mortality in dry environments? a multi-perspective approach. *Ecol. Appl.* **25**, 1054–1071 (2015).

146. Swemmer, A. Locally high, but regionally low: the impact of the 2014–2016 drought on the trees of semi-arid savannas, South Africa. *Afr. J. Range Forage Sci.* **37**, 31–42 (2020).

147. Sáenz-Romero, C. *et al.* Recent evidence of Mexican temperate forest decline and the need for ex situ conservation, assisted migration, and translocation of species ensembles

as adaptive management to face projected climatic change impacts in a megadiverse country. *Can. J. For. Res.* 1–12 (2020) doi:10.1139/cjfr-2019-0329.

148. Allen, C. D. Interactions Across Spatial Scales among Forest Dieback, Fire, and Erosion in Northern New Mexico Landscapes. *Ecosystems* **10**, 797–808 (2007).

149. Rodríguez-Catón, M., Villalba, R., Srur, A. & Williams, A. P. Radial Growth Patterns Associated with Tree Mortality in Nothofagus pumilio Forest. *Forests* **10**, 489 (2019).

150. Das, A. J. *et al.* TREE MORTALITY IN BLUE OAK WOODLAND DURING EXTREME DROUGHT IN SEQUOIA NATIONAL PARK, CALIFORNIA. *Madroño* **66**, 164 (2020).

151. Stephenson, N. L., Das, A. J., Ampersee, N. J., Bulaon, B. M. & Yee, J. L. Which trees die during drought? The key role of insect host-tree selection. *J. Ecol.* **107**, 2383–2401 (2019).

152. Csank, A. Z., Miller, A. E., Sherriff, R. L., Berg, E. E. & Welker, J. M. Tree-ring isotopes reveal drought sensitivity in trees killed by spruce beetle outbreaks in south-central Alaska. *Ecol. Appl.* **26**, 2001–2020 (2016).

153. Kannenberg, S. A., Schwalm, C. R. & Anderegg, W. R. L. Ghosts of the past: how drought legacy effects shape forest functioning and carbon cycling. *Ecol. Lett.* **23**, 891–901 (2020).

154. Schuldt, B. *et al.* A first assessment of the impact of the extreme 2018 summer drought on Central European forests. *Basic Appl. Ecol.* **45**, 86–103 (2020).

Supplementary Information for Chapter IV: DEAD OR DYING? QUANTIFYING THE POINT OF NO RETURN FROM HYDRUALIC FAILURE IN DROUGHT-INDUCED TREE MORTALITY.

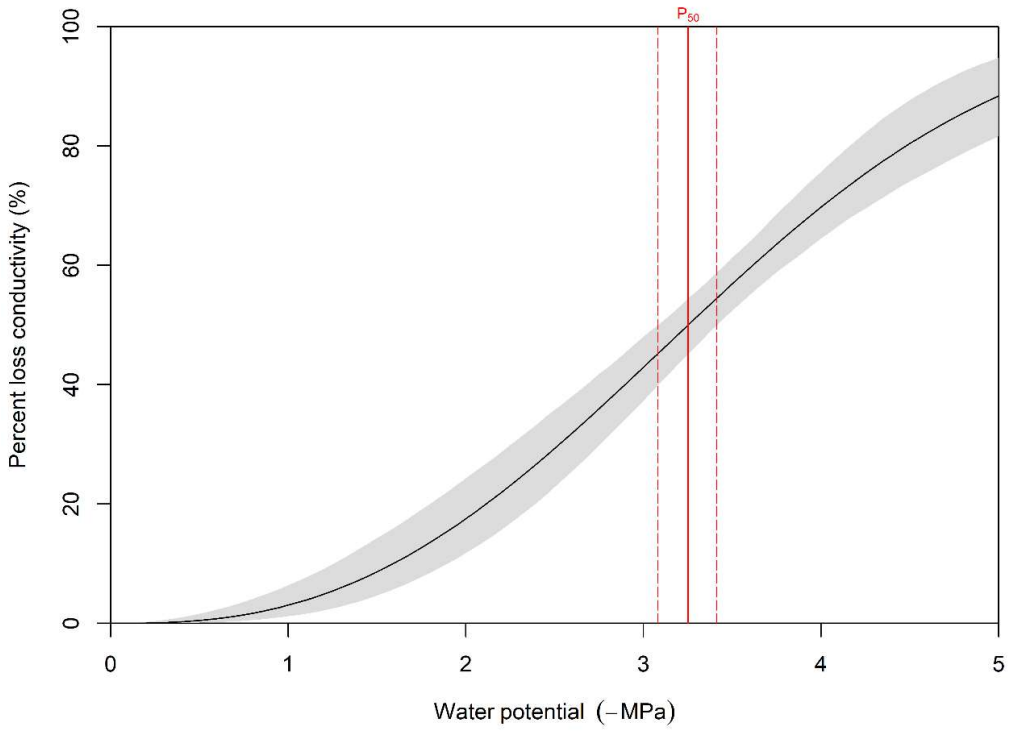

Figures S1. Vulnerability curve of *Pinus taeda*, loblolly pine, generated with samples from six saplings of the experimental population, using centrifugation to induce embolism. The water potential at 50 PLC (P_{50}), -3.22 MPa, is shown with a solid red line, and the 95% confidence interval for P50 (-3.05 to -3.37 MPa) is shown with dashed red lines. We fitted the curve using R package 'fitplc' (Duursma & Choat, 2017).

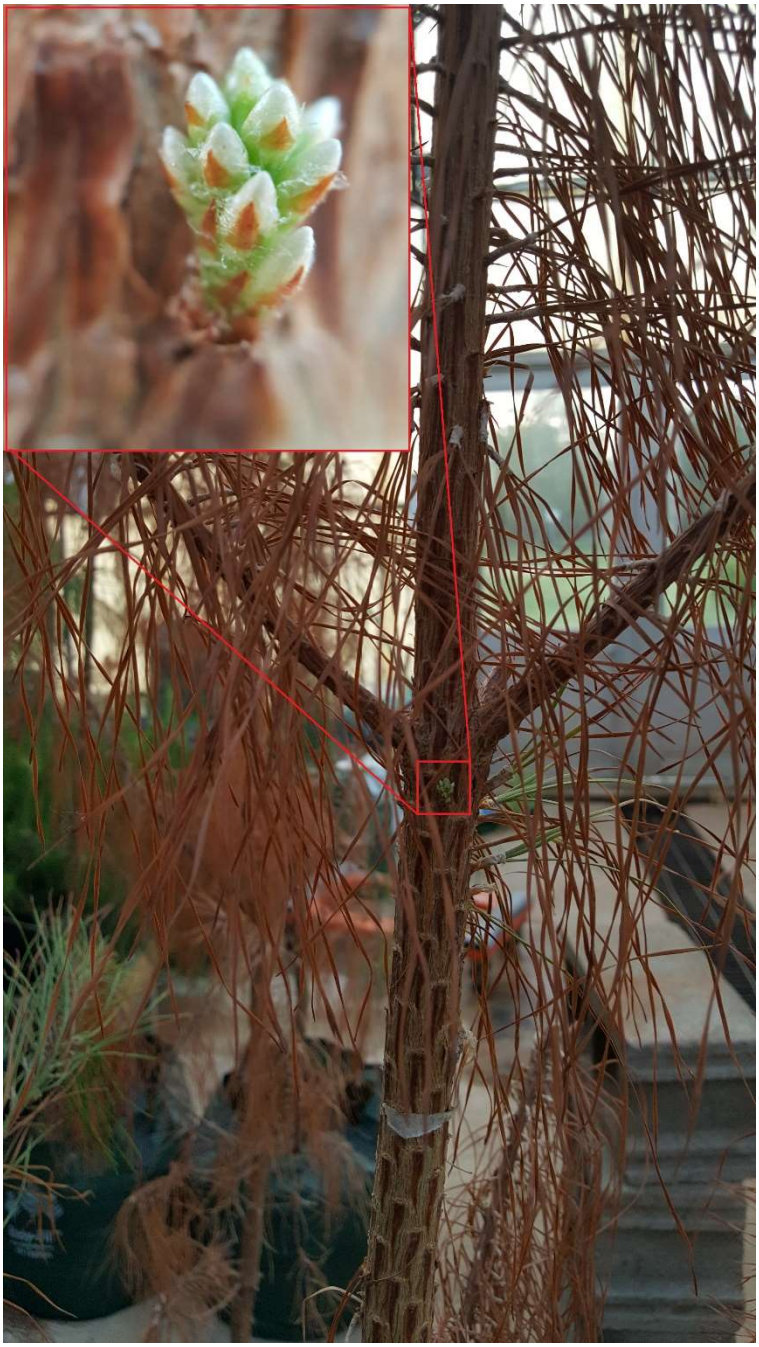

Figure S2. Epicormic re-sprouting on loblolly pine just after re-watering. All existing foliage was completely browned, appearing dead, and epicormic re-sprouts appeared shortly after re-watering. While epicormic re-sprouts did not die within 60 days of re-watering, all epicormic re-sprouts eventually died (within 120 days). Due to this, these two trees were excluded from our calculations of the lethal hydraulic threshold.

Supplemental Text for Figure S2:

Of note, we observed four trees re-sprout basally after re-watering, a rare response in loblolly pine that is more often observed in response to fire or wounding. Two trees also re-sprouted epicormically (~1m above soil level) after complete canopy die-back, which has not been previously reported for drought-stressed loblolly pine (Fig. S2). Trees that produced epicormic shoots had a 72.5 and 95 PLC, indicating that their water-stress approached the limits of survival. The basally re-sprouted tissues died within 60 days of re-watering and were included in the analysis as dead trees. However, trees with epicormic shoots survived beyond 60 days, so these two trees were excluded from our analysis although they eventually died at a later date.

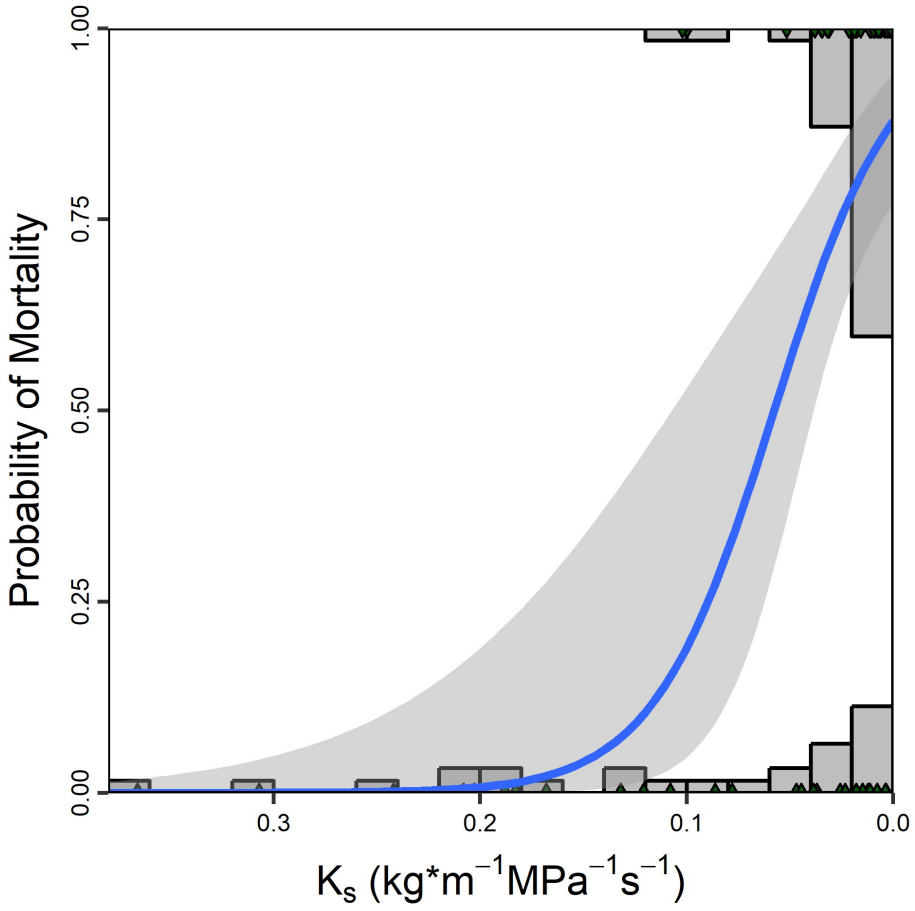

Figure S3. A logistic regression to determine the 50% lethal dose (LD50) of native conductivity (K_s) during drought, which was 0.06 (95% Wald Confidence for probability of mortality had a minimum K_s = .04 and maximum K_s = 0.11 at LD50). Bars represent proportion of all trees in 20 bins across the observed range of K_s, scaled to the height of Y-axis. Solid blue line is the logistic regression fit, with shaded grey area representing a Wald 95% confidence interval for the logistic regression.

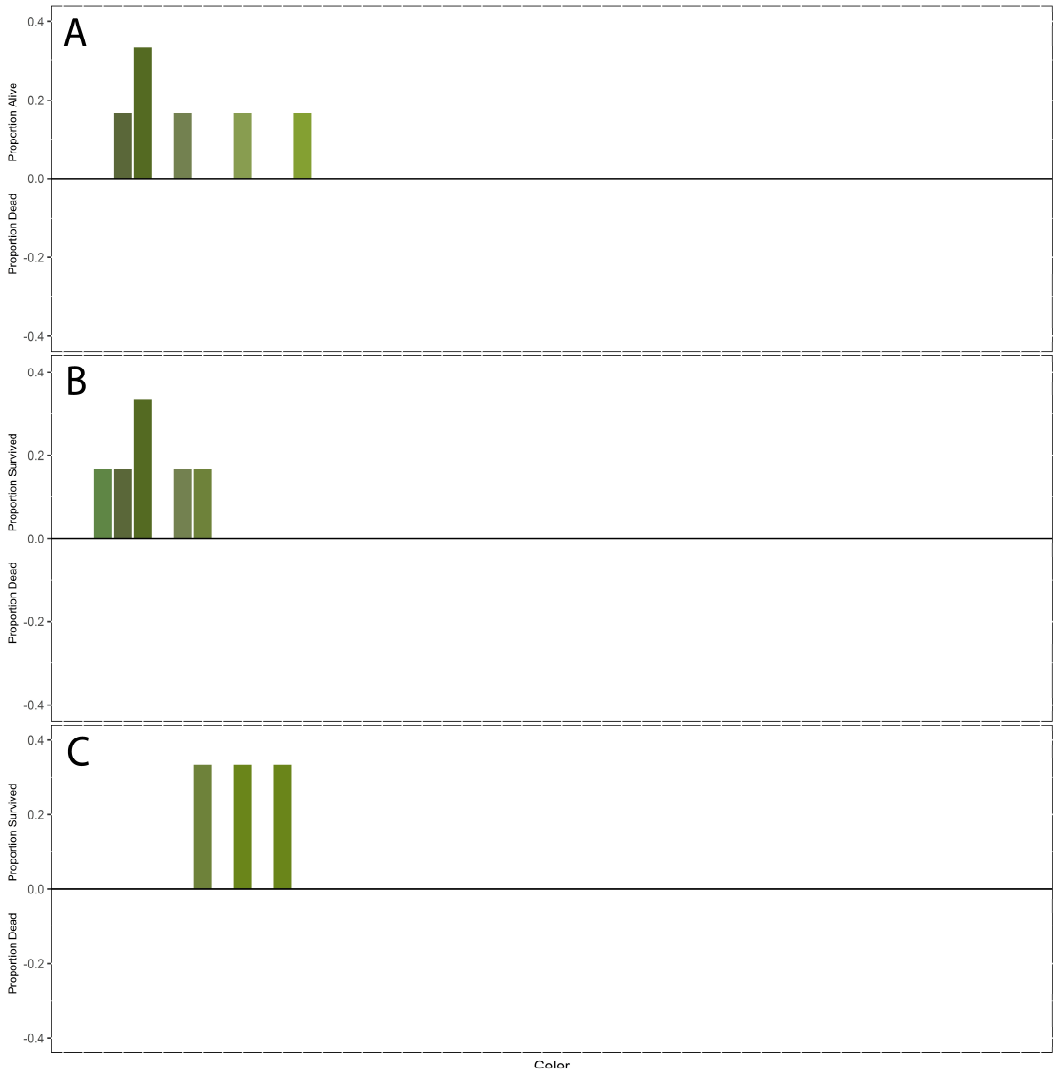

Figure S4. **This figure is a companion to** Figure 3 **in the main text—containing data for only the six watered control trees (which are not included in Figure 3). The x-axis remains the same as Fig. 3, observed canopy color, arranged from darkest green to deepest red-brown. Bar height indicates the proportion of trees that survived (positive proportions) or the trees that died (negative proportions) at a given color. Bars are filled with the observed foliar color recorded from a representative sample. Panel A shows canopy foliar color at the beginning of the experiment, before drought, and foliar color of all trees was a deep green. Panel B shows canopy foliar color at the end of the re-watering period. Panel C shows canopy foliar color 60 days after re-watering of the last droughted tree in the experiment. Canopy color was consistently green, without yellowing or browning of the canopy during the experimental drought and recovery periods.**

Author's note: *Table S1 and Table S2 are published online, at https://doi.org/10.1111/nph.15922 under supplemental material, and are not included in this appendix due to their excessive size. However, their captions are below:*

Table S1. Logistic regression model predictions for probability of mortality given percent loss of conductivity values (PLC) ranging from 0 to 100, by 0.1. Model fit is provided, along with lower (lwr) and upper (upr) 95% Wald CI's for probability of mortality.

Table S2. Logistic regression model predictions for probability of mortality given specific conductivity values (K_s) ranging from 0 to 0.366 (the range of observed values during this experiment), by 0.001. Model fit is provided, along with lower (lwr) and upper (upr) 95% Wald CI's for probability of mortality.

Suppelemental References for chapter IV:

Duursma RA, Choat B. 2017. fitplc: an R package to fit hydraulic vulnerability curves. *Journal of Plant Hydraulics* **4**.

VITA

William Michael Hammond

Candidate for the Degree of

Doctor of Philosophy

Thesis: WHAT KILLS TREES? DRIVERS, MECHANISMS, AND TIMING OF CLIMATE-INDUCED TREE MORTALITY.

Major Field: Plant Biology

Biographical:

Education:

Completed the requirements for the Doctor of Philosophy in Plant Biology at Oklahoma State University, Stillwater, Oklahoma in May, 2021.

Completed the requirements for the Bachelor of Science in Biology at University of Central Oklahoma, Edmond, Oklahoma, USA, 2016.

Experience:

National Science Foundation Graduate Research Fellow (NSF GRFP)
2018 “Make Our Planet Great Again” Laureate (Campus France)

For a full list of experience, see my *curriculum vitae* at
https://wmammond.com/cv

Professional Memberships:

American Geophysical Union (2016-Present)
Ecological Society of America (2016-Present)
European Geophysical Union (2021-Present)